Adaptive Multiuser Detection with Decision Feedback Equalizer for Interference Cancellation

By

Waleed Abdulwahed Saif

A Thesis Presented to the
DEANSHIP OF GRADUATE STUDIES

In Partial Fulfillment of the Requirements
for the degree

MASTER OF SCIENCE

IN

TELECOMMUNICATION ENGINEERING

KING FAHD UNIVERSITY
OF PETROLEUM & MINERALS

Dhahran, Saudi Arabia

June 2003

ACKNOWLEDGEMENTS

In the name of Allah, the Most Gracious and the Most Merciful

All praise and glory to Almighty Allah (SWT) who gave me courage and patience to carry out this work.

Acknowledgement is due to King Fahd University of Petroleum and Minerals for providing support for this work as well as the Telecommunication Research Laboratory. Also, acknowledgment is due to KACST for financial support of this work.

My deep appreciation goes to my thesis advisor and co-advisor Dr. A. U. H. Sheikh and Dr. A. Zerguine for their constant help, guidance and the countless hours of attention he devoted throughout the course of this research work. Their priceless suggestions made this work interesting and learning for me.

Also, thanks are due to Dr. Mohammad Adnan Al-Andalusi for his interest, invaluable cooperation and support.

Acknowledgement is due to A. Bentrcia, Sajid Khan, Kamran Arshad, Moinuddin, and Hamid who helped me at various stages of this work.

Special thanks are due to my friends and colleagues for their help and encouragement. A few of them are Hashim and Hani Al-Shehri, Wail Al-Gamdi, Hamad Al-Ammar, Rakan Al-Ohali, Badr Al-Dohan, Badr Al-Jarallah, Abduallah Manda, Fahd, W. Al-Qoti, M. Khames, Tawfiq, Afiff and Najib. They have made my work and stay at KFUPM very pleasant.

And finally, my heartfelt thanks to my parents, my brothers and sisters. Their prayers and support are always with me.

CONTENTS

List of Tables

List of Figures

THESIS ABSTRACT

Name: Waleed Saif

Title: Adaptive Multiuser Detection with Decision Feedback Equalizer for Interference Cancellation

Degree: MASTER OF SCIENCE

Major Field: Telecommunication Engineering

Date of Degree: June 2003

Multiple access interference (MAI) is considered the major air interference for the 3G radio communication systems in which code division multiple access (CDMA) technique is used for allocating certain number of users the same channel at the same time. Canceling MAI is a major task in the 3G system. Multiuser detection (MUD) receivers can provide better interference rejection than the conventional detector used in 2G system (like IS-95). The optimal MUD detector which is the maximum likelihood detector is too complex for practical implementation with today's technology. Due to this complexity, most of researches have focused on finding suboptimal low complexity multiuser detectors solutions that are feasible to implement. In this thesis, we investigate the performance of a new receiver structure which uses decision feedback equalizer (DFE) as a multiuser detector. A modified DFE structure in which error feedback filter (EFF) is added to the main structure is also investigated. The performance of these proposed structures will be compared to the decorrelator detector (DD). The proposed structure is shown to exhibit good MAI rejection as well as near-far resistance.

Keywords: *CDMA, Multiuser detection, Adaptive equalization, Decision feedback Equalizer, Error feedback, LMS algorithm, Decorrelator, Multiple Access Interference.*

King Fahd University of Petroleum Minerals, Dhahran
June 2003

ARABIC ABSTRACT

ملخص الرسالة

الإسم: وليد عبدالواحد سيف

عنوان الرسالة: الكشف التكيفي متعدد المستعملين بمعادل تعليقات الفرار لإلغاء التداخل

التخصص: هندسة الإتصالات

تاريخ التخرج: يونيه 2003

يعتبر تداخل الوصول المتعدد (MAI) التشويش الجوي الرئيسي لنظام الجيل الثالث لإتصالات الراديو و الذي يُستخدم في تقنية وصول قسم الرمز المتعدد (CDMA) لتخصيص عدد معين من المستعملين لنفس القناة في نفس الوقت . إلغاءMAI مهمة رئيسية في نظام الجيل الثالث للإتصالات . الكشف المتعدد المستعملين يستطيع التقليل من التشويش أفضل من الكاشف التقليدي المستخدم في نظام الجيل الثاني . إن الكاشف المثالي معقد جدا للتطبيق العملي. بسبب هذا التعقيد أغلب البحوث تركز على اكتشاف حلول كاشفات المتعددة للمستعملين منخفض التعقيد و عملي قابل للتطبيق. في هذه الأطروحة نتحرى آداة تركيب مستقبل إتصالات جديد و الذي يستعمل معادل تعليقات الفرار (DFE) ككاشف متعدد المستعملين. أيضا التحري في آداء التركيب معدل من (DFE) و الذي أضيف إليه مرشح تعليقات الخطأ. آداء هذه التراكيب المقترحة ستقارن إلى كاشف (DD). إن التركيب المقترح يقوم بالتقليل الجيد من التشويش بالإضافة غلى المقاومة البعيدة تقريبا.

Chapter 1

Introduction

Mobile communication is rapidly becoming a necessity for everyday activities. As a result, more users need to be accommodated. However, availability of bandwidth should be taken in consideration particularly in cellular radio systems for spectrum conservation. Capacity of the system can be increased by allowing users to share the same channel or frequency bandwidth. This can be done by using multiple access systems or multiaccess communications in which each user is provided with a certain frequency band or a time slot or both, without disturbing other users communication [1][2]. Several examples of multiple access methods, e.g. Frequency Division Multiple Access (FDMA), Time Division Multiple Access (TDMA) and Code Division Multiple Access (CDMA) are the most commonly used multiple access systems.

All third generation (3G) technologies use CDMA which provides high data and voice capacity and low cost. The CDMA technique is based on spread spectrum technology in which the message signal is spread to a relatively wide bandwidth by using pseudo-random codes or pseudo-noise (PN) sequences to achieve low power per unit bandwidth [3][4]. In this technique, several independent users are simultaneously share the same frequency band, and are separated only by different user codes called spreading sequences.

Transmission over time varying multipath mobile radio channels will produce both Intersymbol Interference (ISI) and Multiple Access Interference (MAI) between data symbols of different users. At the receiver, ISI and MAI can be treated in different ways.

The conventional single user receiver implemented as a matched filter considers each user as if it was the only one transmitting, and this is often inefficient because it treats the MAI from other users as noise. Another problem with the conventional receiver is the *near-far problem* [1]. This problem appears when the number of active users in the system becomes large or when the power level of certain users increases, the detection of weak users with the conventional detector becomes difficult.

The optimum multiuser detector such as the maximum likelihood multiuser detector is too complex to be implemented with the present day technology. Therefore, suboptimum detectors are used. Furthermore, they show on one hand a better performance than the conventional receiver and on the other hand have a lower computational complexity than the maximum likelihood detector.

Some of the suboptimum detectors are based on zero forcing and minimum mean square error (MMSE) equalization. Equalization can be linear or non-linear, with or without decision feedback. Also, equalization can be adaptive; either they use training or work blindly. Equalization with multiuser detection is a good solution for overcoming ISI, MAI and other factors that affect transmission in CDMA such as near far resistance [1][5].

1.1 Equalization

Equalization plays an important role in a communication system. In some applications, the channel parameters and their statistics are not known in advance.

Moreover, they may change from time to time, specially in wireless communications [6]. So, it is important to track the channel characteristics. Adaptive equalization employs adaptive algorithms such as Least Mean-Square (LMS) to adjust the equalizer filter coefficients to minimize the Mean Square Error (MSE). In the receiver, the *equalizer,* which is a compensator for channel distortion, is placed before the detection process at the receiver in order to reduce the ISI as much as possible and hence maximize the probability of correct decisions.

There are three types of equalizers that are commonly used:

- Maximum Likelihood (ML) Sequence Detection which is the optimal equalizer but in some cases impractical for implementation due its complexity.
- Linear Equalizers such as the taped-delay-line equalizer (also known as linear Transversal equalizer (LTE)) which is widely used and simple for implementation.
- Non-Linear Equalizes such as Decision feedback equalizer.

Since the LTE and the DFE will be used in this thesis, these two only will be discussed here.

1.1.1 Linear Transversal Equalizer:

The linear transversal equalizer (LTE) is the simplest equalizer among others and it is most widely used in channel equalization. It is also known as the tapped-delay-line equalizer. Figure 1.1 shows the structure of the linear transversal filter used in LTE.

The output of the equalizer having N taps at the n^{th} instant and is given by:

$$y_{eq}(n) = \sum_{k=0}^{N-1} w(k)\, y(n-k) \tag{1.1}$$

where $w(k)$, k=1,2, ...,N-1, are the coefficients of the equalizer and $y(n)$ is the input to the equalizer.

The error, as it can be seen from Figure 1.1, is computed as follow:

1) In the training mode, the error is the difference between the training sequence (transmitted $x(n)$) and the output of the equalizer, that is:

$$e(n) = x(n) - y_{eq}(n) \tag{1.2}$$

2) In the decision-directed mode, the error is the difference between the estimated transmitted sequence, $x'(n)$, and the output of the equalizer and thus is given by:

$$e(n) = x'(n) - y_{eq}(n) \tag{1.3}$$

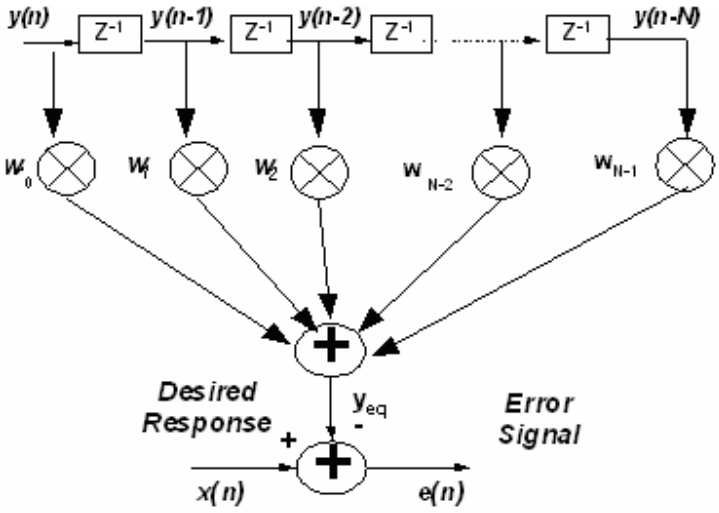

Figure 1.1: Linear Transversal Filter.

The error signal is used to update the tap coefficients of the equalizer based on some minimization criteria or adaptive algorithms. Three of the most widely used algorithms are LMS, Discrete Cosine Transform (DCT)-LMS and Recursive Least Square (RLS).

1.1.2 Decision Feedback Equalizer

The decision feedback equalizer (DFE) is a nonlinear equalizer. As the name implies, the DFE uses decisions on the symbols to estimate the error and cancel the interference from the symbols that have already been detected. An example of the structure of DFE is shown in Figure 1.2. It consists of two linear transversal filters, the feedforward and feedback filters. The output of both filters is the equalized signal. The decision made on this signal is fed back via the feedback filter in order to cancel ISI caused by previously detected symbols [6][7]. The coefficients of the DFE can be updated simultaneously by using the same equation used to update LTE coefficients. The goal of updating the coefficients is to minimize the MSE.

The major disadvantage of DFE is error propagation. This happens when an incorrect fed back decision affects the next few symbols. This will lead to multiple errors following the first one. However, the DFE can compensate for amplitude distortion better than LTE [6]. In general, up to some noise level, DFE perform better than LTE. After that level, DFE will cause error propagation.

Let us define the feed forward DFE coefficients $\mathbf{w_f}$ and the feedback coefficients $\mathbf{w_b}$ as:

$$\mathbf{w_f} = [w_{f1} \quad w_{f2} \quad \cdots \quad w_{fN_f}]^T \tag{1.4}$$

$$\mathbf{w_b} = [w_{b1} \quad w_{b2} \quad \cdots \quad w_{bN_b}]^T \tag{1.5}$$

where N_f and N_b are the number of feed forward and feedback taps, respectively.

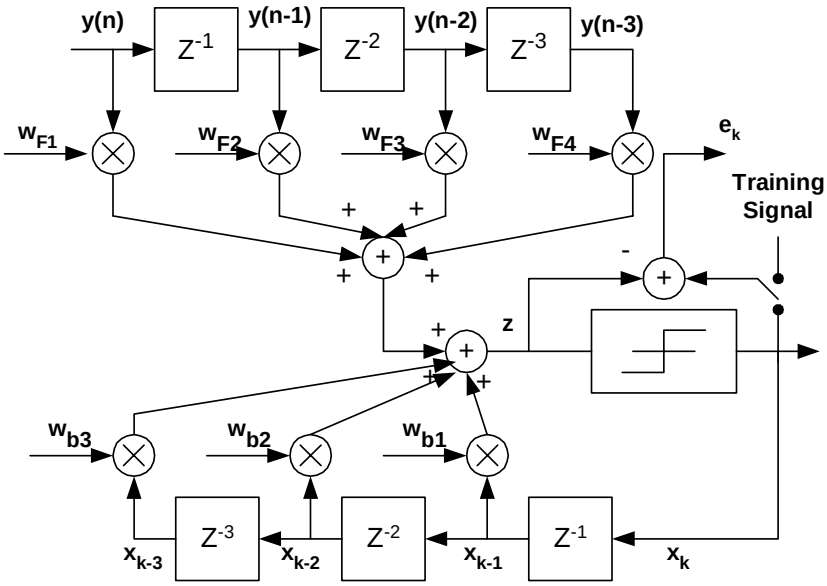

Figure 1.2: Decision feedback equalizer

The input vectors to the forward and feedback filters are given by:

$$\mathbf{y}(n) = \begin{bmatrix} y(n+1) & y(n+2) & \cdots & y(n+N_f-1) \end{bmatrix}^T \tag{1.6}$$

$$\hat{\mathbf{x}}(n) = \begin{bmatrix} \hat{x}(n+1) & \hat{x}(n+2) & \cdots & \hat{x}(n+N_b-1) \end{bmatrix}^T \tag{1.7}$$

Now the output of the DFE before the decision device y_{eq} can be found to be given by

$$\begin{aligned} z(n) &= \mathbf{w_f^T y}(n) + \mathbf{w_b^T}\hat{\mathbf{x}}(n) \\ &= \begin{bmatrix} \mathbf{w_f^T} & \mathbf{w_b^T} \end{bmatrix} \begin{bmatrix} \mathbf{y}(n) \\ \hat{\mathbf{x}}(n) \end{bmatrix} \end{aligned} \tag{1.8}$$

By using the result of (1.8) with (1.3), we get the error signal. As mentioned before, the error is used to update the tap coefficients for both feedforward and feedback filters using selected adaptive algorithms such as LMS, Normalized-LMS (NLMS), RLS, algorithms.

1.2 Multiuser Detection

In CDMA receivers, there are two categories of receivers; single-user detectors and multiuser detector as shown in Figure 1.3.

The conventional detection (single-user detector), also known as the matched filter, simply correlates the received signal with the desired user's spreading code and samples the output at the bit rate. This detector doesn't consider the MAI. It follows a single user detection in which each user is detected separately without taking into account other users. In this type of receiver, the MAI is considered as noise [5][8].

Many different linear and non-liner detectors have been developed for multiuser CDMA system (see Figure 1.3). These detectors differ in their computational complexity and actual performance. Some of these detectors are:

1.2.1 Maximum Likelihood Sequence (MLS) Detector

This detector was proposed and analyzed by Verdu [1]. It is known as the optimal multiuser detector and can be stated as follows [1]:

"*For K users, given the statics* $(y_1,...,y_K)$ *from the output of the matched filters, find an estimate of the transmitted bit-vector* $(b_1,...,b_K)$ *that optimizes (minimizes) the probability of error.*" The ML criterion is based on selecting the input bit that minimizes the Euclidean distance between the transmitted bits and the received ones.

This detector is too complex for practical Direct Sequence (DS)-CDMA. Because of its complexity, most of the research has focused on finding suboptimal multiuser detectors solutions, which are feasible to implement.

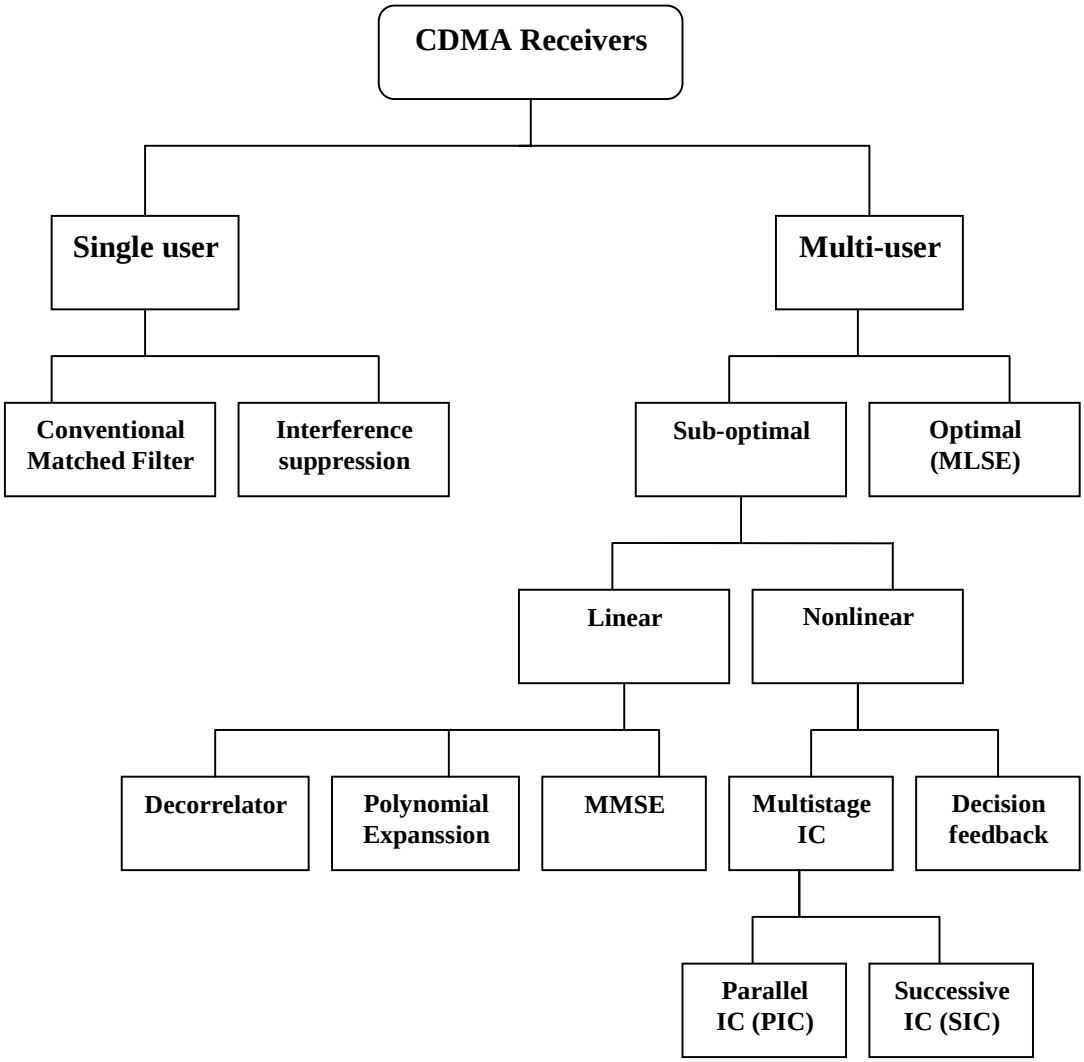

Figure 1.3: Hierarchy of various CDMA receiver techniques.

1.2.2 Decorrelating Detector

This detector was initially proposed in [9][10] and it is extensively analyzed by Lupas and Verdu in [11][12]. It is a linear detector which applies the inverse of the correlation matrix of user spreading codes to the output of the conventional detector. In matrix form, the soft decision output for *K*-users system is given by [1]:

$$\mathbf{y} = \mathbf{RAd} + \mathbf{n} \tag{1.9}$$

where the vector **d**, **n** and **y** are *K*-vectors that hold the data, noise and matched filter output of all users, respectively. The matrix **A** is a diagonal matrix containing the corresponding received amplitudes. The matrix **R** is $K \times K$ cross-correlation matrix whose entries contain the values of cross-correlation between every pair of codes. Now, the soft estimate of this detector, assuming the matrix **R** is invertible, is found to be [1]:

$$\hat{\mathbf{d}} = \mathbf{R}^{-1}\mathbf{y} = \mathbf{Ad} + \mathbf{R}^{-1}\mathbf{n} \tag{1.10}$$

This detector outperforms the conventional one. It removes all MAI which implies that the power of each user does not have to be estimated [5]. On the other hand, this detector has some drawbacks such as noise enhancement caused by the term $\mathbf{R}^{-1}\mathbf{n}$ in (1.10). Also, it has no way of removing ISI caused by the channel. The complexity of this detector is in the order of $O(K^3)$ due to the inverse of a cross-correlation matrix [13].

1.2.3 Zero-Forcing Detector

The zero-forcing (ZF) detector, also known as ZF equalizer, is a natural progression of the decorrelating detector. In addition of removing MAI, it eliminates the ISI as well [5]. This can be done by taking into consideration each user channel impulse response. The equalizer is used to estimate the channel information including channel impulse response, users spreading codes and timing. The ZF equalizer suffers from noise enhancement problem as the decorrelating detector does. To improve the performance in the presence of noise, the MMSE equalizer is used.

1.2.4 MMSE Detectors

Two detectors can be considered here. They are the linear MMSE detector and the adaptive MMSE detector, as discussed next.

A. Linear MMSE Detector

It is a linear detector which takes into account the background noise and utilizes the knowledge of the received signal power. It minimizes the MSE between the actual data and the soft output of the conventional detector. It provides better probability of error performance than the decorrelating detector since it considers the background noise [1][5].

B. Adaptive MMSE Detector

Both the previous detector and the decorrelator detector involve matrix inversion. Although, there are ways to speed up such computation, it is better to avoid using them, especially in asynchronous time varying channels. Eliminating the need of matrix inversion can be accomplished with an adaptive implementation of MMSE linear detector. In the adaptive MMSE detector, either training adaptive equalization or blind equalization is used with the appropriate adaptive algorithm.

1.2.5 Subtractive Interference Cancellation Detectors

The basic principle of these detectors is that separate estimates of the MAI contributed by each user at the receiver is done in order to subtract out some or all of the MAI seen by each user. These detectors are similar to feedback equalizers. Some of these detectors are Successive Interference Cancellation (SIC) [14], Parallel Interference Cancellation (PIC) [15] and ZF decision-feedback (DF) detectors.

The SIC detector takes a serial approach to get out the MAI. It makes a decision, regenerates and cancels out the additional direct-sequence user at a time. On the other hand, the PIC detector uses the parallel approach in which it estimates and subtracts out all the MAI for each user in parallel.

The ZF-DF detector performs two operations. First, linear preprocessing is done then followed by a form of SIC detection. The first operation tends to decorrelate the users without enhancing the noise [5]. The SIC operation makes the decision and subtracts out the MAI from one additional user at a time.

Direct performance of SIC, partial PIC, Decorrelating and MMSE detectors can be found in [16][17].

1.3 Motivation and Thesis Contribution

CDMA technology became a leading candidate for 3G systems because of its notable advantages such as interference resistance, anti-jamming and high system capacity. However, CDMA is susceptible to the Near-Far Effect, in which strong signals interfere with weaker ones, limiting the total number of simultaneous transmission. Also, as mentioned earlier in this chapter, the MAI is one of the main factors that limits both capacity and performance of CDMA.

Another factor that affects the detection process is ISI produced by the channel. Fortunately, ISI can be removed using equalization at the receiver. Equalization can be used for channel estimation as well. It is impossible to find a fixed receiver structure specially in case of time varying channels, which is common in wireless communication.

The conventional detector cannot remove all the MAI. This problem gives rise to multiuser detection. Since the optimum receiver which is based on the maximum likelihood sequence detector is too complex for practical DS-CDMA systems, many studies have been conducted for finding a good suboptimal receiver. Systems designers try to develop a suboptimal receiver which has a close performance to the optimal one with reasonable complexity.

In this thesis work, a multiuser detector based on modified decision feedback equalizer is used. The structure is an adaptive decision feedback detector with error feedback which was proposed by Kim [18] and used in the context of equalization for combating ISI in magnetic recoding channels, but not in the context of multiuser detection. In [18], it was shown that the performance of DFE with error feedback is better than its counterpart with no error feedback. This is due to the correlation reduction of error signal that cannot be reduced by the feedforward or feedback filters. The complexity of this structure is minimal since it requires only additional few taps [18].

The aim of this work is to get a good receiver structure that overcomes the previous mentioned problems, i.e. MAI, ISI and near far effect. The performance of the receiver will be compared with the conventional DFE detector as well as the DFE-Decorrelator. During the simulations, the following items are considered in the evaluation process:

- Synchronous CDMA system.
- Simple BPSK data.
- Three types of channels are used: a static channel, a Pedestrian (slowly frequency selective fading) channel with three paths and Vehicular (slowly

frequency selective fading) channel with three paths, each path has a different Doppler frequency.

1.4 Thesis Organization

This thesis is organized as follow:

- Chapter 2 presents an overview of multiple access techniques with an emphasis on the CDMA system. Pseudo-noise codes and their properties such as the Maximal length, Gold and Walsh codes are discussed. Mathematical representations of synchronous and asynchronous CDMA models are presented. Finally, a brief overview of multiuser detection, that discusses the conventional and decorrelator detectors, is given.
- Chapter 3 presents an overview on mobile fading channels, types of fading and their statistics and modeling fading channels.
- Chapter 4 presents the concept of adaptive equalization, the effect of ISI and its mathematical representation, ways of combating ISI and some adaptive algorithms.
- Chapter 5 presents an adaptive multiuser detector with decision feedback equalizer (DFE) for interference cancellation. A modified version of decision feedback equalizer in which an error feedback filter (EFF) is incorporated to the conventional DFE is presented. The MSE for both structures is derived in this chapter.

- Chapter 6 presents the simulation results comparing the conventional DFE, DFE based multiuser detector and DFE-Decorrelator detector. The same structures are also compared when EFF is added to the conventional DFE.
- Chapter 7 presents some observations and conclusions as well as possible future work directions.

Chapter 2

Code Division Multiple Access Spread Spectrum System

2.1 Introduction

Wireless cellular telephony has been growing at a faster rate than wired-line telephone networks [19]. This growth is a result of the recent improvements in the capacity of wireless channels due to the use of multiple access techniques, which allow many users to share the same channel for transmission, in association with advanced signal processing algorithms. CDMA is becoming a popular technology for cellular communications, which is based on spread spectrum technology [20]. Unlike other multiple access techniques such as FDMA and TDMA, which are limited in frequency band and time duration respectively, CDMA uses all of the available time-frequency space.

In general, spread spectrum signals are commonly used for [7]:

- Combating or suppressing the detrimental effects of interference due to jamming, interference arising from other users of the channel, and self-interference due to multipath propagation.

- Hiding a signal by transmitting it at low power spectral density and, thus making it difficult for an unintended listener to detect in the presence of background noise.
- Achieving message privacy in the presence of other listeners.

The purpose of this chapter is to give an overview of CDMA system. First, multiple access techniques including TDMA, FDMA and CDMA will be discussed briefly. Then, CDMA system will be discussed in details including Direct Sequence (DS)-CDMA and spreading codes.

2.2 Multiple Access Techniques

A multiple access system has a design, which allows multiple users to transmit information over the same channel, or frequency bandwidth, to a receiver. In a cellular communication system, this corresponds to the multitude of mobile units all transmitting to a single base station as shown in Figure 2.1.

Since there are multiple users transmitting over the same channel, a method must be used so that individual users will not disrupt one another. There are essentially three ways in which to do this; FDMA, TDMA, and CDMA.

For radio systems there are two resources, frequency and time. Division by frequency, so that each pair of communicators is allocated part of the spectrum (band) for all of the time, results in FDMA. The receiver can tune to the specified band and demodulate the information. If only a small number of users are active, not the whole resource (frequency-spectrum) is used. Assignment of the channels can be done centrally or by carrier-sensing in a mobile. The latter technique enables random-access.

On the other hand, division by time, so that each pair of communicators is allocated whole (or at least a large part) of the spectrum for part of the time (time-slot), results in TDMA. Transmission of data is only possible during this time-slot, after that the transmitter has to wait until it gets another time-slot. Synchronization of all users is an important issue in this concept. Consequently, there must be a central unit (base-station) that controls the synchronization and the assignment of time-slots. This means that this technique is difficult to apply in random-access systems.

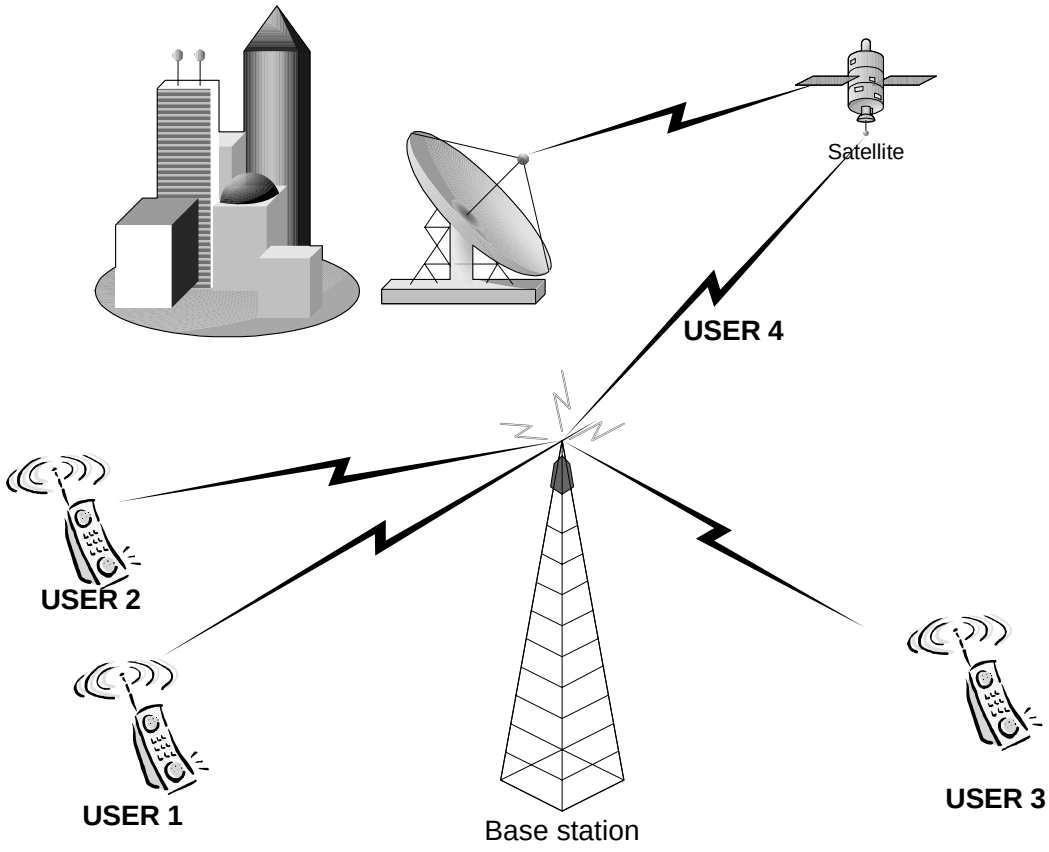

Figure 2.1: Multiple Access System

In the previous two systems, each user is essentially orthogonal in either time or frequency, which makes detection and demodulation a relatively easy task. However, these systems cannot take advantage of the properties of the transmitted data. Voice data tends to be very bursty in nature, so much of the time no data is being sent over the channel. This inefficiency tends to limit the capacity of the system.

In CDMA, every communicator will be allocated the entire spectrum all of the time. The message signal is spread to a relatively wide bandwidth by using pseudo-random codes or pseudo-noise (PN) sequences and transmits it with low power per unit bandwidth [3][4]. Synchronization between links is not strictly required and so random-access is possible. A practical application at the moment is the cellular-*cdma* phone system IS-95 [21]. The CDMA concept will be discussed in the next sections.

2.3 Code Division Multiple Access

CDMA is a system which is based on spread spectrum technology. It was initially developed for military antijamming. Since 1940's spread spectrum systems were developed for *antijam* and *low probability of intercept* (LPI) applications [3][20][22]. A spread spectrum signal is characterized by the bandwidth which is used to decrease the transmitting power and eliminate interference from other users as well as interference from the same user. In a CDMA system the users are spread across both frequency and time in the same channel. The capacity of this system depends on the amount of interference from the other users since the fundamental problem of CDMA is that each user causes *multiple access interference* (MAI) affecting all the other users.

The pseudo-random codes or PN sequences used to increase the bandwidth are essential for providing security as the situation in *antijaming*. In the antijam systems spectral spreading secures the signal against narrowband interferers [23] to make the detection as difficult as possible for an unwanted interceptor by hiding the signal in the noise as shown in Figure 2.2.

The PN codes spread the baseband data before transmission. The signal is transmitted in a channel, which is below noise level. The receiver then uses a correlator to “despread” the wanted signal, which is passed through a narrow bandpass filter. Unwanted signals will not be “despread” and will not pass through the filter. Codes take the form of a carefully designed one/zero sequence produced at a much higher rate than that of the baseband data. The rate of a spreading code is referred to as chip rate rather than bit rate.

There are many advantages of using CDMA. Some of these advantages are [2]:

- **Low power spectral density.** As the signal is spread over a large frequency-band, the Power Spectral Density is getting very small, so other communications systems do not suffer from this kind of communications. However the Gaussian Noise level is increasing.
- **Privacy due to unknown random codes.** The applied codes are - in principle - unknown to a hostile user. This means that it is hardly possible to detect the message of another user.
- **Applying spread spectrum implies the reduction of multi-path effects.**
- **Random access possibilities.** Users can start their transmission at any arbitrary time.

- **Capacity.** The capacity of CDMA system has been very controversial issue. The capacity of CDMA system is good compared to other systems. For example comparing CDMA with AMPS can be found [24]. However this is not fair, because AMPS is first generation system and CDMA is not. Third generation wideband CDMA and enhanced GSM is compared in [25] and the result is that there is no great differences in capacities.

On the other hand, there are some disadvantages:

- **Wide bandwidth:** High bit rates are difficult to achieve, because CDMA requires a lot of bandwidth. Due to intra-cell interference a single cell capacity is lower than in other cellular systems.
- **Near-far-problem**: CDMA requires good power control; otherwise near-far problem will decrease capacity.
- **Soft handover:** More interference and more complex network structure.

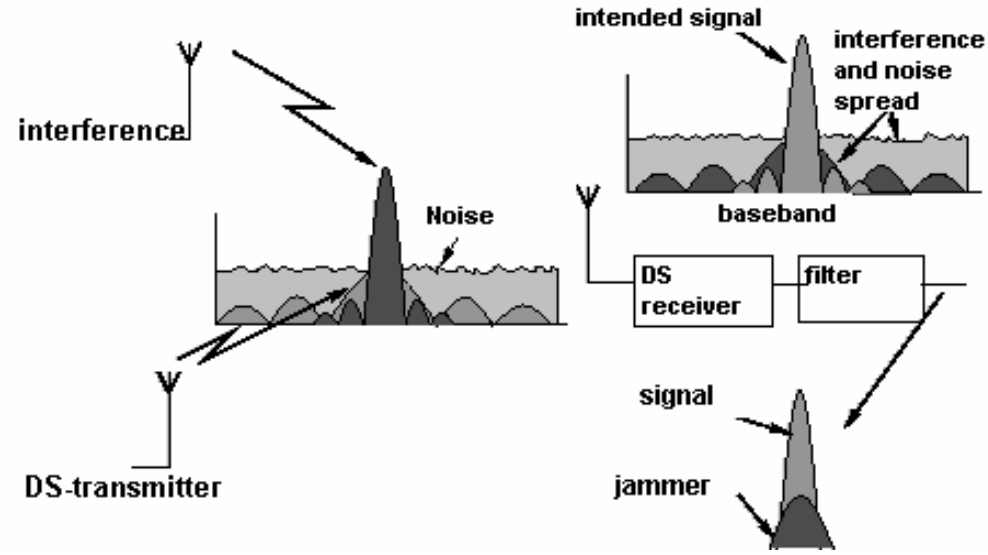

Figure 2.2: Spread spectrum and CDMA concept

There are many possible ways of spreading the signal in CDMA system. Some of these techniques are Direct-Sequence (DS), Frequency-Hopping (FH) and Time-Hopping (TH) [26]. They are the most common spreading techniques. In this thesis we will deal with the DS-CDMA spreading technique.

2.4 DS-CDMA

In DS-CDMA, modulating the message signal with higher rate chip sequence can achieve band spreading by using PN codes. Figure 2.3 illustrates the principle of DS-CDMA. Each symbol has duration of T_s. The information bandwidth is $W=1/T_s$ Hz. This bandwidth is spread a larger bandwidth called the transmission bandwidth which is $B=1/T_c$, where T_c is the chip duration, $T_c < T_s$. Hence we can define the spreading factor of processing gain as the ratio of the transmission bandwidth to the information bandwidth:

$$P_G = \frac{B}{W} = \frac{T_s}{T_c} \tag{2.1}$$

Processing gain (P_G) determines the amount of redundancy injected during modulation process. There are two major benefits from high processing gain:

- Interference rejection: the ability of the system to reject interference is directly proportional to P_G.
- System capacity: the capacity of the system is directly proportional to P_G.

So the higher the PN code bit rate is (the wider the CDMA bandwidth), the better the system performance.

At the receiver, the same PN codes used for spreading are generated. The received signal is correlated with that code to extract the data. We can summarize the DS-CDMA spreading as follow:

- Signal transmission consists of the following steps:
  1. A PN code is generated, each user or channel has different code.
  2. The Information data or transmitted signal is “spread” by the PN code.
  3. The resulting signal modulates a carrier.
  4. The modulated carrier is amplified and broadcasted.
- Signal reception consists of the following steps:
  1. The carrier is received and amplified.
  2. The received signal is mixed with a local carrier to recover the spread digital signal.
  3. A PN code is generated, matching the anticipated signal.
  4. The receiver acquires the received code and phase locks its own code to it.
  5. The received signal is correlated with the generated code, extracting the Information data.

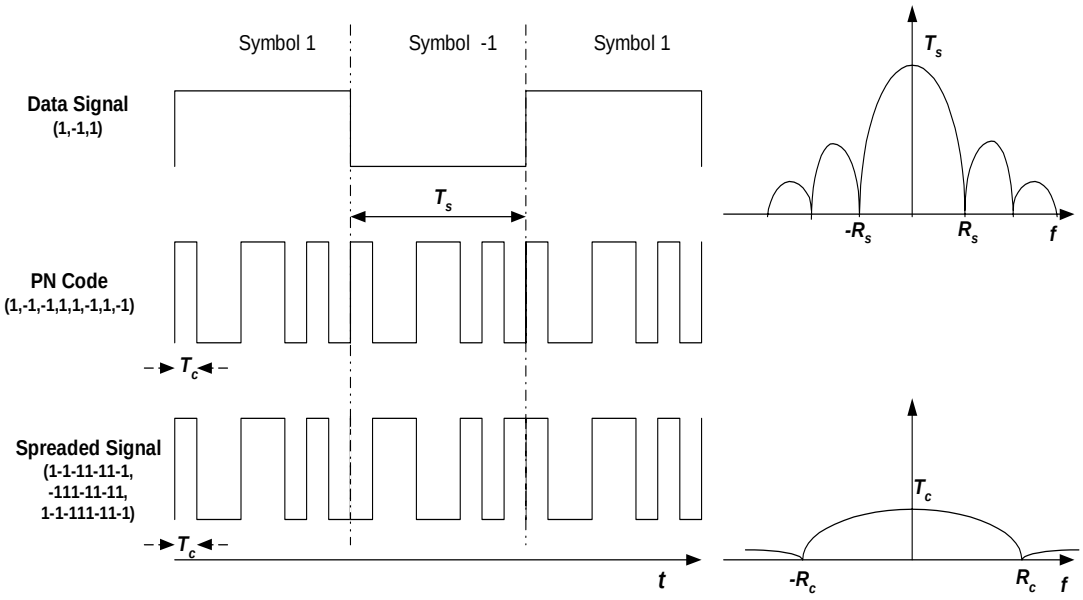

Figure 2.3: Direct-Sequence Spread Spectrum, time and frequency domain $R_s << R_c$.

2.5 Spreading Codes

In CDMA system, a user signal is multiplied by pseudo random sequence at the transmitter. This sequence must be known to receiver in order to recover the information bearing signal. A PN code is a sequence of chips valued -1 and 1 (polar) or 0 and 1 (non-polar) and has noise-like properties.

The desired properties of PN sequences depend clearly on the target application. The detailed requirements depend on the target system type, such as whether the system is a military or civilian system, is it a cellular system, what are the code length requirements and is the mode of operation synchronous or asynchronous.

There are many PN sequences such as *m*–sequences[27], Gold sequences[28], Walsh codes Barker sequences and Kasami sequences. Only the first tree types of sequences will be discussed in this section.

2.5.1 Maximal length sequences (m-sequences)

The maximum-length shift-register sequence, or shortly *m*-sequence, is probably the most widely known PN sequence. It can be generated by *m*-stage shift register with linear feedback as shown in Figure 2.4. The sequence length generated is $N=2^m-1$ chips long, meaning that they are as long as a shift register can produce. To construct *m* sequences of length *N*, (*N* is also the period of the sequence), one needs a primitive polynomial *h(x)* of degree *m*,

$$h(x) = h_0 x^m + h_1 x^{m-1} + h_2 x^{m-2} + \ldots + h_{m-1} x + h_m \qquad (2.2)$$

where h_0=h_m=1. A primitive generator polynomial [27] always yield an *m-sequence.* This polynomial specifies a linear feedback shift register. If the register contains $s_{m-1.}, s_{m-2.}, ..., s_{1.}, s_0$. at time *n*=*m*-1, then the output at time *n*=*m* is:

$$s_n = -\sum_{i=1}^{m} h_i s_{n-i}, \qquad n \geq m, \qquad h_i \in [0,1] \tag{2.3}$$

The *m sequences* have good autocorrelation property and are being used in many applications including IS-95. As the cross-correlation property of these sequences is relatively poor compared to Gold codes, the same sequence with different offset are usually used for different users or for different base stations. With this method, the discrimination property between different spreading codes only depends on partial autocorrelation property.

2.5.2 Gold Sequences

The Gold codes were invented in 1967 at the Magnavox Corporation by Robert Gold. They were invented specifically for multiple acces applications of spread specturm [27][28]. Gold codes have well controlled cross-correlation properties. Some pairs of *m*-sequences with the same degree can be used to generate Gold codes by linearly combining two *m* sequences with different offset in Galois field. All pairs of *m*-sequences do not yield Gold codes and those which yield Gold codes are called *preferred pairs* [27]. Usually, a set of Gold sequences consists of 2^{m+1} sequences having the period $N=2^m-1$ that are generated by a preferred pair of *m*-sequences. A typical Gold code genertor is shown in Figure 2.5 which can produece 32 Gold sequences of length 31.

Because the Gold codes are not maximul length sequence excpet the preferred pairs, the Gold codes have three-valued autocorrelation and cross-correlation function with values,

$$\begin{matrix} -\frac{1}{N}t(m) \\ -\frac{1}{N} \\ \frac{1}{N}[t(m)-2] \end{matrix} \tag{2.5}$$

where

$$t(m)=\begin{cases} 2^{(m+1)/2}+1 & \text{for m odd} \\ 2^{(m+2)/2}+1 & \text{for m even} \end{cases} \tag{2.6}$$

A considerably more thorough discussion of these codes can be found in [29].

2.5.3 Short versus. Long Codes

The temporal length of one code period of a *short* code sequence is equal to the symbol period ($P_G = N$, $T_s = N \cdot T_c$). The code period (N) of a *long* code sequence contains several symbol periods ($P_G << N$, $T_s << N \cdot T_c$). Short codes are used by multiuser detection systems because they use the bit periodic property of the short codes for MAI canceling. Otherwise, the long codes are preferred because the interference from all users becomes identical on the average [30].

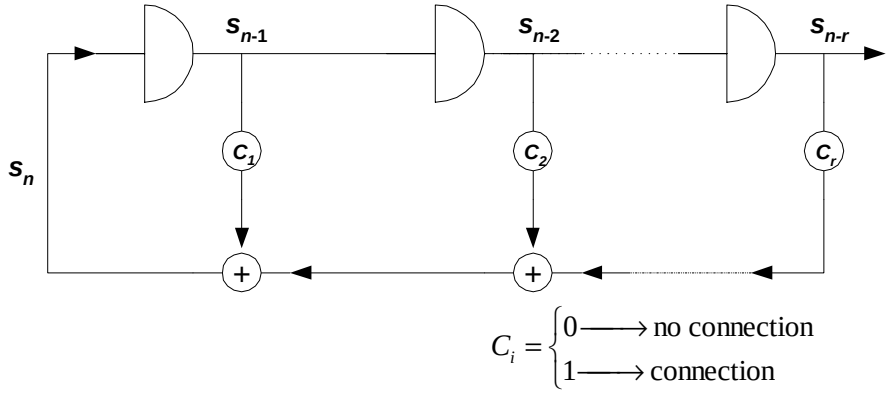

Figure 2.4 Linear shift register sequence generator

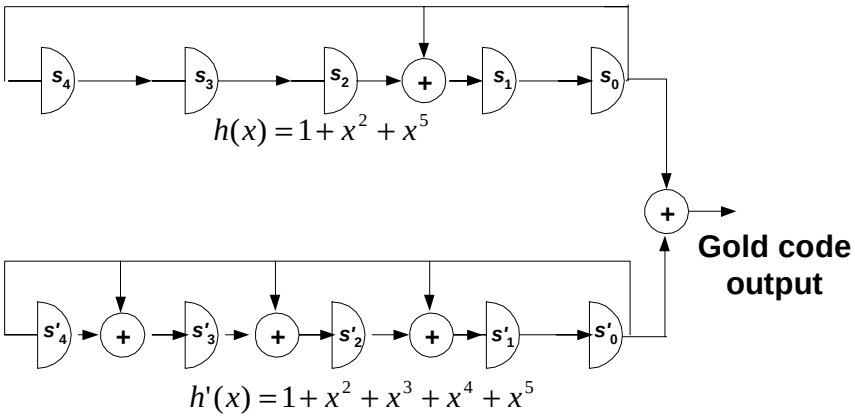

Figure 2.5: Typical Gold Generator

2.6 System Model

2.6.1 Synchronous DS-CDMA

In synchronous DS-CDMA channel, all bits of all K-user are aligned. This means that the *K*-users DS-CDMA signal model in additive white Gaussian noise (AWGN) consists of the sum of antipodally modulated synchronous wave signature [1][5] which is given by:

$$r(t) = \sum_{k=1}^{K} A_k(t) b_k(t) s_k(t) + n(t) \quad t \in [0, T_s] \tag{2.8}$$

where

- T_s is the symbol period;
- $s_k(t)$ is the deterministic signature waveform (PN code waveform) assigned to the k^{th} user, normalized so as to have unit energy

$$\|s_k\|^2 = \int_0^{T_s} s_k(t)dt = 1 \tag{2.9}$$

  The signature waveforms are assumed to be zero outside the interval [0, T_s], and therefore, there is no intersymbol interference [1];

- $A_k(t)$ is the received amplitude of the k^{th} user's signal. A_k^2 is referred to as the energy of the k^{th} user;
- $b_k(t) \in [-1,1]$ is the bit transmitted by the k^{th} user; and
- *n(t)* is white Gaussian noise with two sided power spectral density of *No/2* W/Hz.

The performance of various demodulation strategies depends on the signal-to-noise ratios, $2A_k/No$, and on the similarity between the signature waveforms, quantified by their crosscorrelation defined as:

$$\rho_{ij} = \langle s_i, s_j \rangle = \int_0^{T_s} s_i(t) s_j(t) dt \tag{2.10}$$

The crosscorrelation matrix

$$\mathbf{R} = \{\rho_{ij}\}, \; i = 1,..., K, \; j = 1,..., K \tag{2.11}$$

has diagonal elements equal to 1 and is symmetric nonnegative definite. Therefore, the crosscorrelation matrix **R** is positive definite if and only if the signature waveforms [s_1, s_2,..., s_k] are linearly independent [1].

2.6.2 Asynchronous DS-CDMA

In practical DS-CDMA applications, users can transmit at any time i.e. with different delays. In this case, the received signal is sampled at chip rate and the observation interval will be of length 2T in order to guarantee that one complete bit from the desired user will fall in that interval [5]. In the case of asynchronous DS-CDMA the crosscorrelation between PN codes is different than for synchronous case [1][31]. This means that Equation 2.10 is no longer valid for determining the performance. Two different crosscorrelation parameters based on delay between the signals should be defined between every pair of PN codes. For the *l*th bit of a given user *i*, an interfering user creates interference by either bits (*l*-1) and *l* or bits *l* and (*l*+1), depending on the positive or negative delay of the interfering user to user *i*. In Figure 2.6 the two possible scenarios are depicted. Assuming the delay of user *j* relative to user *i* is represented by τ where $\tau \in [0, T_s]$. As shown in Figure 1.7, user *j* has a positive delay relative to user *i*. This will result in interference to the *l*th bit of user *i* with bits (*l*-1) and *l*. similarly, user *k* has a negative delay relative to user *i* and creates interference to the *l*th bit of user *i* with

bits l and (l+1). In order to express the left and right bits interference, we define two types of crosscorrelation parameters between PN codes of any two user i and j. If $\tau \geq 0$, case of user j in Figure 2.7, then:

$$\rho_{ji} = \int_0^{\tau} s_i(t) s_j(t + T_s - \tau) dt \tag{2.11}$$

$$\rho_{ij} = \int_{\tau}^{T_S} s_i(t) s_j(t - \tau) dt \tag{2.12}$$

and if $\tau < 0$, case of user k in Figure 2.7, then:

$$\rho_{ik} = \int_0^{T_S + \tau} s_i(t) s_k(t - \tau) dt \tag{2.13}$$

$$\rho_{ki} = \int_{T_S + \tau}^{T_S} s_i(t) s_k(t - T_s - \tau) dt \tag{2.14}$$

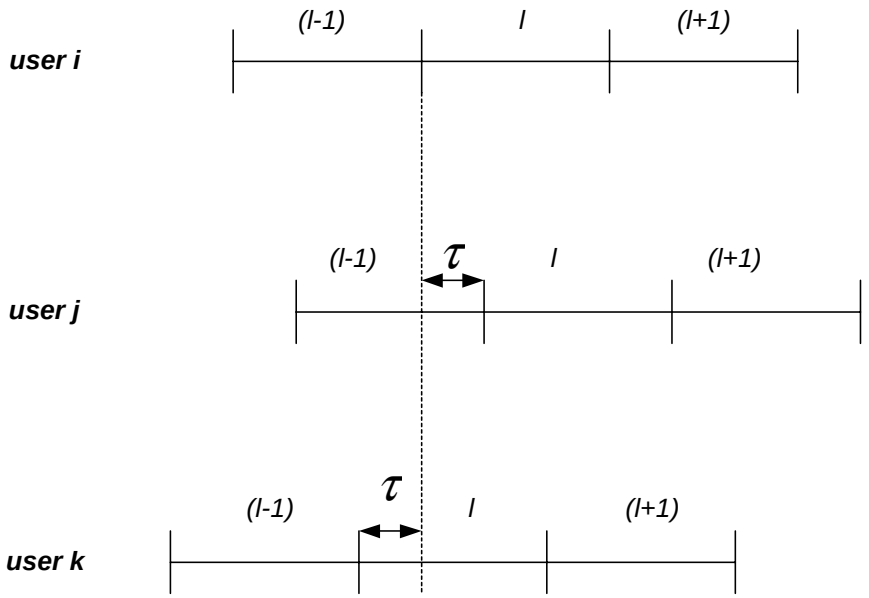

Figure 2.6: Asynchronous CDMA model.

2.7 Multiuser Detection

DS-CDMA has some attractive properties such as potential increase in capacity compared to other multiple access systems, anti-multipath capabilities, soft capacity and soft handoff. However, the performance and capacity of the DS-CDMA system are limited by Multiple Access Interferences (MAI). MAI is caused by the cross-correlation between spreading codes of active users.

In chapter 1, a brief overview on the development of multiuser detection (MUD) techniques for DS-CDMA during the past decade was presented. In this section we will focus on the conventional and Decorrelator detectors.

2.7.1 The Conventional Detector

The detection in the 2G system, namely, IS-95, is based on matched filtering. This detector is also known as the conventional detector. At the base station it consists of a bank of K correlators, as shown in Figure 2.7. Each user is treated separately in such detector. The received signal is correlated with the desired user's PN code and the output is sampled at the bit rate, which yields soft estimates of the transmitted data. The final hard data (± 1) decisions are made according to the signs of the soft output [5][32].

It is clear from Figure 2.7 that the conventional detector follows a single user detector strategy. Each branch detects one user without considering the other existing users. This means that the conventional detector treats MAI as noise. Thus, the performance and capacity of the system is highly dependent on the number of the active users in the system since there is no sharing of multiuser information.

Assume there are K users in a synchronous CDMA system. The baseband received signal was given in Equation (2.8)

The received signal will be matched to the corresponding users' PN codes as shown in Figure 2.8. If L is the processing gain defined in Chapter 2, then the output of the j^{th} correlator is given by:

$$y_j = \sum_{l=1}^{L} r(l)s_j(l) \tag{2.15}$$

$$y_j = \sum_{i=1}^{K} A_i b_i \left(\sum_{l=1}^{L} s_i(l)s_j(l) \right) + \sum_{l=1}^{L} n(l)s_j(l) \tag{2.16}$$

$$= \sum_{i=1}^{K} A_i b_i \rho_{ij} + n_j \tag{2.17}$$

where,

$$n_j = \sum_{l=1}^{L} n(l)s_j(l) \tag{2.18}$$

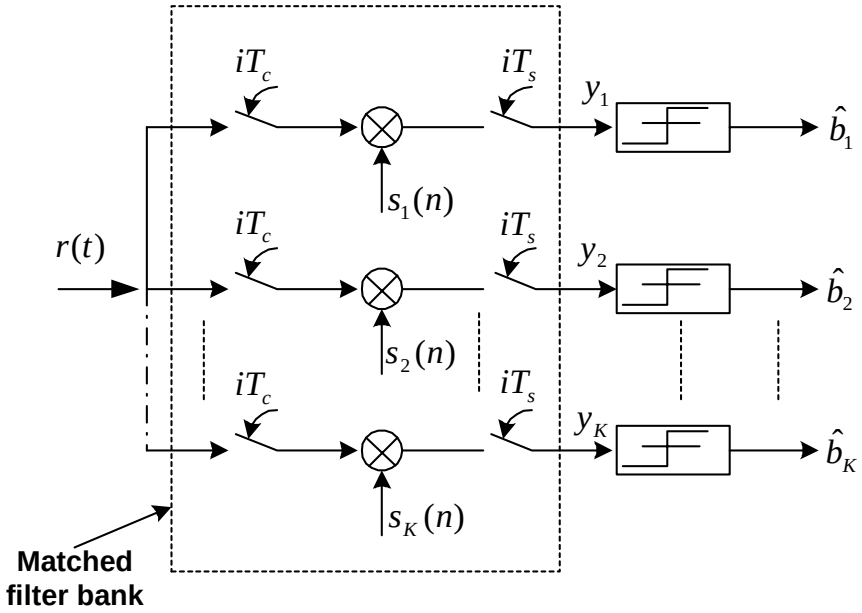

Figure 2.7: The Conventional Detector

and ρ_{ij} is the normalized cross-correlation of the signature waveforms defined as:

$$\rho_{ij} = \left\langle s_i, s_j \right\rangle = \frac{1}{\sqrt{L}} \sum_{l=1}^{L} s_i(l) s_i(l) \tag{2.19}$$

From (2.17) the output of the k^{th} user's correlator for a particular bit interval is:

$$\begin{aligned} y_k &= A_k b_k + \sum_{\substack{i=1 \\ i \neq k}}^{K} A_i b_i \rho_{ij} + n_j \\ &= A_k b_k + MAI_k + n_k \end{aligned} \tag{2.20}$$

It is clear form (2.20) that the correlation with the k^{th} user itself gives rise to the recovered data (1st term), correlation with all other active users gives rise to MAI (2nd term) and the correlation with the thermal noise yields to the noise term (3rd term).

In order to reduce the effect of MAI on user *k*, usually PN codes are generally designed to have very low crosscorrelation relative to autocorrelation (i.e. $\rho_{k,j} << 1$) [5].

As mentioned earlier, the conventional detector depends on the number of active users in which MAI has a significant impact on the capacity and performance of conventional DS-CDMA system. As the number of interfering users increases, the amount of MAI increases.

Another problem that causes the degradation in the performance of the conventional detector is the *near-far effect*. This is the case where the users' signals arrive at the receiver at different power levels due to the different geographical locations of the transmitters relative to the receiver. In such a case, weaker users may be overwhelmed by stronger users. As illustrated in Figure 2.8, although the cross-correlation between the codes of 1st and 2nd users is low, the interfering user is close to the receiver in which its signal is received at higher power level compared to the intended users. This might affect the proper data detection of the intended user.

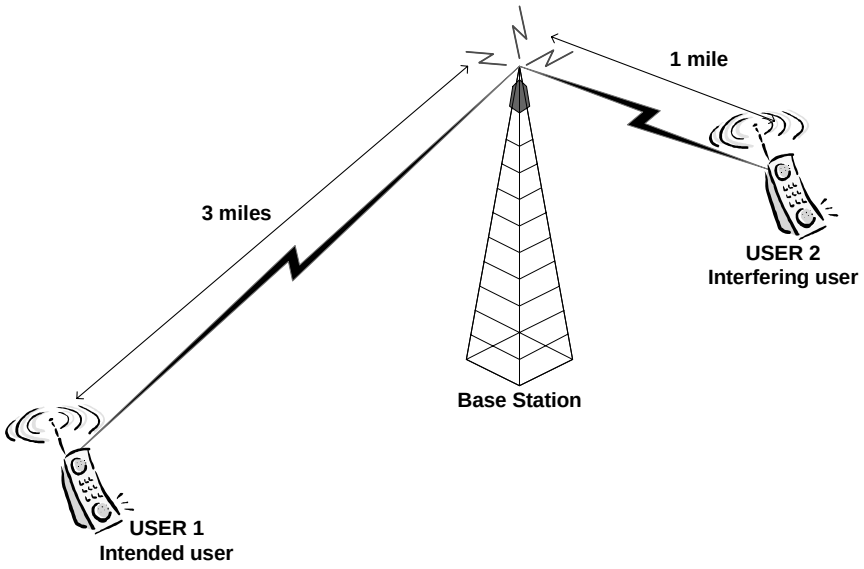

Figure 2.8: The near-far Effect Scenario.

To mitigate the near-far problem, power control is employed in the 2G CDMA systems, e.g. IS-95 system. Ideal power control ensures all users have identical signal power level when they arrive at the receiver.

2.7.2 The Decorrelator Detector

Although the conventional detector is easy and simple to implement, it suffers from the MAI and near-far problem which affect the performance of the detector. As discussed in the pervious section, the conventional detector has no information of multiple users which can be jointly used to better detect each individual user. Due to this lack of multiuser information, there has been great interest in enhancing DS-CDMA detection through the use of multiuser detectors.

Verdu shows in [33] that the optimal MU detection can be achieved by the maximum likelihood sequence detector that uses the Viterbi algorithm. The optimal detector shows

a huge performance and capacity enhancement over the conventional detector. However, its complexity grows exponentially with the number of active users. Due to this problem, the optimal detector is too complex for practical DS-CDMA systems. Therefore, most of the research has focused on finding suboptimal low complexity detectors solutions that are more feasible to implement.

The decorrelator detector is a linear multiuser detector where a linear transformation is applied to the soft output of the conventional detector in order to produce a new set of decisions with MAI completely decoupled. It offers many desirable features, such as: it yields an optimal value of near-far resistance performance and does not need to estimate the received signal amplitude.

We can define a cross-correlation matrix **R** as,

$$\mathbf{R} = \begin{bmatrix} \rho_{11} & \rho_{12} & \cdots & \rho_{1K} \\ \rho_{21} & \rho_{22} & \cdots & \rho_{2K} \\ \vdots & \vdots & \ddots & \vdots \\ \rho_{K1} & \rho_{K2} & \cdots & \rho_{KK} \end{bmatrix} \tag{2.21}$$

the matrix **R** has the following properties

- It is symmetric,
- The diagonal elements are equal to 1 (normalized),
- In general, the matrix is non-negative definite.

The receiver in case of DS-CDMA consists of a bank of matched filters.

Equation (2.17) can be set into a matrix form,

$$y_j = \mathbf{r}_j \mathbf{A}\mathbf{b} + n_j \tag{2.22}$$

where,

- $\mathbf{r}_j = [\rho_{j1}, \quad \rho_{j2}, \quad \cdots, \quad \rho_{jK}]$, the cross-correlation vector of the j^{th} user with all other users.
- $\mathbf{A} = diag(A_1, \quad \cdots, \quad A_K)$, the matrix of received signal amplitudes.
- $\mathbf{b} = [b_1, \quad \cdots, \quad b_K]^T$, the vector of the transmitted bits.

If the outputs of all users are considered, the above equation can be written as,

$$\begin{bmatrix} y_1 \\ y_2 \\ \vdots \\ y_K \end{bmatrix} = \begin{bmatrix} \rho_{11} & \rho_{12} & \cdots & \rho_{1K} \\ \rho_{21} & \rho_{22} & \cdots & \rho_{2K} \\ \vdots & \vdots & \ddots & \vdots \\ \rho_{K1} & \rho_{K2} & \cdots & \rho_{KK} \end{bmatrix} \begin{bmatrix} A_1 & 0 & \cdots & 0 \\ 0 & A_2 & \cdots & 0 \\ \vdots & \vdots & \ddots & \vdots \\ 0 & 0 & \cdots & A_K \end{bmatrix} \begin{bmatrix} b_1 \\ b_2 \\ \vdots \\ b_K \end{bmatrix} + \begin{bmatrix} n_1 \\ n_2 \\ \vdots \\ n_K \end{bmatrix} \tag{2.23}$$

In a compact matrix notation, the previous equation can be expressed as,

$$\mathbf{y} = \mathbf{RAb} + \mathbf{n} \tag{2.24}$$

The decorrelator detector (shown in Figure 2.9) applies the inverse of the correlation matrix **R,** that is $\mathbf{R}^{-1}$, to the output of the conventional detector in order to decouple the data. From (2.24), the soft estimate of this detector is:

$$\hat{\mathbf{b}} = \mathbf{R}^{-1}\mathbf{y} = \mathbf{Ab} + \mathbf{R}^{-1}\mathbf{n} \tag{2.25}$$

Thus, the decorrelator detector completely eliminates the MAI at the expense of noise enhancement at the output of decorrelator detector as it can be seen in (2.25).

Another disadvantage of the decorrelator detector is that the computations needed to compute the inverse of the matrix **R** are difficult to perform in real time, specially for asynchronous CDMA.

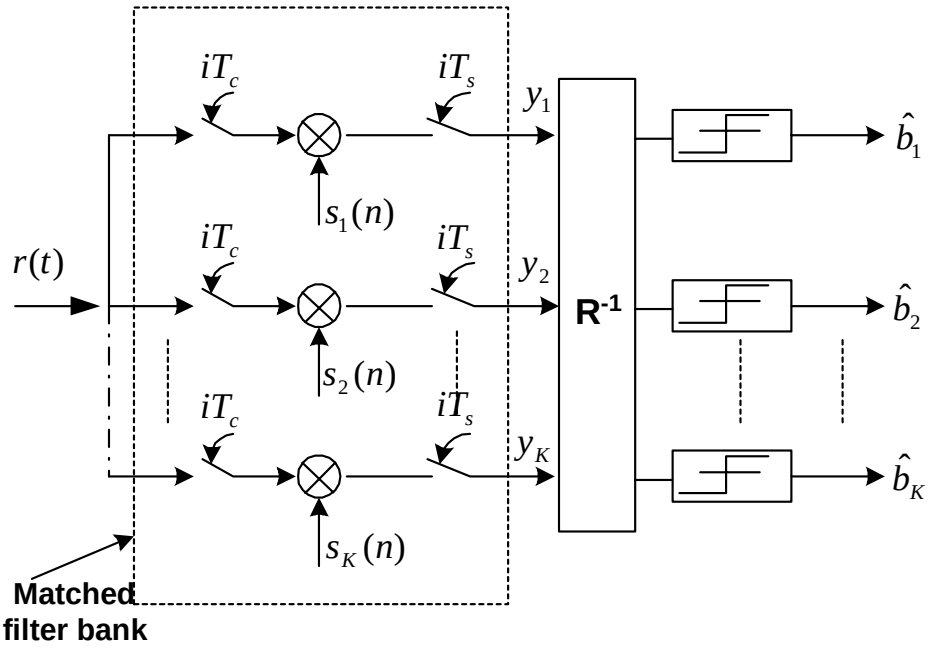

Figure 2.9: The Decorrelator Detector.

Chapter 3

The Mobile Radio Channel

3.1 Introduction

In a wireless mobile communication system, information transmission from a fixed station to one or more mobile stations is considerably influenced by the characteristics of radio channel. The mechanisms of fading channels were first modeled in the 1950s and 1960s. These models are quite useful in characterizing fading effects in mobile digital communications systems [34]. The purpose of this chapter is to give a brief description of multipath fading channels encountered in mobile radio communications.

3.2 Fading Channels

A channel is defined as the frequency band in the frequency domain, or its digital time slot equivalent in the time domain, established to provide a communication path between the transmitter and receiver. Also, a channel can be described as everything from source to the destination of a radio signal which may include the physical medium such as free space, fiber optics link or waveguide structure [35]. The term fading refers to the time-varying channel conditions such as amplitude [7]. When the transmitted signal

travels over multiple reflective paths, *multipath propagation* phenomenon rises. This is a common phenomenon in a wireless mobile communication system which can cause fluctuations in the received signal's amplitude, phase and angle of arrival giving rise to *multipath fading* [19][34]. The performance of mobile communication system is primarily affected by the dynamics of multipath fading [36].

Another factor influencing fading is the *Doppler Shift*. The time variations in the channel are evidenced as Doppler broadening and perhaps, in addition as a Doppler shift of a spectral line. Doppler spread is used to quantify the signal fading due to Doppler shift.

Fading in the cellular environment which results from multipath propagation of the transmitted signal can be divided in two types, *large-scale fading* and *small-scale fading*. ***Large-scale fading*** which represents the average signal power attenuation or path loss due to motion over large areas. On the other hand ***small-scale fading*** refers to the dramatic changes in signal amplitude and phase that can be experienced as a result of small changes in spatial separation between receiver and transmitter [19][34]. Small-scale fading also known as Rayleigh fading because if there are multiple reflective paths with no line-of-sight signal component, the envelope of the received signal is statistically described by Rayleigh probability density function (pdf) which is defined as [34]:

$$f_G(g) = \frac{g}{\sigma^2} e^{-g^2/2\sigma^2} \tag{3.1}$$

where $\sigma^2 = E[GG^*]$ is the variance of the Gaussian process. The phase pdf has a uniform distribution [7][19]:

$$f_\Theta(\theta) = \frac{1}{2\pi}, \quad 0 \leq \quad \theta \quad \leq 2\pi \tag{3.2}$$

When the received signal is made up of multiple reflective signals as well as a significant non-fading line-of-sight component, the envelope of the received signal is no more statistically described by Rayleigh pdf. Instead, the small-scale fading envelope is described by a Rician pdf [7][19][34].

Propagation in free space is the ideal case. However, when propagation takes place close to obstacles, the following propagation mechanisms occur [19]:

a) ***Reflection –*** Occurs when a radio wave strikes an object with dimensions that are large relative to its wavelength, i.e., buildings.

b) ***Diffraction*** – Occurs when a radio wave is obstructed by surfaces with sharp irregularities and with large dimensions relative to its wavelength. Secondary waves arise from the obstructing surface and give rise to the bending of waves around and behind obstacles.

c) ***Scattering –*** Occurs when a radio wave travels through a medium containing lots of small objects compared to wavelength.

3.3 Types of Fading

The type of fading experienced by signal propagation through a mobile radio channel depends on the nature of the transmitted signal (such as bandwidth and symbol duration) with respect to the characteristics of the channel (delay and Doppler spreads). While multipath delay spread leads to time dispersion and frequency selective fading, Doppler spread leads to frequency and time selective fading [19].

The received signal will undergo ***flat fading***, If a mobile radio channel has a constant gain and linear a phase response over a bandwidth which is greater than the bandwidth of the transmitted signal [19].

If the spectrum of the transmitted signal has a bandwidth which is greater than the *coherence bandwidth* B_c of the channel, then the received signal will undergo ***frequency selective fading***. The coherence bandwidth is a statistical measure of the range of frequencies over which the channel can be considered flat.

In a ***fast fading*** channel, the channel impulse response changes rapidly within the symbol duration. That is, the coherence time *Tc* of the channel is smaller than the symbol period *Ts* of the transmitted signal. The coherence time is the time domain dual of the Doppler spread and is used to characterize the time-varying nature of the frequency dispersiveness of the channel in the time domain.

On the other hand, the channel impulse response in a ***slow fading*** channel changes at a rate much slower than the transmitted baseband signal i.e. $Ts << Tc$.

3.4 Modeling of Fading Channels

With the advent of statistical communication theory in 1950's the research in the characterization and modeling of fading channels gained considerable attention. Over many years, a large number and a wide range of experiments were carried out to investigate the fading channels. Earlier work in this area includes the contribution form Bello [37], Jakes [38] and Clark [39].

Jakes developed a model of fading channel which accommodates the Doppler spread. He also presented a realization for the simulation of the fading channel model. His simulator has been widely used and extensively studied over the past three decades. Recently, Pop and Beaulieu [40] have highlighted few shortcomings in the Jakes model. They came up with a modified Jakes simulator.

3.4.1 Discrete-Time Channel Model

Assuming low-pass equivalent model for the channel, the received signal $r(t)$ over a fading multipath channel can be represented by:

$$r(t) = \int_{-\infty}^{\infty} h(\tau, t)x(t-\tau)d\tau \tag{3.3}$$

where $x(t)$ is the transmitted signal and $h(\tau, t)$ is the time-varying channel impulse response at delay τ and time instant t. In discrete form Equation (3.3) can be written as:

$$r(n) = \sum_{i=-\infty}^{\infty} h(iT_c, n)x(n-iT_c) \tag{3.4}$$

where T_c is the chip duration and n represents the sampling index. Defining a compact notation for the time varying channel coefficients in the form $h_i(n) = h(iT_c,n)$, Equation (3.4) can be written as:

$$r(n) = \sum_{-\infty}^{\infty} h_i(n)x(n-iT_c) \tag{3.5}$$

The form of the received signal in Equation (3.5) suggests that the impulse response of fading multipath channel can be modeled as a tapped delay line filter (shown in Figure 3.1) , modeled as a finite impulse response (FIR) filter, with tap spacing T_c and time varying tap coefficients $h_i(n)$. For all practical purposes one can use truncated tapped delay line filter with $L = \frac{T_m}{T_c} + 1$ taps, where T_m is the multipath spread and T_c is the chip rate [7], i.e.:

$$r(n) = \sum_{i=1}^{L} h_i(n)x(n-iT_c) \tag{3.6}$$

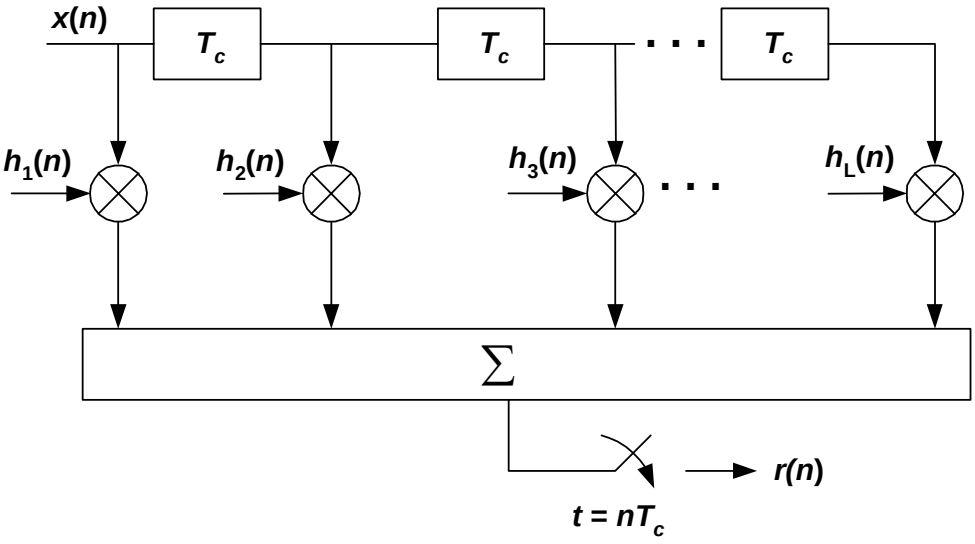

Figure 3.1: Tapped delay line model of fading channel.

The time varying complex coefficients $h_i(n)$ are characterized as random processes because of the constantly changing physical characteristics of the media. The tap weights, $h_l(n)$, in Figure 3.2 can be expressed as:

$$h_l(n) = \sqrt{\rho_l}\, G_l(n) \tag{3.7}$$

where ρ_l is the strength of the lth path and $G_l(n)$ is the complex stochastic process specified by its mean square value and power spectrum density.

3.4.2 Simulation Model of Fading Channel

As mentioned earlier (Section 3.4.1) a fading channel can be represented by a tapped delay line FIR filter with tap weights as given by (3.7). This section describes the method that will be used to simulate the channel.

Jakes [38] presented a realization for the simulation of the fading channel model which generates real and imaginary parts of the channel tap coefficients as weighted sum

of sinusoids. Jakes simulator has been widely used and extensively studied intermittently the past three decades [64]. Recently, Pop and Beaulieu [40] have highlighted few shortcomings in the Jakes model. They proposed to include a random phase in the low frequency oscillators of the Jakes model. In this thesis, we have used this modified semi-deterministic Jakes model as fading channel simulator.

The real and the imaginary components of the channel tap are generated by [38]:

$$\begin{aligned} g_I(t) &= 2\sum_{n=1}^{N_o} \cos\beta_n \cos(\omega_n t + \varphi_n) + \sqrt{2}\cos\alpha\cos\omega_m t \\ g_Q(t) &= 2\sum_{n=1}^{N_o} \sin\beta_n \cos(\omega_n t + \varphi_n) + \sqrt{2}\sin\alpha\cos\omega_m t \end{aligned} \tag{3.8}$$

where β_n, ω_n and N_o are defined, respectively, as:

$$\beta_n = \frac{n\pi}{N_o + 1}, \quad \omega_n = \omega_m \cos\left(\frac{2\pi n}{N}\right), \quad N_o = \frac{1}{2}\left(\frac{N}{2} - 1\right) \tag{3.9}$$

$t = kT_s$ and $\varphi_1, ..., \varphi_{N_o}$ are uniformly distributed random variables over $[0, 2\pi]$ and α is the angle of arrival. For multipath uncorrelated scattering, I used the technique proposed by Jakes [38] whose correct version is available in [64]. In this technique, the nth oscillator is given an additional phase shift $\gamma_{nl} + \beta_n$ with gains as before. For lth path the in-phase and quadrature components of the fading can be written as:

$$\begin{aligned} g_l^I(t) &= 2\sum_{n=1}^{N_o} \cos\beta_n \cos(\omega_n t + \theta_{nl} + \varphi_n) + \sqrt{2}\cos\alpha\cos\omega_m t \\ g_l^Q(t) &= 2\sum_{n=1}^{N_o} \sin\beta_n \cos(\omega_n t + \theta_{nl} + \varphi_n) + \sqrt{2}\sin\alpha\cos\omega_m t \end{aligned} \tag{3.10}$$

$$\theta_{nl} = \gamma_{nl} + \beta_n, \quad \beta_n = \frac{n\pi}{N_o + 1}, \quad \gamma_{nl} = \frac{2\pi(l-1)n}{N_o + 1} \tag{3.11}$$

The normalized complex channel tap for lth path is:

$$G_l(t) = g_l^I(t) + jg_l^Q(t) \tag{3.12}$$

which will be normalized such that $E[G_l G^*_l] = 1$. Thus, the complete channel tap for the model shown in Figure 3.2 can be obtained by combining Equations (3.7), (3.10) and (3.12).

3.5 Fading Statistics

Fading describes the rapid fluctuation of the amplitude of radio signal when passing through radio channels over a short period of time or travel distance. The complex stochastic process $G_l(n)$ in (3.7) represents the fading and can be completely characterized by specifying the pdf of its amplitude and phase. The simplest process that can exhibit both time-selective and frequency-selective fading is *wide-sense stationary uncorrelated scattering* (WSSUS) process introduced by Bello [37]. The number of uncorrelated paths is sufficiently large so that the quadrature components of the fading process are Gaussian distributed according to the central limit theorem. The Gaussian WSSUS model fits well to land mobile radio channels and have been specified in the ITU's test environment [43]. It was mentioned earlier that in the absence of direct path, the Gaussian process has zero mean and the pdf of the envelope is Rayleigh and the phase is uniform given by Equations (3.1) and (3.2), respectively.

A typical and often-assumed shape for the power spectral density, also known as Doppler Spectrum, of the fading process for mobile radio channels is given by Jakes' Spectrum [38][39][40]:

$$S(f) = \begin{cases} \dfrac{\sigma^2}{\pi f_m \sqrt{1-(f/f_m)^2}}, & |f| \le f_m \\ 0, & elswhere \end{cases} \tag{3.14}$$

where f_m is the maximum Doppler frequency shift given by:

$$f_m = \frac{v f_c}{C} \tag{3.15}$$

in which v, f_c and C are the vehicle speed, frequency of the carrier and speed of light respectively. The autocorrelation function of the fading process is given by [20][38][39]:

$$R(\tau) = \sigma^2 I_0(2\pi f_m \tau) \tag{3.16}$$

where $I_0(.)$ is the zeroth order Bessel function of the first kind.

3.6 Types of Channel Used in Simulation

In this thesis, four channels were used in the simulations. One channel is static channel and the others are frequency selective Rayleigh fading channel with 3 paths.

3.6.1 Channel 1, Static Channel

The static channel has a power delay profile equivalent to the raised cosine function given by:

$$h(n) = \begin{cases} \frac{1}{2}(1 + \cos(\frac{2\pi}{s}(n-2))), & \text{n} = 1,2,3 \\ 0, & otherwise \end{cases} \tag{3.17}$$

where s controls the eigenvalue spread $\chi(\mathbf{R})$ of the correlation matrix of the input vector to the receiver. In our case s = 3.5, which corresponds to $\chi(\mathbf{R})$ = 46.8216, was used.

3.6.2 Rayleigh Fading channel

A. Channel 1; ***Pedestrian channel***: This channel is Pedestrian channel with 3 independent slowly fading paths and Doppler frequency equal to 10Hz. This frequency corresponds to a speed of 5km/h assuming a carrier frequency of 2.2GHz. The power delay profile is given in Table 3.1. The term “CLASSIC” for Doppler spectrum refers to

Jakes' Spectrum and the fading statistics are assumed to be Rayleigh. The pdf distributions of the three paths are presented in Figures 3.2-3.4.

Tap	Relative Delay [ns]	Average Power [dB]	Doppler Spectrum
1	0	0	CLASSIC
2	260.4	-12.77	CLASSIC
3	512.8	-25.48	CLASSIC

Table 3.1: Pedestrian Test Environment Tapped delay line parameters [43]

B. Channel 2; Vehicular Channel 1: This channel has the same power delay profile of Channel 1 but each path has different Doppler frequency. The 1st, 2nd and 3rd paths have Doppler frequency of 100Hz, 66Hz and 33 Hz, respectively. The pervious Doppler frequencies correspond to a speed of 49.1km/h, 32.4km/h and 16.2km/h, respectively.

C. Channel 3; Vehicular Channel 2: This channel is the same as the previous channel but the Doppler frequency of each path had been increased. The 1st, 2nd and 3rd paths have Doppler frequency of 135Hz, 90Hz and 45 Hz, respectively. The pervious Doppler frequencies correspond to a speed of 66.3km/h, 44.2km/h and 22.1km/h, respectively. The pdf distributions of the three paths are presented in Figures 3.5-3.7.

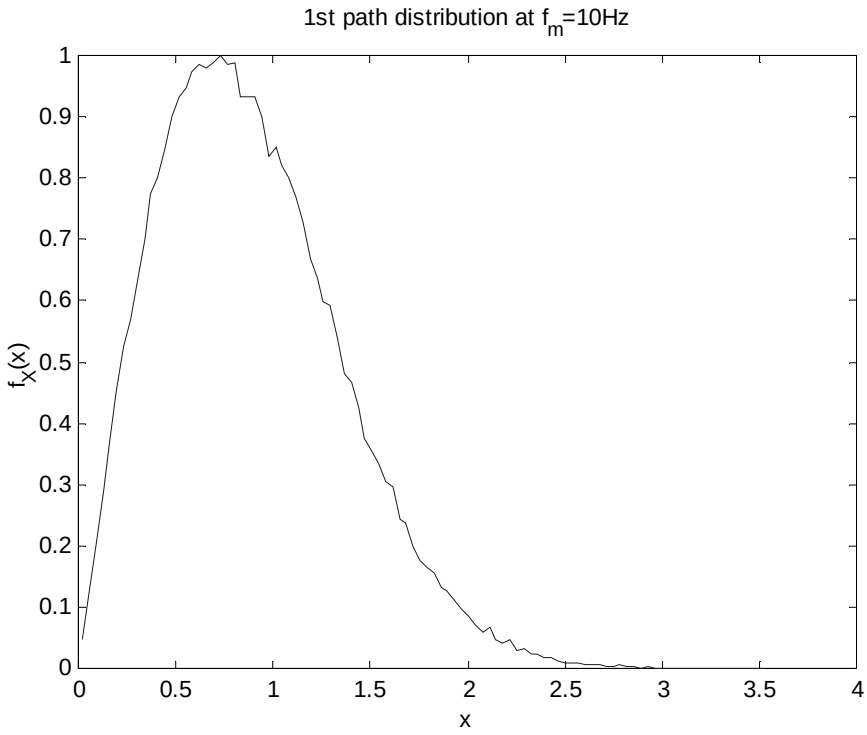

Figure 3.2: The pdf distribution of the first path; Channel 1

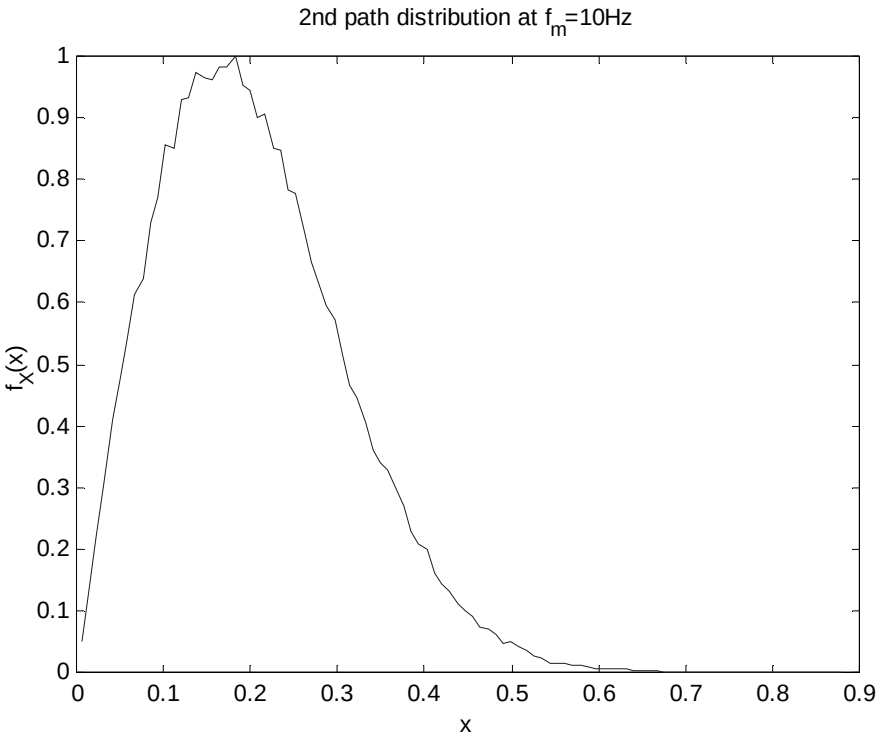

Figure 3.3: The pdf distribution of the second path; Channel 1

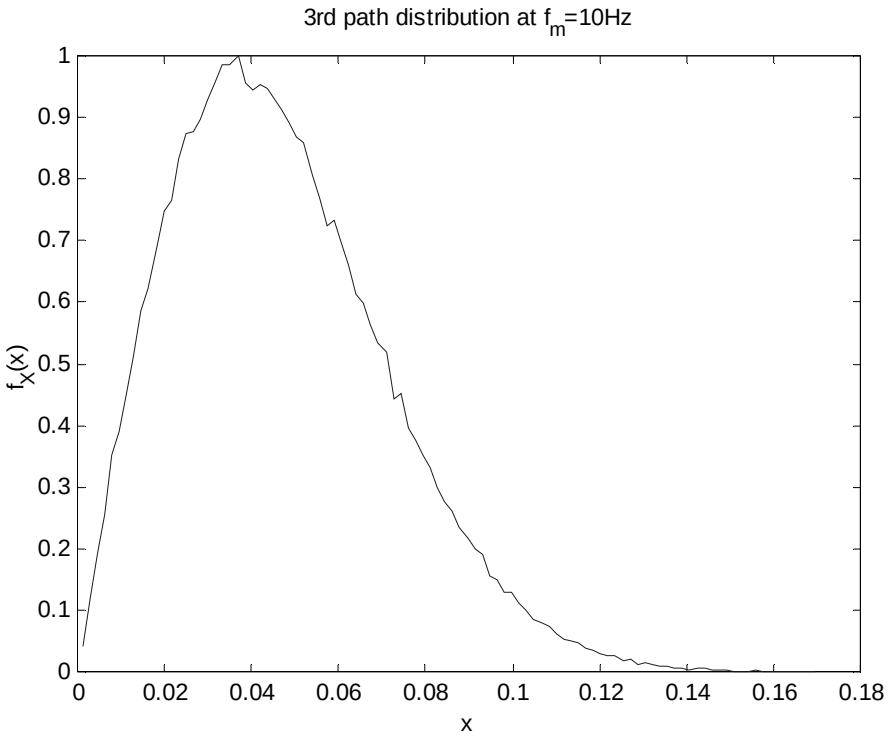

Figure 3.4: The pdf distribution of the third first path; Channel 1

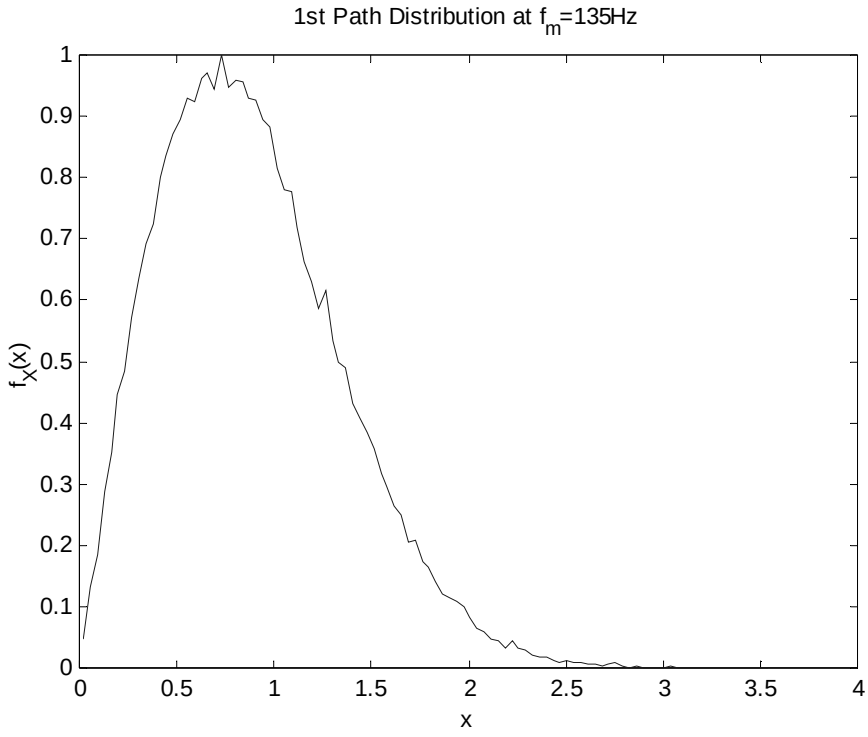

Figure 3.5: The pdf distribution of the first path; Channel 3

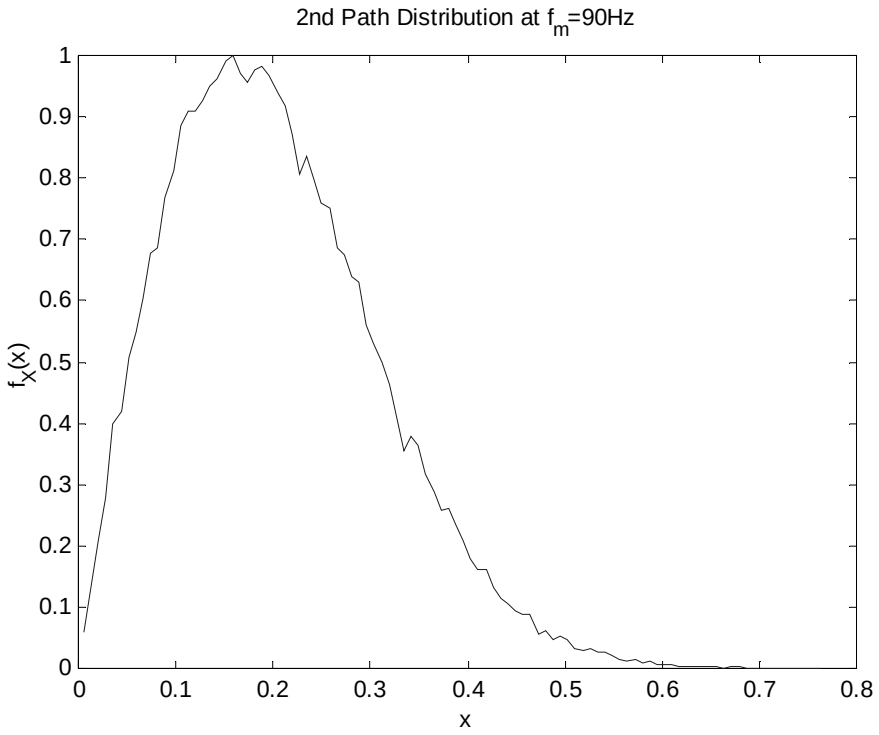

Figure 3.6: The pdf distribution of the second path; Channel 3

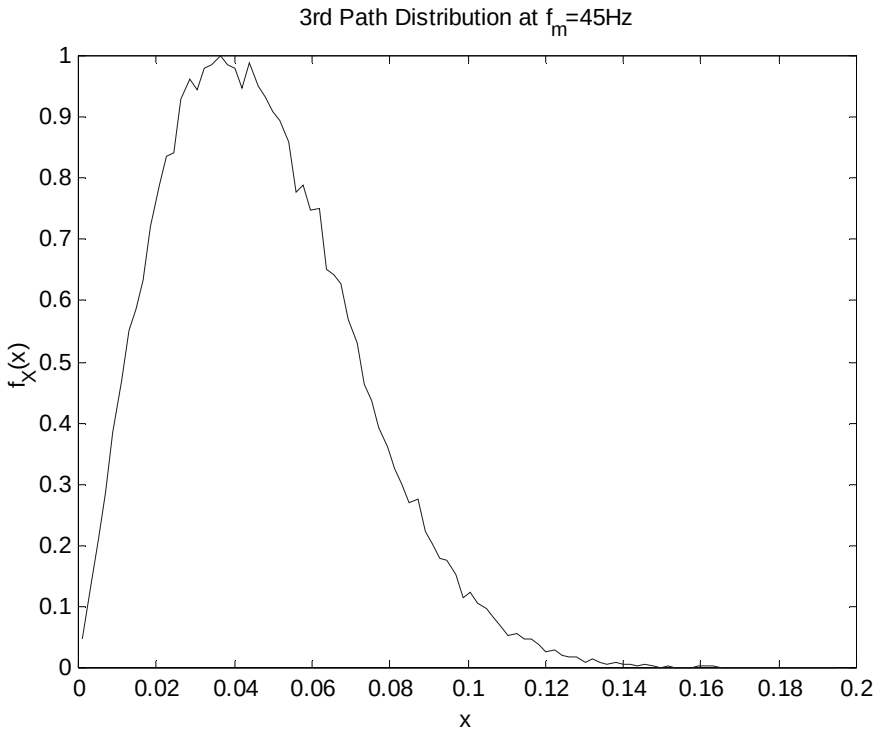

Figure 3.7: The pdf distribution of the third path; Channel 3

Chapter 4

Adaptive Equalization

4.1 Introduction

Adaptive filtering plays an important role in the field of communication systems where early adaptive engineering systems have been designed in this area. The concept of adaptive filtering constitutes an important part of the statistical signal processing. When the filter is linear and all the pertinent statistics are known, the solution can be obtained from the Wiener filter [44], which is optimum in the mean-square sense. However, when there is a requirement to process signals that result from an unknown statistics of an environment, the use of an adaptive filter gives an attractive solution to the problem.

Adaptive filters are generally defined as filters whose characteristics can be modified to achieve desired objectives and accomplish this modification or adaptation automatically without user involvement. Recursive algorithms which adaptive filters rely on make it possible for the filter to perform suitably in an environment where complete knowledge of the relevant signal characteristics is not available. In telecommunication systems, adaptive filters proved to be extremely effective in achieving high efficiency, high quality and high reliability. Thus, adaptive filters are successfully applied in such

diverse fields as equalization [6], noise cancellation [45], linear prediction [46] and in system identification [44][47].

In this chapter, we will discuss briefly the subject of adaptive equalization. The next section describes the Intersymbol Interference (ISI) mathematically and *Nyquist Criterion* for Zero ISI. After that, adaptive equalization and its use in communication systems is discussed followed by a brief overview on some adaptive algorithms.

4.2 Intersymbol Interference

In simple terms, Intersymbol Interference (ISI) can be defined as a distortion caused as a result of overlapping of the received symbols [6]. This phenomenon arises in all digital pulse modulation systems and in which the channel is bandlimited and dispersive, such as cable lines [48][49]. Another example where ISI can occur is in mobile communications due to multipath propagation in which there are many propagation paths from transmitter to the receiver. The incoming radio waves reach the destination from several directions with different amplitude and time delays.

For a bandlimited non-distorting channel, the amplitude response should be constant and the phase should be linear [7]. Figure 4.1 shows the characteristics of a bandlimited channel.

4.2.1 Mathematical Representation of ISI

To represent ISI mathematically assuming the following:

x(t) is the input signal,*r(t)* is the received signal, *h(t)* is the channel impulse response and *z(t)* is Additive White Gaussian Noise (AWGN).

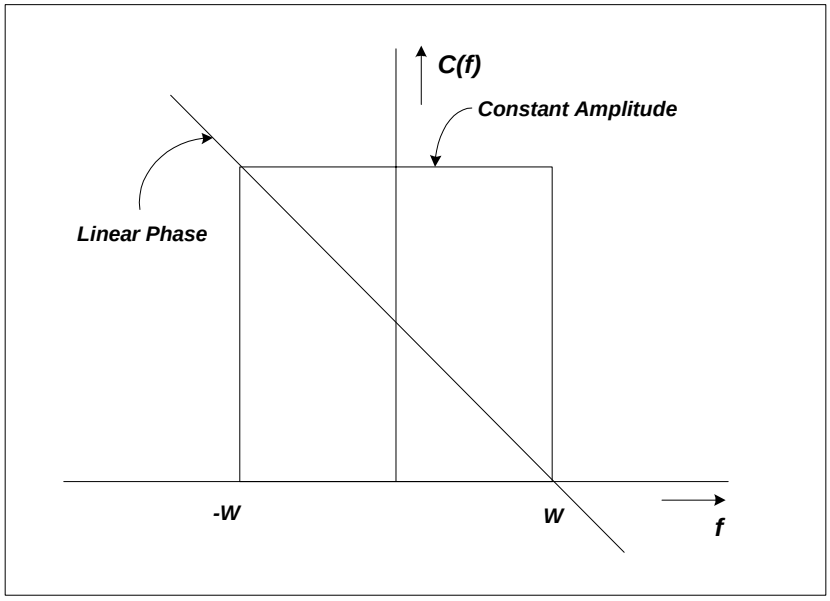

Figure 4.1: Characteristics of a Bandlimited Channel

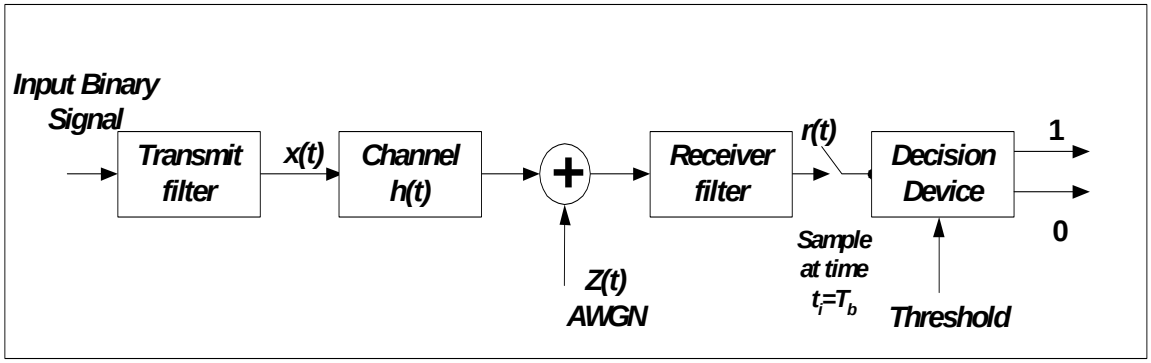

Figure 4.2: Communication System.

In the communication system shown in Figure 4.2, the received signal is given by the following equation:

$$r(t) = \int_{-\infty}^{+\infty} h(\tau)x(t-\tau)d\tau + z(t) \tag{4.1}$$

The component *x(t)* is the input pulse train which consists of periodically transmitted impulses of varying amplitudes. This means,

$$\begin{cases} x(t) = 0 \quad for \quad t \neq kT \\ \\ x(t) = x_k \quad for \quad t = kT \end{cases} \tag{4.2}$$

where *T* is the symbol period. Equation (4.2) implies that the only significant values of the variable of (4.1) are those for which $\tau = kT$. The other values of τ are multiplied by zero. Therefore, (4.1) can be written as

$$r(t) = \sum_{k=-\infty}^{\infty} x_k h(t-kT) + z(t) \tag{4.3}$$

Now, the received signal should be sampled at the symbol transmit rate. This can be represented mathematically by replacing t with nT, where T is the symbol transmit rate:

$$r(nT) = \sum_{k=-\infty}^{\infty} x_k h(nT-kT) + z(nT) \tag{4.4}$$

or

$$r_n = \sum_{k=-\infty}^{\infty} x_k h_{n-k} + z_n \tag{4.5}$$

which can also be written as

$$r_n = x_n + \sum_{\substack{k=-\infty \\ k\neq n}}^{\infty} x_k h_{n-k} + z_n \tag{4.6}$$

where h_0 is equal to 1.

The first term on the RHS of the above equation represents the desired information symbol at the n^{th} sampling instant. The ISI is represented by the second term and the last term is the AWGN term.

4.2.2 Nyquist Criterion for Zero ISI

In order to get zero ISI at the sampling rate, the second term of Equation (4.6) should satisfy the following condition:

$$h(kT) = \begin{cases} 1 & k = 0 \\ 0 & k \neq 0 \end{cases} \tag{4.7}$$

Equation (4.7) simply means that there are zero crossing at the sampling instants and the ISI is zero at that instant, that is $h(kT)=0$ for $k \neq 0$. This criterion is known as Nyquist condition for zero ISI. Therfore, it is possible to shape the transmitted pulses in a way such that the effects of ISI on the received signal is minimized.

In frequency domain, Equation (4.7) can be represented as follow:

$$\sum_{m=-\infty}^{\infty} H(f + m/T) = T \tag{4.8}$$

Now, if the channel bandwidth is W and the channel response is zero for $|f| > W$, this will lead $H(f) = 0$ for $|f| > W$**.** There are two possible cases in which zero ISI can be satisfied.

1. The sampling rate is twice the bandwidth (*1/T=2W)*. In this case only one possibility exists such that Equation (4.8) is met. This leads to the following pulse:

$$h(t) = \frac{\sin(\pi t / T)}{\pi t / T} \tag{4.9}$$

The problem with the pulse in Equation (4.9) is that *h(t)* is non-causal and therefore can not be used unless a delay is introduced between the input time and the output response. A second problem is the slow decay of the pulse tails (1/t) [7].

2. The sampling rate is grater than twice the bandwidth (*1/T>2W*). This case leads to very well known pulse called the raised cosine spectrum and it overcomes the disadvantages of the previous pulse (case 1). The raised cosine pulse is represented by the following mathematical expression:

$$h(t) = \frac{\sin(\pi t / T)}{\pi t / T} \frac{\cos((\pi \beta t / T))}{1-(2\beta t / T)^2} \qquad (4.10)$$

where β is the rolloff factor. Figure 4.3 shows the pulse shape of the two cases.

The presence of ISI in the received signal limits the digital transmission rate. Therefore, there should be a way by which the impacts of ISI as well as the channel distortion are eliminated substantially. The effect of ISI is removed by channel equalization, which will be the next topic of our discussion.

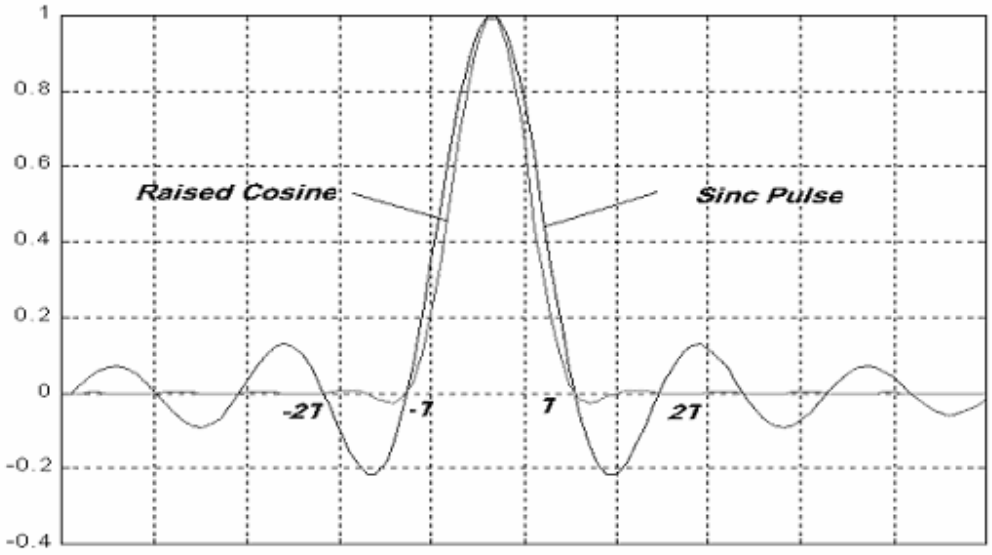

Figure 4.3: The Sinc Pulse & the Raised Cosine Pulse.

4.3 Adaptive Equalization

Actual implementations of adaptive equalizers were realized in 1965 by Bell Laboratories [50]. In this application, the adaptive filter is used to provide an inverse model that represents the best fit to the unknown system. Thus, at convergence, the inverse of the transfer function of the unknown system is approximated by the adaptive filter. The primary objective of adaptive equalization is for reducing the effect of ISI in digital receivers. This is achieved through the use of channel equalization for digital communications [6].

In wireless communication systems, an equalizer is helpful in reducing the effect of multipath time-varying radio channel and ISI. Also it is useful in estimating the channel characteristics and parameters that are not known in advance and in which they may change from time to time, specially in wireless communications [7][48]. Hence, it is important to keep track the channel characteristics. To do such a tracking, an equalizer uses an adaptive algorithm to update its tap gains such that the Mean Squared Error (MSE) is minimized. Three of the most well known algorithms are Least Mean Square (LMS), Discrete Cosine Transform LMS (DCT-LMS) and Recursive Least Square (RLS) [44].

Before going to adaptive algorithms, let's take a look to the adaptive equalizer presented in Figure 4.4. The following symbols are used in the analysis:

$x(n)$ is the transmitted signal,

$x'(n)$ is the estimated transmitted signal such that $x'(n) \cong x(n)$,

$r(n)$ is the received signal,

$y_{eq}(n)$ is the output of the equalizer, and $e(n)$ is the error signal.

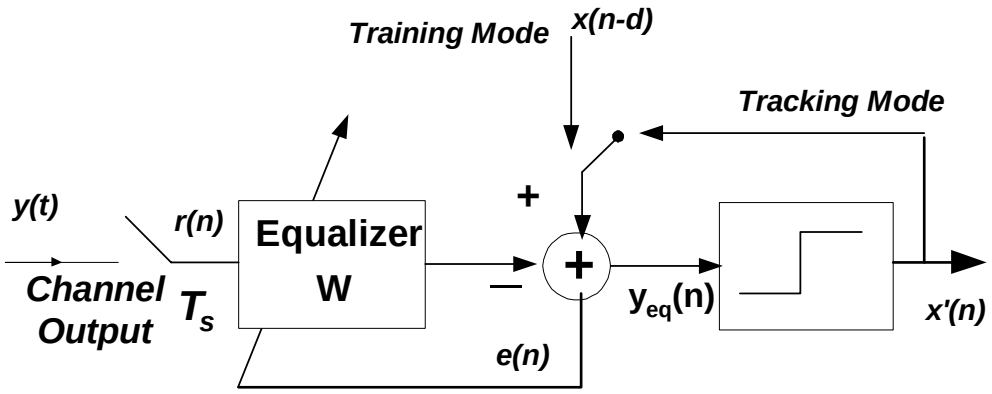

Figure 4.4: Adaptive equalization.

The output of the equalizer can be written as follow:

$$y_{eq}(n) = \sum_{i=0}^{N-1} w_i(n) r(n-i) \tag{4.11}$$

where $\{w_i , i=0,1,2,\ldots,N-1\}$ are the N tap gains of the linear transversal equalizer with N taps. The decision device will give the following:

$$x'(n-d) = \text{sgn}[y_{eq}(n-d)] \tag{4.12}$$

where d represents delay and sgn[ ] is the sign function. The purpose of Equation (4.12) is to satisfy the following criterion:

$$x'(n-d) \equiv x(n-d) \tag{4.13}$$

In a time-varying environment, it is difficult to find a fixed equalizer so that the channel meets Nyquist criterion because the channel characteristics change. Therefore, the adaptive equalizer works in two different modes in order to track the channel variations. These two modes are the training mode and tracking mode (decision direction mode). In the training mode, the adaptive equalizer uses a known signal (training sequence) to update the equalizer tap gains and identifies as closely as possible the channel characteristics. Therefore, the equalizer changes to tracking mode and the

receiver uses the converged weights which are no longer updated if the channel is static; otherwise, they should be updated continuously in order to track the channel changes. The main disadvantage of the training mode in the case of time-varying channel is the waste of bandwidth [48]. In Figure 4.5, a scenario for training and tracking modes is presented in which two consecutive frames of date are transmitted. Each frame consists of 100 symbols. The first 20 symbols (known sequence) are used in the training mode to update the tap gains. Now, if the channel is stationary, the remaining symbols of the frame will be the data and the tap gains will no be longer updated. On the other hand, if the channel is not stationary, the process is repeated every frame.

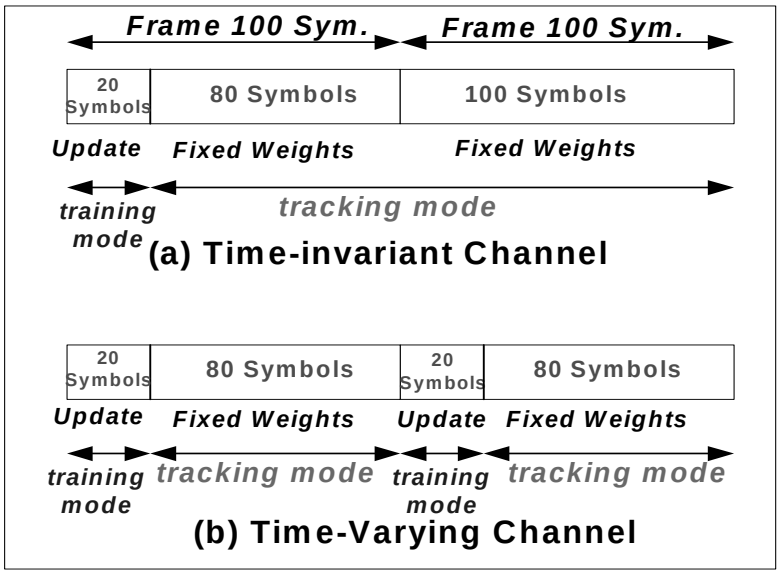

Figure 4.5: Two Consecutive Frames (a) Stationary Channel
(b) Time-Varying Channel

4.4 Adaptive Algorithms

In this section, one of the most widely used adaptive algorithms which is used to update the tap gain coefficients will be discussed. This algorithm is the Least Mean Squares (LMS) algorithm [44][51].

The Recursive Least Squares (RLS) is another well known adaptive algorithm which updates the inverse of the $N \times N$ covariance matrix (N is the length of the filter), therefore, its computational complexity amounts to $O(N^2)$ operations. To reduce the computational complexity of the RLS algorithms, some fast versions of the RLS (FRLS) algorithms have been developed, such as the Fast Kalman [52], which reduces the order of the complexity to $O(N)$. Practical use of the fast RLS algorithms in real time applications has been prevented because of its divergence due to numerical error accumulation in the prediction parameters.

4.4.1 Least Mean-Square (LMS) Algorithm

The LMS algorithm was presented by Widrow and Hoff in 1960 [6]. The LMS algorithm is used in the equalization process so that the equalizer coefficients are obtained to minimize the MSE.

Using the procedure used to obtain the LMS algorithm [49], we can start from Equation (4.11). The error, as it can be seen from Figure 4.4, can be computed as follow:

1) In the training mode, the error is the difference between the training sequence (transmitted) and the output of the equalizer.

$$e(n) = x(n-d) - y_{eq}(n) \tag{4.13}$$

2) In the decision direct mode, the error is the difference between the estimated transmitted sequence and the output of the equalizer.

$$e(n) = x'(n) - y_{eq}(n) \tag{4.14}$$

In our analysis, we will consider (4.14).

Now, our aim is to achieve the MSE criterion, which is the minimization of the output mean square error and is defined as:

$$J(n) = \mathrm{E}[e(n)^2] \tag{4.16}$$

where $\mathrm{E}[\ ]$ is the statistical expectation. By using Equations (4.11), (4.14) and (4.16) the gradient of the MSE *J(n)* with respect to the k^{th} tap weights w_k

$$\begin{aligned} \frac{\partial J(n)}{\partial w_k} &= 2\mathrm{E}\left[e(n) \frac{\partial e(n)}{\partial w_k} \right] \\ &= -2\mathrm{E}\left[e(n) \frac{\partial y_{eq}(n)}{\partial w_k} \right] \\ &= -2\mathrm{E}[e(n) r(n-k)] \end{aligned} \tag{4.17}$$

The expectation E[*e(n) r(n-k*)] is the cross-correlation between the error signal *e(n*) and the input signal *r(n)* for a lag of *k* samples. Therefore,

$$R_{er}(k) = \mathrm{E}[e(n) r(n-k)] \tag{4.18}$$

Now, to have a minimum MSE, the following optimum condition should be satisfied:

$$\begin{aligned} &\frac{\partial J(n)}{\partial w_k} \approx 0 \\ &or \qquad , \quad \text{for } k = 0, 1, 2, \ldots, N\text{-}1 \\ &R_{er}(k) \approx 0 \end{aligned} \tag{4.19}$$

The result in Equation (4.19) is known as the principle of orthogonality [49].

The MSE performance can be visualized as a parabolic surface like bowl shape. The surface is a function of the tap weights. The process of adjusting these taps is like seeking the bottom of the bowl where the MSE attains its minimum value. This is the basic idea of the steepest decent algorithm [49] which can be described mathematically by the following recursive formula:

$$w_k(n+1) = w_k(n) - \frac{1}{2}\mu \frac{\partial J(n)}{\partial w_k}, \text{ for } k = 0, 1, 2, \ldots, N\text{-}1 \tag{4.20}$$

where μ is a small positive constant called the step-size parameter.

Since the use of steepest decent algorithm requires exact knowledge of the cross-correlation function $R_{er}(k)$, and as this parameter is not available, we can use instead the instantaneous estimate for $R_{er}(k)$. The following estimate may be used [49]:

$$\hat{R}_{er}(k) = e(n)r(n-k), \text{ for } k = 0, 1, 2, \ldots, N\text{-}1 \tag{4.21}$$

Using equations (4.18), (4.20) and (4. 21) we get the following recursive formula for updating the tap weights of the equalizer:

$$w_k(n+1) = w_k(n) + \mu e(n)r(n-k), \text{ for } k = 0, 1, 2, \ldots, N\text{-}1 \tag{4.22}$$

This algorithm is known as the least mean-square (LMS) algorithm where $w_k(n+1)$ is the current value of the k^{th} tap weights, $w_k(n)$ is the previous value of the k^{th} tap weights and $\mu e(n)r(n-k)$ is the correction applied to compute the updated value (current value $w_k(n+1)$).

4.4.2 Convergence of LMS Algorithm

The convergence of the tap weights using the LMS algorithm depends on the value of the step size parameter μ. For large value of μ the tracking capability of the equalizer will

be high [6][48][53]. Practically, the value of the step size is chosen for fast convergence during the training mode and then reduced for fine tuning during the decision directed mode [6].

For stable adaptation, the following limit on μ is applicable [7][53]:

$$0 < \mu < \frac{2}{\lambda_{\max}} \tag{4.23}$$

where $\lambda_{\max}$ is the maximum eigenvalue of the autocorrelation of *r(n)*.

Now, the LMS algorithm can be summarized as follows:

1. Initialize the algorithm by setting the tap weights of the equalizer to zero at *n=1*, that is $w_k(1)=0$ for all *k*.
2. For n=1, 2, …, compute the results of Equations (4.11), (4.14) or (4.15) and (4.22).
3. Continue the computation until the tap weights converge.

Figure 4.6 shows the signal flow graph representation of the LMS algorithm.

The LMS algorithm is simple to use, involves few computations per iteration and allows tracking of a varying channel. However, the main disadvantage of this algorithm is its low adaptation rate [6][48][49]. Although, a large step size μ can result in a faster convergence, it may cause oscillation of the coefficients around the optimum set of values corresponding to the minimum point on an error surface.

To improve the performance of the LMS one can use a time varying step size in the standard LMS [54][55]. This is based on using large step size when the algorithm is far from the optimal solution, thus speeding up the convergence rate, and when the algorithm is near the optimum, small step size is used to achieve a low level of miss- adjustment, thus achieving a better overall performance.

4.4.3 The Normalized LMS Algorithm

The LMS algorithm provides a solution to the optimal Weiner Filter criterion minimizing the mean square value of the error in a stochastic approximation sense. The LMS algorithm belongs to the gradient type algorithmic schemes, thus inheriting their low computational complexity i.e. $O(N)$ operations, and their slow convergence, especially on highly correlated signals like speech. Therefore, the LMS algorithm performs badly with correlated input signals due to the direct dependency of the algorithm on the input vector $r(n)$. When the eigenvalue spread of $r(n)$ is large, LMS algorithm experiences a gradient noise amplification. In order to overcome this problem, the input signal is normalized by the input signal power. Thus, the filter coefficients are adapted according to the following recursion [56]:

$$w_k(n+1) = w_k(n) + \mu \frac{e(n)r(n-k)}{\|r(n)\|^2}, \text{ for } k = 0, 1, 2, \ldots, N\text{-}1 \qquad (4.24)$$

This algorithm is known as normalized LMS (NLMS) algorithm. Due to normalization, the NLMS algorithm is made to have more stable behavior for a known step size range ($0 < \mu < 2$), less sensitive to colored input signal (as the effect of the eigenvalue spread of the input vector is reduced), and converges faster than the LMS algorithm [57].

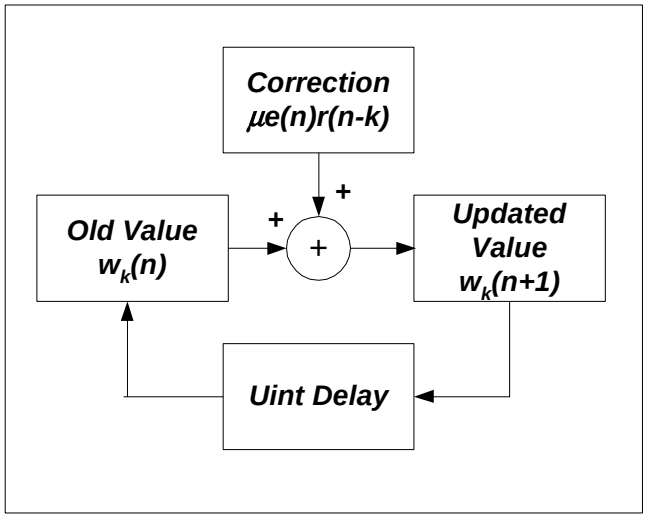

Figure 4.6: Signal-flow graph representation of the LMS algorithm

Chapter 5

Adaptive Decision Feedback Equalizer with Error Feedback for Multiuser Detection in Synchronous CDMA

5.1 Introduction

Wireless cellular telephony has been growing at a faster rate than wired-line telephone networks [19]. This growth is a result of the recent improvements in the capacity of wireless links due to the use of multiple access techniques, which allow many users to share the same channel for transmission, in association with advanced signal processing algorithms. Code Division Multiple Access (CDMA) has become the technology of choice for cellular communications [20]. In CDMA-Spread Spectrum (SS) systems users are assigned different spreading codes, also called pseudo-noise (PN) sequences, to spread their signals, prior to transmission, over a bandwidth much wider than the information bandwidth.

To accomplish signal spreading, Direct Sequence (DS)-SS technique is used in which the transmitted data stream is multiplied by a higher rate PN code to spread the information's energy over a wider bandwidth [1]. Already, Chapter 2 of this thesis has detailed this subject.

There has been substantial interest in DS-CDMA technology in recent years because of its many attractive properties for wireless communications [5]. However, the measure of MAI in CDMA places a limit on the system performance and capacity. MAI is caused by the cross-correlation between PN codes of active users. In the 2nd generation CDMA system, namely IS-95, single user detection receiver has been used [58]. IS-95 uses limited signal processing and interference suppression [59]. The receiver structure is based on the matched filter detector which treats MAI as noise. The matched filter, also known as the conventional detection, simply correlates the received signal with the desired user's spreading code and samples the output at the bit rate. The performance of the conventional detector is highly dependent on the number of users [8][59]. Therefore, when the number of active users in the system becomes large or when the power level of certain users increases, weak users with conventional detector suffer from the near-far problem. Mitigating the near-far effect is done by employing very accurate power control to make sure all users have identical signal power level. The effect of MAI in DS-CDMA can be eliminated or reduced by using MUD techniques.

Verdu has shown in [33] that the optimal MUD which is based on maximum likelihood sequence detector uses the Viterbi algorithm. However, this detector is too complex for practical DS-CDMA systems. The complexity is exponential with the number of active users. Therefore, most of research has focused on finding suboptimal low complexity multiuser detectors solutions that are feasible to implement.

Many different linear and non-liner detectors have been developed for multiuser CDMA system [1][5][32][59]. These detectors differ in their computational complexity and performance.

Another problem facing CDMA transmission, specially over time-varying multipath mobile radio channels, is intersymbol interference (ISI) between data symbols. Though Rake receiver can effectively take advantage of multipath interference, but the problem of self and MAI remains. Here, adaptive equalization can be used to combat these interference sources.

An earlier work where equalization was used for interference cancellation in CDMA systems is presented in [60]. The same authors proposed the use of fractionally spaced DFE where they showed the capabilities of this structure in minimizing the effects of interference, multipath, fading and additive white Gaussian noise (AWGN) in a slow acting power control environment [61]. In [8], the zero forcing equalizer (ZFE) with decision feedback was used. It was shown that ZFE with MUD outperform the conventional receiver by combating both ISI and MAI with reasonable computational complexity. In [62], an adaptive DFE was used as multiuser detector. The authors showed that DFE receiver structure is shown to exhibit good near-far resistance. However, the authors didn't compare their results with a well known MUD detector such as the decorrelator detector to see how their receiver structure performs.

In 1996, Kim and his group proposed and analyzed a modified DFE where an error feedback filter (EFF) was added to the conventional DFE [18]. The use of EFF led to an enhancement in the performance with minimal increase in complexity. The enhancement in the performance is achieved by reducing the correlation of error signal which cannot be reduced by the feedback or feedforward filters.

In this work, the performance of DFE-based MUD will be investigated and compared to a combined DFE with the DD as well as the conventional DFE detector. The performance of a modified DFE-MUD where EFF is added is also investigated.

The next section describes briefly the system model for the CDMA system as well as the proposed receiver structures used in this work. Simulation results, which illustrate the performance of these receivers, are presented in Chapter 6.

5.2 System Model

The uplink synchronous DS-CDMA will be considered in this work. PN codes are assumed to be known.

Recall from Chapter 2, the received signal in a synchronous DS-CDMA channel where all bits of all K-user are time aligned, [1][5] is given by:

$$r(t) = \sum_{k=1}^{K} A_k(t) b_k(t) s_k(t) + n(t) \quad t \in [0, T_s] \tag{5.1}$$

where T_s is the symbol period, $A_k(t)$ is the received amplitude of the k^{th} user's signal, $b_k(t) \in [-1,1]$ is the BPSK bits transmitted by the k^{th} user, $s_k(t)$ is the normalized deterministic signature waveform assigned to the k^{th} user and $n(t)$ is white Gaussian noise with unit power spectral density.

The signature waveforms are assumed to be zero outside the interval [0, T_s], and therefore, there is no ISI introduced by the PN codes [1]. The output of the j^{th} matched filter where each user is matched to its PN code is given by:

$$y_j = \sum_{k=1}^{K} A_k b_k \rho_{jk} + n_j \tag{5.2}$$

where ρ_{ij} is the normalized cross-correlation of PN codes and is given by:

$$\rho_{ij} = \frac{1}{\sqrt{L}} \sum_{l=1}^{L} s_i(l) s_j(l) \tag{5.3}$$

$L = T_s / T_c$ is the processing gain and T_c is the chip rate.

We shall consider three receiver structures: the conventional DFE detector, the DFE-Decorrelator detector (DD) and the DFE-based MUD receiver. In these structures the EFF can be added to the DFE resulting three more receivers.

5.2.1 Conventional DFE with and without EFF

The DFE is a simple nonlinear equalizer. As the name implies, the DFE uses decisions on the symbols to cancel the interference from the symbols that have already been detected. The DFE consists of two linear transversal filters, feedforward filter (FFF) and feedback filter (FBF). The outputs of both filters form the equalized signal. The decision made on this signal is fed back via the feedback filter in order to cancel ISI caused by previously detected symbols [6][7]. The coefficients of the DFE are updated simultaneously by using some adaptive algorithms such as LMS and RLS. The goal of updating the coefficients is to minimize the MSE.

The major disadvantage of the DFE is error propagation. This happens when a particular incorrect decision is fed back affecting the future symbols. This will lead to probably more errors follow the first one. However, recently, a new weighted DFE had been proposed [63] which is based on the computation of a reliability value of the output of the conventional DFE. This equalizer doesn't suffer from the error propagation phenomenon [63].

The DFE can compensate for amplitude distortion better than linear transversal equalizer (LTE) [6]. In general, up to some noise level, DFE performs better than LTE.

After that level, DFE will cause error propagation. This problem is well known and has already been addressed by many authors. Often to overcome this problem a known training data sequence to the receiver is transmitted periodically.

In [18], a modifed DFE was proposed in which an EFF was added to the main structure. The use of EFF helps in reducing the correlation of error signal which cannot be reduced by the FFF or FBF. This structure is shown in Figure 5.1.

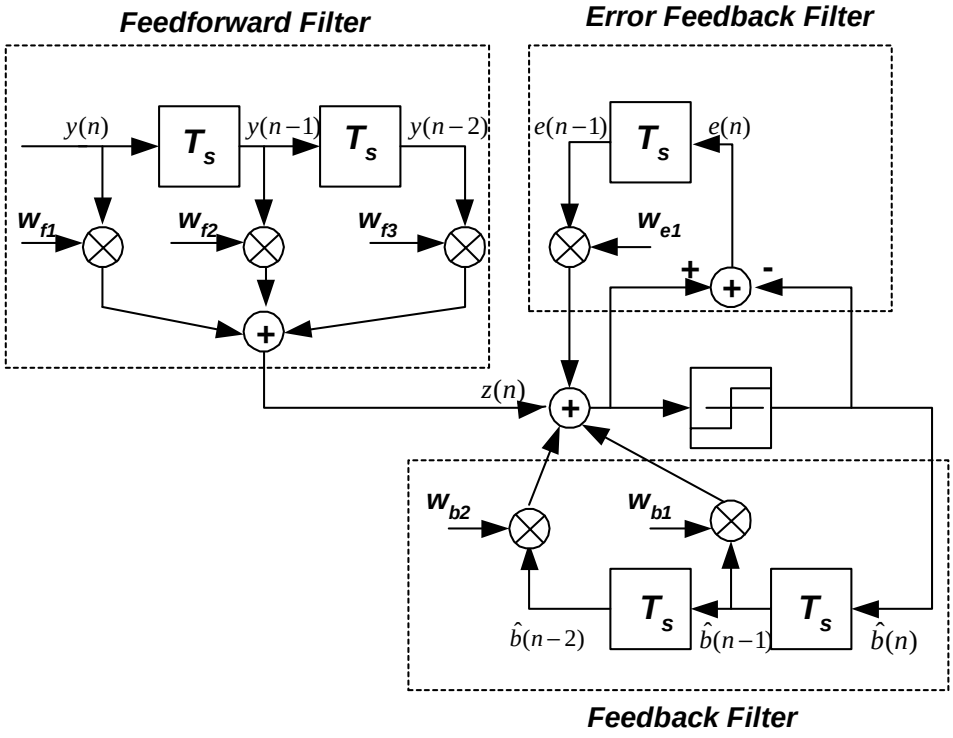

Figure 5.1: An example of a DFE with error feedback filter.

Let us define the FFF coefficients $\mathbf{W}_f$, the FBF coefficients $\mathbf{W}_b$ and the EFF coefficients $\mathbf{W}_e$ for K users as,

$$\mathbf{W}_f = [\mathbf{w}_f^{(1)} \quad \mathbf{w}_f^{(2)} \quad \cdots \quad \mathbf{w}_f^{(K)}]^T; \ \mathbf{w}_f^{(k)} = [w_{f1}^{(k)} \quad w_{f2}^{(k)} \quad \cdots \quad w_{fN_f}^{(k)}], \tag{5.4}$$

$$\mathbf{W}_b = [\mathbf{w}_b^{(1)} \quad \mathbf{w}_b^{(2)} \quad \cdots \quad \mathbf{w}_b^{(K)}]^T; \ \mathbf{w}_b^{(k)} = [w_{b1}^{(k)} \quad w_{b2}^{(k)} \quad \cdots \quad w_{bN_b}^{(k)}] \ , \tag{5.5}$$

$$\mathbf{W}_e = [\mathbf{w}_e^{(1)} \quad \mathbf{w}_e^{(2)} \quad \cdots \quad \mathbf{w}_e^{(K)}]^T; \mathbf{w}_e^{(k)} = [w_{e1}^{(k)} \quad w_{e2}^{(k)} \quad \cdots \quad w_{eN_e}^{(k)}] \ , \tag{5.6}$$

where N_f , N_b and N_e are the number of forward, feedback and error taps, respectively. The superscript (k) in (5.4)-(5.6) is used to indicate the k^{th} user for the purpose of MUD, k=1,..,K.

The input to the forward, feedback and error filters are,

$$\mathbf{Y}_n = [\mathbf{y}_n^{(1)} \quad \mathbf{y}_n^{(2)} \quad \cdots \quad \mathbf{y}_n^{(K)}]^T; \ \mathbf{y}_n^{(k)} = [y_n^{(k)} \quad y_{n-1}^{(k)} \quad \cdots \quad y_{n-N_f+1}^{(k)}], \tag{5.7}$$

$$\hat{\mathbf{B}}_n = [\hat{\mathbf{b}}_n^{(1)} \quad \hat{\mathbf{b}}_n^{(2)} \quad \cdots \quad \hat{\mathbf{b}}_n^{(K)}]^T; \ \hat{\mathbf{b}}_n^{(k)} = [\hat{b}_{n-1}^{(k)} \quad \hat{b}_{n-2}^{(k)} \quad \cdots \quad \hat{b}_{n-N_b+1}^{(k)}], \tag{5.8}$$

$$\mathbf{E}_n = [\mathbf{e}_n^{(1)} \quad \mathbf{e}_n^{(2)} \quad \cdots \quad \mathbf{e}_n^{(K)}]^T; \ \mathbf{e}_n^{(k)} = [e_{n-1}^{(k)} \quad e_{n-2}^{(k)} \quad \cdots \quad e_{n-N_e+1}^{(k)}], \tag{5.9}$$

Now the output vector of the DFE for K users before the decision device $\mathbf{z}$, is given by:

$$\begin{aligned} \mathbf{z}_n &= diag\left(\begin{bmatrix} \mathbf{W}_f & \mathbf{W}_b & \mathbf{W}_e \end{bmatrix} \begin{bmatrix} \mathbf{Y}_n^T \\ \hat{\mathbf{B}}_n^T \\ \mathbf{E}_n^T \end{bmatrix} \right) \\ &= diag(\mathbf{W}_f \mathbf{Y}_n^T + \mathbf{W}_b \hat{\mathbf{B}}_n^T + \mathbf{W}_e \mathbf{E}_n^T) \end{aligned} \tag{5.10}$$

For simplicity let,

$$\mathbf{W} = [\mathbf{W}_f \quad \mathbf{W}_b]^T \tag{5.11}$$

$$\tilde{\mathbf{W}} = [\mathbf{W}_f \quad \mathbf{W}_b \quad \mathbf{W}_e]^T \tag{5.12}$$

$$\mathbf{X} = [\mathbf{Y} \quad \hat{\mathbf{B}}]^T \tag{5.13}$$

and

$$\tilde{\mathbf{X}} = [\mathbf{Y} \quad \hat{\mathbf{B}} \quad \mathbf{E}]^T \tag{5.14}$$

The error signal vector of K users between the desired signal vector $\mathbf{b}_n$ and the DFE output vector $\mathbf{z}_n$ is defined as,

$$\mathbf{e}_n = \mathbf{b}_n - \mathbf{z}_n \tag{5.15}$$

To obtain the mean-square error (MSE), there are two cases [18]. The first case when the EFF is not used, the MSE for a single user is given by:

$$\begin{aligned} J &= E[e_n^2] = E[(b_n - z_n)^2] \\ &= E[b_n^2 - 2b_n z_n + z_n^2] \\ &= E[b_n^2] - 2E[b_n z_n] + E[z_n^2] \end{aligned} \tag{5.16}$$

Note that from (5.10), if we consider the MSE of a single user, then,

$$z = \mathbf{w}^T \mathbf{x} = \mathbf{x}^T \mathbf{w} \tag{5.17}$$

using (5.17) in (5.16) we get:

$$\begin{aligned} J &= E[b_n^2] - 2E[b_n \mathbf{x}^T \mathbf{w}] + E[\mathbf{w}^T \mathbf{x}\mathbf{x}^T \mathbf{w}] \\ &= E[b_n^2] - 2E[b_n \mathbf{x}^T]\mathbf{w} + \mathbf{w}^T E[\mathbf{x}\mathbf{x}^T]\mathbf{w} \\ &= E[b_n^2] - 2\mathbf{p}^T \mathbf{w} + \mathbf{w}^T \mathbf{R}_c \mathbf{w} \end{aligned} \tag{5.18}$$

Where $\mathbf{p}$ is a vector of size $(N_f+N_b)\times 1$ contains the cross-correlation between the desired signal and input signal and $\mathbf{R}_c$ is a matrix of size $(N_f+N_b)\times (N_f+N_b)$ contains the auto-correlation of the input signal, i.e.:

$$\begin{aligned} \mathbf{P} &= E[b_n \mathbf{x}^T] \\ \mathbf{R}_c &= E[\mathbf{x}\mathbf{x}^T] \end{aligned} \tag{5.19}$$

Now by differentiating (5.18) with respect to equalizer taps weights, **w**, to get the gradient of the MSE performance function;

$$\nabla = \frac{\partial J}{\partial \mathbf{w}} = 2\mathbf{R}_c \mathbf{w} - 2\mathbf{p} \tag{5.20}$$

The optimal taps weights are then obtained by setting the gradient to zero.

$$\mathbf{w}_{opt} = \mathbf{R}_c^{-1} \mathbf{p} \tag{5.21}$$

By substituting (5.21) in (5.18), we get the minimum MSE as;

$$J_{\min} = E[b_n^2] - \mathbf{p}^T \mathbf{R}_c^{-1} \mathbf{p} \tag{5.22}$$

The second case when EFF is used with DFE. In this case, with the help of (5.12) and (5.14), Equation (5.17) can be written as follow:

$$z = \tilde{\mathbf{w}}^T \tilde{\mathbf{x}} = \tilde{\mathbf{x}}^T \tilde{\mathbf{w}} \tag{5.23}$$

In the same way, that was used to obtain (5.18), we can find the MSE of DFE-EFF for a single user.

$$J = E[b_n^2] - 2\tilde{\mathbf{p}}^T \tilde{\mathbf{w}} + \tilde{\mathbf{w}}^T \tilde{\mathbf{R}}_c \tilde{\mathbf{w}} \tag{5.24}$$

where, $\tilde{\mathbf{p}}$ is a vector of size (N_f+N_b+ N_e)×1 contains the cross-correlation between the desired signal and input signal and $\tilde{\mathbf{R}}_c$ is a matrix of size (N_f+N_b+ N_e)× (N_f+N_b+ N_e) contains the auto-correlation of the input signal, i.e.:

$$\begin{aligned} \tilde{\mathbf{p}} &= E[b_n \tilde{\mathbf{x}}^T] \\ \tilde{\mathbf{R}}_c &= E[\tilde{\mathbf{x}}\tilde{\mathbf{x}}^T] \end{aligned} \tag{5.26}$$

By using (5.19), (5.26) can be written as:

$$\begin{aligned} \tilde{\mathbf{p}} &= E\begin{bmatrix} b_n \mathbf{x} \\ b_n e_{n-1} \end{bmatrix} \\ \tilde{\mathbf{R}}_c &= \begin{bmatrix} \mathbf{R}_c & \mathbf{h} \\ \mathbf{h}^T & \sigma_e^2 \end{bmatrix} \end{aligned} \tag{5.27}$$

where $\mathbf{h} = E[e_{n-1}\mathbf{X}]$ and $\sigma_e^2 = E[e_{n-1}^2]$.

As in the first case, where EFF was not used, the equalizer optimal weight $\tilde{\mathbf{w}}$ is obtained as follow:

$$\tilde{\mathbf{w}} = \tilde{\mathbf{R}}_c^{-1} \tilde{\mathbf{p}} \tag{5.28}$$

Then, the minimum MSE is given by:

$$J_{\min} = E[b_n^2] - \tilde{\mathbf{p}}^T \tilde{\mathbf{R}}_c^{-1} \tilde{\mathbf{p}} \tag{5.29}$$

We can continue further by finding $\tilde{\mathbf{R}}_c^{-1}$ to compare between the conventional DFE and DFE-EFF.

By employing the block matrix inverse given below:

$$\begin{bmatrix} A & D \\ C & B \end{bmatrix}^{-1} = \begin{bmatrix} A^{-1} + E\Delta^{-1}F & -E\Delta^{-1} \\ -\Delta^{-1}F & \Delta^{-1} \end{bmatrix} \tag{5.30}$$

where $\Delta = B - CA^{-1}D$, $E = A^{-1}D$ and $F = CA^{-1}$.

By substituting (5.27) into (5.30), we obtain:

$$\tilde{\mathbf{R}}_c^{-1} = \begin{bmatrix} S & T \\ U & V \end{bmatrix} \tag{5.31}$$

where

$$\begin{aligned} S &= \mathbf{R}_c^{-1} + \mathbf{R}_c^{-1}\mathbf{h}(\sigma_e^2 - \mathbf{h}^T\mathbf{R}_c^{-1}\mathbf{h})^{-1}\mathbf{h}^T\mathbf{R}_c^{-1} \\ T &= -\mathbf{R}_c^{-1}\mathbf{h}(\sigma_e^2\mathbf{h}^T\mathbf{R}_c^{-1}\mathbf{h})^{-1} \\ U &= -(\sigma_e^2\mathbf{h}^T\mathbf{R}_c^{-1}\mathbf{h})^{-1}\mathbf{h}^T\mathbf{R}_c^{-1} \\ V &= (\sigma_e^2 - \mathbf{h}^T\mathbf{R}_c^{-1}\mathbf{h})^{-1} \end{aligned}$$

Using this result, the second term on right-hand side of (5.29) can be represented by:

$$\begin{aligned} \tilde{\mathbf{p}}^T\tilde{\mathbf{R}}_c^{-1}\tilde{\mathbf{p}} &= \begin{bmatrix} \mathbf{p}^T E[b_n e_{n-1}] \end{bmatrix}\tilde{\mathbf{R}}_c^{-1}\begin{bmatrix} \mathbf{p} \\ E[b_n e_{n-1}] \end{bmatrix} \\ &= \mathbf{p}^T\mathbf{R}_c^{-1}\mathbf{p} + (\sigma_e^2 - \mathbf{h}^T\mathbf{R}_c^{-1}\mathbf{h})^{-1} \\ &\quad (E[b_n e_{n-1}] - \mathbf{h}^T\mathbf{R}_c^{-1}\mathbf{p})^2 \end{aligned} \tag{5.32}$$

Thus, the minimum MSE of the DFE-EFF can be obtained by substituting (5.32) in (5.29):

$$J_{\min} = E[b_n^2] - \mathbf{p}^T\mathbf{R}_c^{-1}\mathbf{p} - (\sigma_e^2 - \mathbf{h}^T\mathbf{R}_c^{-1}\mathbf{h})^{-1}(E[b_n e_{n-1}] - \mathbf{h}^T\mathbf{R}_c^{-1}\mathbf{p})^2 \tag{5.33}$$

Since e_n and **x** are orthogonal, **h** reduced to a zero vector and hence the minimum MSE is given by:

$$J_{\min} = E[b_n^2] - \mathbf{p}^T \mathbf{R}_c^{-1} \mathbf{p} - (\sigma_e^2)^{-1} (E[b_n e_{n-1}])^2 \tag{5.34}$$

Now simplifying (5.34) further with the help of (5.15) by considering:

$$\begin{aligned} E[b_n e_{n-1}] &= E[(e_n - y_{eq}) e_{n-1}] \\ &= E[e_n e_{n-1} - y_{eq} e_{n-1}] \\ &= E[e_n e_{n-1}] - E[y_{eq} e_{n-1}] \end{aligned} \tag{5.35}$$

The second term of (5.35) vanishes to zero. Finally, the minimum MSE can be expressed as follow:

$$J_{\min} = E[b_n^2] - \mathbf{p}^T \mathbf{R}_c^{-1} \mathbf{p} - (\sigma_e^2)^{-1} (E[e_n e_{n-1}])^2 \tag{5.36}$$

by looking to (5.36), the first two terms corresponds to the minimum MSE of the conventional DFE expressed in (5.22). The last term of (5.36) is always positive [18] and therefore the MSE of DFE with EFF is smaller than that of the conventional one.

The optimum weighting coefficients can be found through adaptive algorithm such that MSE, given by (5.22) or (5.36) in the case of using EFF, is minimized. In this work we use the LMS algorithm for updating the filter taps and which is given by,

$$\mathbf{W}(n) = \mathbf{W}(n-1) + \mu\, e(n-1)\mathbf{X}(n-1) \tag{5.37}$$

where **W** and **X** are given by (5.11) and (5.13), respectively, if no EFF is used, otherwise (5.12) and (5.14), respectively, if EFF is used. μ is the step size parameter of LMS algorithm and it is chosen to ensure that MSE remains bounded. The conventional DFE-EFF receiver structure is shown in Figure 5.2.

5.2.2 The combined DFE-Decorrelator detector

The previous detector is considered as the conventional detector since it treats MAI as noise and follows single user detection. The use of DFE is useful in combating ISI as well as suppressing noise.

In order to cancel MAI, we combined both the DFE and the decorrelator detector (DD) in one structure is shown in Figure 5.3. As we can see, there are two stages. The first stage consists of DFE (with or without EFF). This stage will treat ISI as well as suppressing noise. The output of first stage is fed to the second stage which is the DD consisting of the inverse of the cross-correlation matrix of PN codes. The DD will help in canceling the MAI. The DD is a simple, natural strategy and optimal according to three different criteria, namely the least squares, near-far resistance and maximum likelihood as detailed [1] when the received amplitudes are unknown. The problem with DD is the noise enhancement. To avoid such a problem we used the DFE in the first stage to suppress noise followed by the DD. The main disadvantage of this structure is its complexity. If we have K active users and the DFE has a total of N taps, then this detector has KN multiplications and $K(N\text{-}3)$ additions per bit plus the complexity of the decorrelator which is in the order of $O(K^3)$ due to the need of matrix inversion.

5.2.3 The DFE based MUD

The third DS-CDMA receiver structure is the DFE (with or without EFF) based MUD. This detector cancels both ISI and MAI as well as suppressing noise. The output of the decision device is fed back to the FBF to cancel ISI from previously detected bits. Also, the current decisions are used to cancel MAI at the input of the DFE. The receiver structure is shown in Figure 5.4.

In this structure, the input to the FFF is no more given by (5.7), since MAI is canceled at the input of DFE. Let $q_n^{(k)}$ represents the MAI coming form all users other than the desired user k, which is given by:

$$q_n^{(k)} = \sum_{\substack{i=1 \\ i \neq k}}^{K} \hat{b}_{n-1}^{(i)} \tag{5.38}$$

where $\hat{b}_n^{(i)}$ is defined in (5.8). Accordingly, (5.7) is modified and expressed as:

$$\begin{aligned} \mathbf{Y}_n^{(k)} &= [\mathbf{y}_n^{(1)} - \mathbf{q}_{n-1}^{(1)} \quad \mathbf{y}_n^{(2)} - \mathbf{q}_{n-1}^{(2)} \quad \cdots \quad \mathbf{y}_n^{(K)} - \mathbf{q}_{n-1}^{K1)}]; \\ \mathbf{y}_n^{(k)} - \mathbf{q}_n^{k1)} &= [y_n^{(k)} - q_{n-1}^{(k)} \quad y_{n-1}^{(k)} - q_{n-2}^{(k)} \quad \cdots \quad y_{n-N_f+1}^{(k)} - q_{n-N_f}^{(k)}] \end{aligned} \tag{5.39}$$

The advantage of this detector is its ability to treat ISI, noise and MAI at the same time. This detector gives an acceptable performance compared DFE-DD as we will see in Chapter 6. Another advantage of this detector is its reasonable complexity compared to the DFE-DD since it requires KN multiplications and $K^2+K(N-1)-3$ additions per bit. However, the main disadvantage of this detector is the error propagation as a result of wrong decision.

5.3 Simulation results

In this section, a MSE comparison between the DFE and DFE-EFF is done. Simple communication system is considered with BPSK data stream. The equalizer has 15, 6 and 2 feedforward, feedback and error feedback taps, respectively. The channel used is the static channel described in Chapter 3. The Eb/No used is 20dB.

Figure 5.5 shows the learning curves of both DFE and DFE-EFF. The DFE has a step size parameter equal to 0.05 as well as the EFF. We can see that the DFE-EFF outperforms the conventional DFE in both rate of convergence and lower MSE level. Moreover, DFE-EFF is more stable than the conventional DFE. To enhance the DFE-EFF performance more, a smaller step size parameter is given to the EFF which is 0.005 as we can see in Figure 5.5. This enhancement is due to the reduction in adding errors to the output of the equalizer. More results are presented in the next chapter.

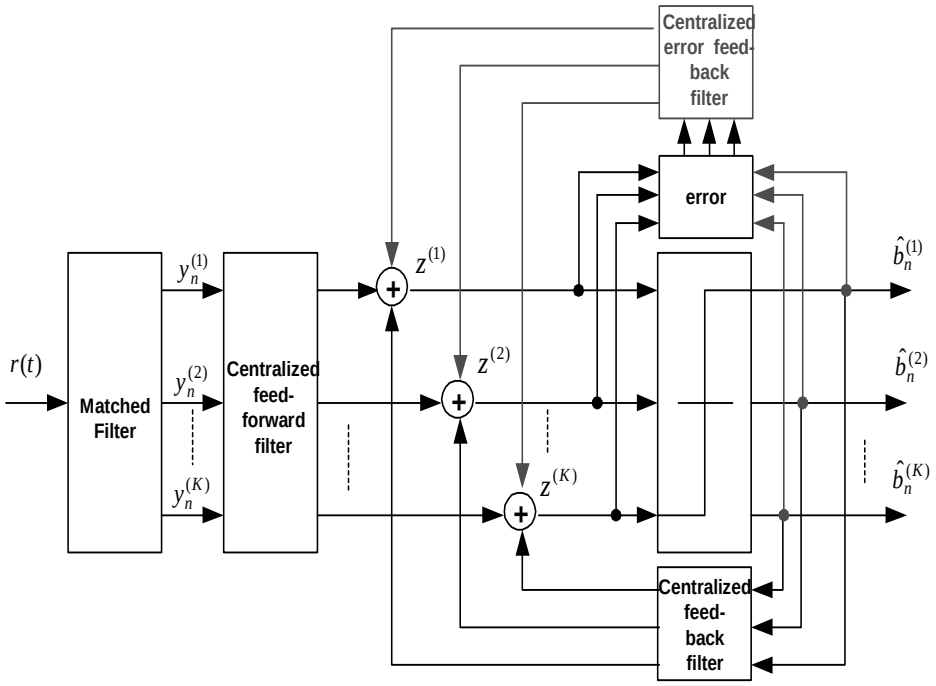

Figure 5.2: The conventional DFE-EFF detector

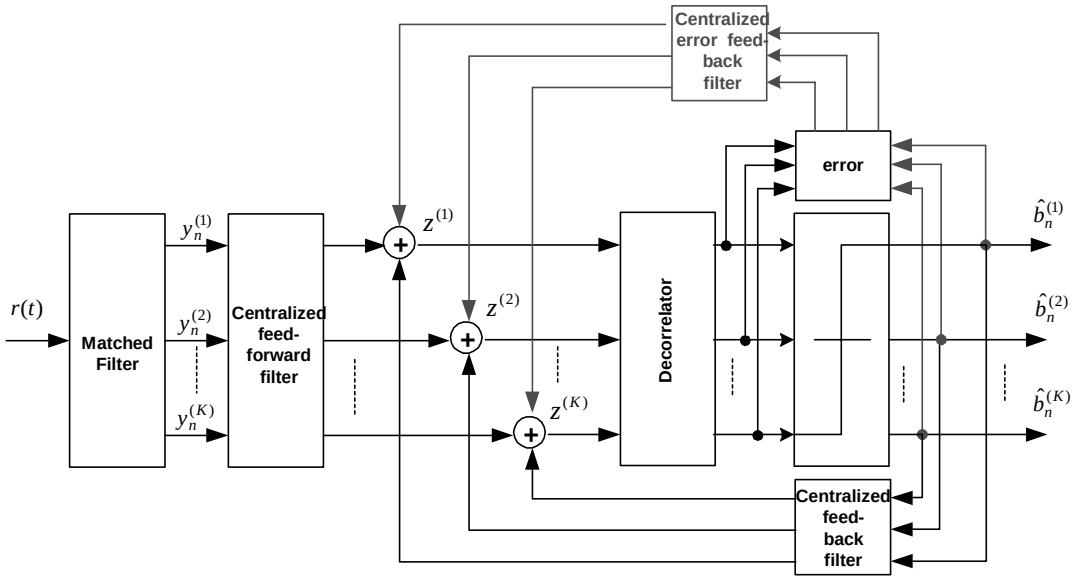

Figure 5.3: The DFE-EFF Decorrelator detector

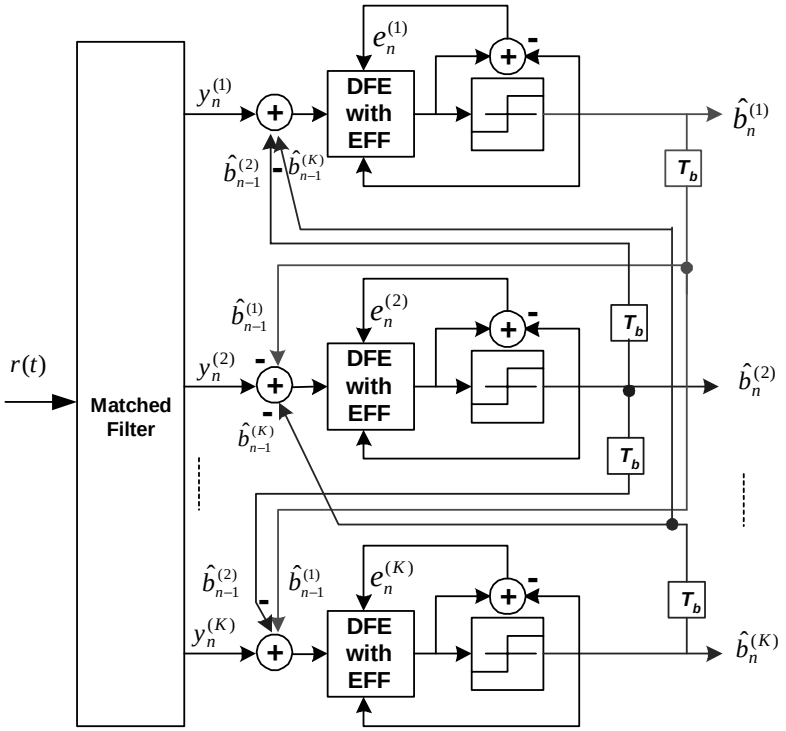

Figure 5.4: The DFE-EFF based multiuser detector

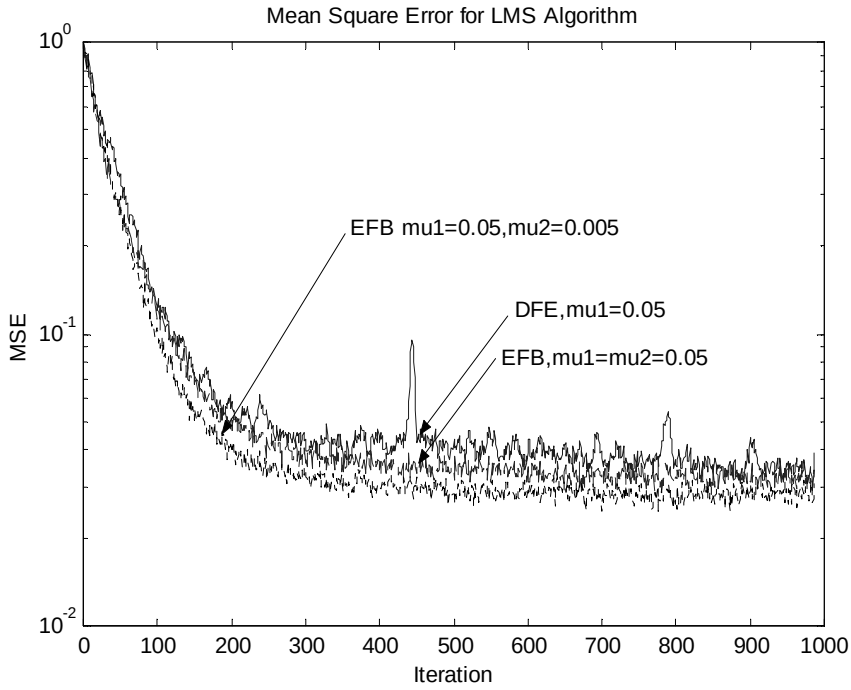

Figure 5.5: MSE comparison between DFE and DFE-EFF.

Chapter 6

Performance of Adaptive DFE with EFF for MUD in Synchronous CDMA

6. 1 Introduction

In this chapter, simulation results will be presented and discussed. The BER performance, system capacity and the effect of near-far problem will be used to compare among the different receiver structures.

Mainly, there are three different structures that will be compared. These structures are the conventional DFE detector, the DFE-based MUD and the DFE-DD. However, adding EFF to the DFE will result in more three structures which mean 6 structures will be compared.

The channels used in the simulation are 4 channels and they had been discussed in Chapter 3.

6. 2 Simulation Parameters

In the simulation of this chapter the following parameters where used:

- Simple BPSK data stream.
- Gold Code with length of 31 chips.
- A bandwidth of 3.84MHz.
- LMS algorithm for updating the equalizer taps.

- Synchronous CDMA channel model had been used.
- Four Channels had been used, one static channel and 3 fading channel. For more information about channels please see Chapter 3, section 3.6.
- DFE(EFF) has (16,5,2) feedforward, feedback and error feedback taps respectively.

The following things have been assumed:

- Full phase recovery.
- Channel doesn't change within a bit in case of fading channels.
- For DFE, correct decisions are fed back to avoid error propagation.

6. 3 Simulation Results under Static Channel

Figure 6.1 shows the BER performance verses Eb/No comparison among different structures under static channel. Seven users are in the system. $NFR^{(1)}$ is set to 0dB, i.e. all users are transmitting at same power level (perfect power control). The step size parameter used to update the equalizer taps including EFF is 0.001. From this figure we can see that the DFE-DD is close to the single user bound. At BER=10^{-3}, 0.1 dB difference is noted. Another thing can be observed from this figure is that there is no much improvement gained by using DFE-based MUD over the conventional DFE detector specially at high Eb/No. Around 0.15 dB difference is noted between the single user bound and both conventional DFE and DFE-based MUD's at BER=10^{-3}. However, this is not the case when an EFF is added to the DFE. Figure 6.2 shows the BER performance of conventional DFE-EFF, DFE-EFF-based MUD, DFE-EFF-DD and DFE-DD. Both DFE-EFF-based MUD and DFE-EFF-DD approach the single

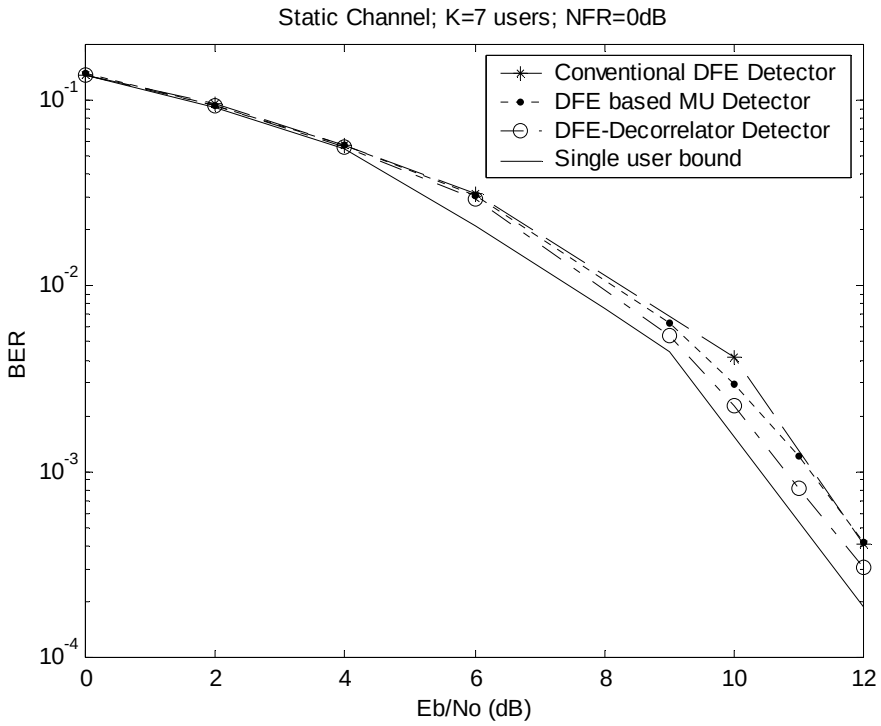

Figure 6.1: BER performance of conventional DFE, DFE-based MUD and DFE-DD under static channel.

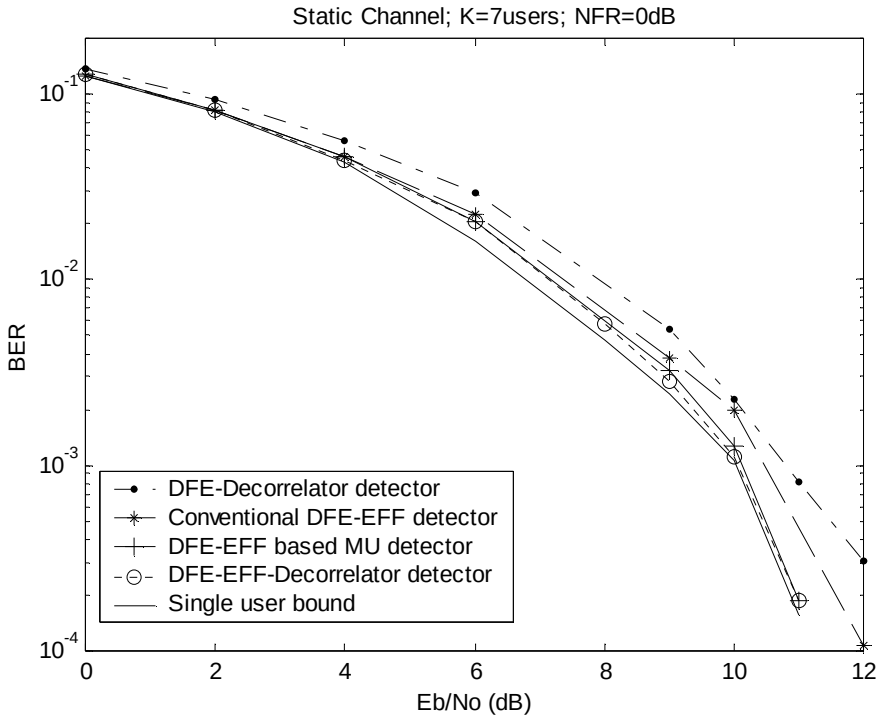

Figure 6.2: BER performance of conventional DFE-EFF, DFE-EFF-based MUD, DFE-EFF-DD and DFE-DD under static channel.

user bound giving around 0.4dB improvement over the conventional DFE-EFF detector, at BER=10^{-3}.

Table 6.1 presents a comparison among different receiver structures at a given BER. One more thing can be noted form this Table is that around 1.1dB improvement is noted between the single user conventional DFE-D and DFE-EFF detector at BER==10^{-3}.

Structure	**Number of users (K)**	**BER**	**Eb/No**
One user DFE-D	1	10^{-3}	11.1 dB
One user DFE-EFF-D	1	10^{-3}	10 dB
Conventional DFE-D	7	10^{-3}	11.25 dB
Conventional DFE-EFF-D	7	10^{-3}	10.47 dB
DFE-based MUD	7	10^{-3}	11.23 dB
DFE-EFF-based MUD	7	10^{-3}	10.12 dB
DFE-Decorrelator D	7	10^{-3}	11.2 dB
DFE-EFF-Decorrelator D	7	10^{-3}	10.05 dB

Table 6.1: BER comparison among different receiver structures (NFR=0dB)

Figure 6.3 shows the system capacity of the conventional DFE, DFE-based MUD and the DFE-DD under static channel. Eb/No was set to 10dB and all users are assumed transmitting at same power level (i.e. NFR=0dB). As it can be seen from the figure, both DFE-based MUD and DFE-DD have close BER performance. Also, they have a considerable improvement over the conventional DFE detector. At BER=1.7×10^{-3}, the conventional DFE detector can accommodate around 10 users while both DFE-based MUD and DFE-DD can accommodate approximately 20 users which means double of that in conventional DFE detector.

Now considering the case where EFF is added to the DFE, the system capacity of different receiver structures is presented in Figure 6.4. As we can see, at BER=10^{-3}, the conventional DFE-EFF can accommodate around 6 users while both DFE-EFF-base

MUD and DFE-EFF-DD can accommodate around 19 users, assuming all users transmitting at same power level and Eb/No is set to 10dB. As in the pervious result we can see the close performance of DFE-EFF-base MUD to DFE-EFF-DD. One thing can be noted is that adding and EFF to the DFE will improve the system capacity 6 times in the cases of DFE-based MUD and DFE-DD at BER=10^{-3}. This improvement came from reducing the correlation of the error signal that could not be reduced the both the feedforward and feedback filters of the DFE. Table 6.2 presents some system capacity among all different receiver structures.

Structure	BER	System Capacity (K-users)
Conventional DFE-D	10^{-3}	2.4
Conventional DFE-EFF-D	10^{-3}	6.4
DFE-based MUD	10^{-3}	3
DFE-EFF-based MUD	10^{-3}	20
DFE-Decorrelator D	10^{-3}	3.5
DFE-EFF-Decorrelator D	10^{-3}	20

Table 6.2: System capacity comparison among different receiver structures under static channel (Eb/No=10dB and NFR=0dB)

Figure 6.5 and 6.6 show the BER performance comparison verses NFR among different receiver structures. Eb/No is set to 10dB and 7 users are in the system. One user is transmitting at higher power level compared to the desired user. As we can see from Figure 6.5 the performance of DFE-based MUD approaches the performance of DFE-DD at high NFR. However, in the case of using EFF (Figure 6.6), the performance of DFE-EFF-based MUD and DFE-EFF-DD is almost the same specially at lower NFR. We can also see that all structures can resist up to around 6dB after which a power control is needed. Table 6.3 presents some NFR values comparison among different receiver structures.

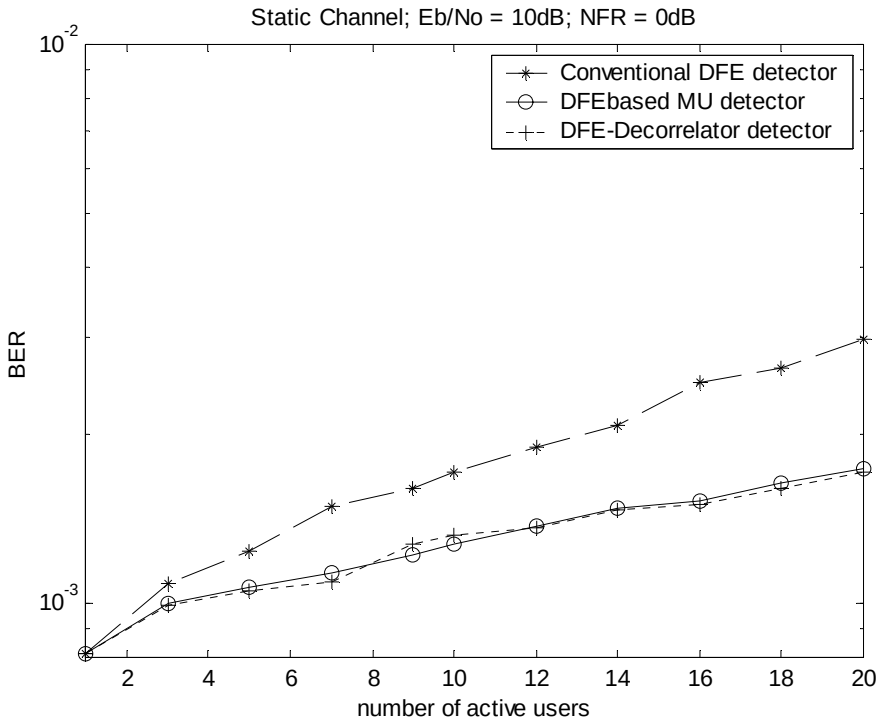

Figure 6.3: System capacity of conventional DFE, DFE-based MUD and DFE-DD under static channel.

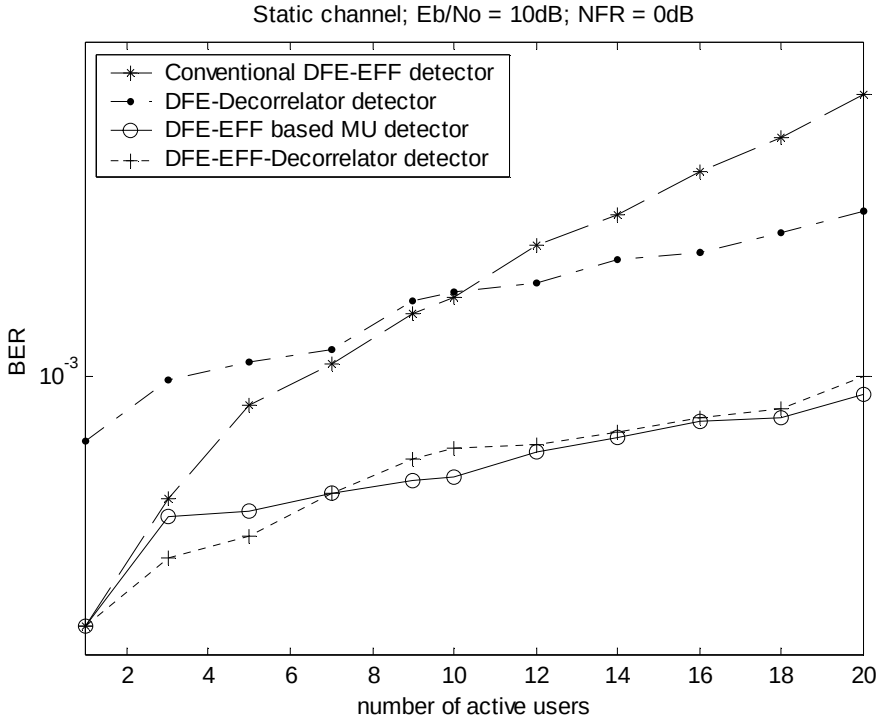

Figure 6.4: System capacity of conventional DFE-EFF, DFE-EFF-based MUD and DFE-EFF-DD as well as DFE-DD under static channel.

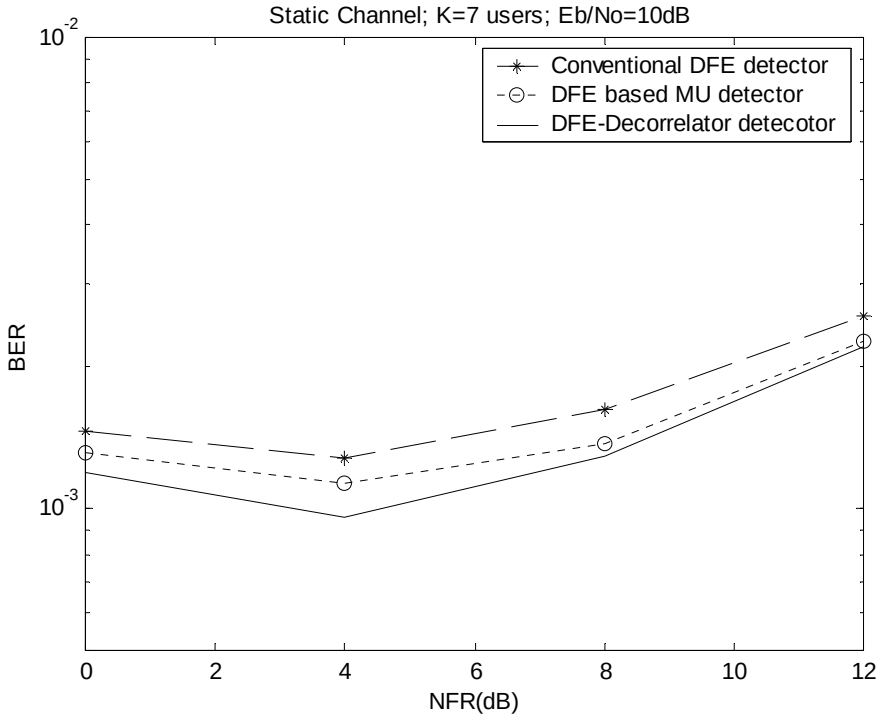

Figure 6.5: NFR comparison of the Conventional DFE, DFE-base MUD and DFE-DD under static channel.

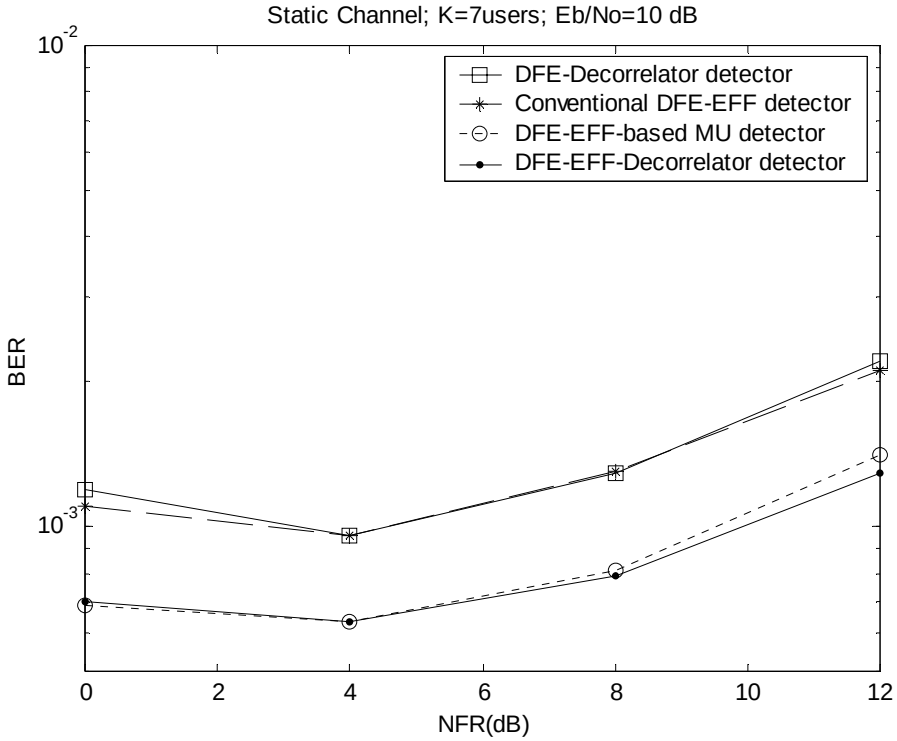

Figure 6.6: NFR comparison of the Conventional DFE-EFF, DFE-EFF-base MUD, DFE-EFF-DD and DFE-DD under static channel.

Structure	BER (1)	NFR(1) (dB)	BER (2)	NFR(2) (dB)
Conventional DFE-D	1.3×10^{-3}	3.9	1.3×10^{-3}	3.9
Conventional DFE-EFF-D	10^{-3}	2.9	1.3×10^{-3}	7.8
DFE-based MUD	1.3×10^{-3}	6.9	1.1×10^{-3}	4
DFE-EFF-based MUD	10^{-3}	9.6	1.1×10^{-3}	10.4
DFE-Decorrelator D	1.3×10^{-3}	8.1	0.95×10^{-3}	4
DFE-EFF-Decorrelator D	10^{-3}	10.1	0.95×10^{-3}	9.6

Table 6.3: NFR comparison among different receiver structures (Eb/No=10dB)

From previous figures (Figure 6.1 through 6.6) the following conclusions can be obtained:

- Adding EFF to the DFE will enhance the overall performance by around 1 dB at BER=10^{-3} under static channel.
- The performance of DFE-EFF-based MUD approaches the performance of the DFE-EFF-DD at high Eb/No under the assumption of perfect power control which means same performance with low complexity.
- The performance of the conventional DFE(EFF) detector under near-far problem degrades while both DFE(EFF) based MUD and DFE(EFF)-DD give a reasonable performance. The reason for bad performance of the conventional DFE(EFF) is that this detector has no way of canceling MAI as a result of increasing the number of active users.

6. 4 Simulation Results under Pedestrian Channel

Now we can switch our attention to the performance of previous MUDs under fading channels. The same simulation done for static channel was repeated for fading channels. The fading channel used in the simulation was presented in Chapter 3 (see section 3.6.2).

Figure 6.7 shows the single user bound of both conventional DFE and DFE-EFF detector under Pedestrian channel. The step size parameter, μ, for the LMS algorithm used is set to $1/aN$, where N is the total number of taps and a is any number grater than one such that the condition stated in Equation (4.24) is satisfied. It is known that $1/N$ gives the fastest rate of convergence of the equalizer's taps with the expense of high MSE.

In the simulation of Figure 6.7, the parameter a was set to 32. The step size parameter of the EFF (μ_e) was set to 0.005. As we can see the performance of DFE-EFF at low Eb/No is close to the conventional DFE detector. For example at BER=10^{-2} a difference of 0.5dB was noted. However, at high Eb/No the DFE-EFF outperforms the conventional DFE by approximately 1.75dB at BER=10^{-3}.

As we start to increase the step size parameter μ (i.e. decrease a) a considerable gap between the performance of the conventional DFE and DFE-EFF is noted. For example, Figure 6.8 shows the single user bound of both conventional DFE and DFE-EFF detector under Pedestrian channel for $\mu=1/aN$, where a was set to 5. In this case, as we can see from Figure 6.8, at BER=10^{-2}, 3.8dB difference is noted and at BER=6×10^{-3} around 9.5dB difference is noted. By comparing Figure 6.7 and 6.8 we can observe degradation in the BER performance in case of high step size parameter. At this point it is worth to state the relationship among BER, MSE and the step size parameter of LMS algorithm. Small step size parameter will result in low level of miss-adjustment of the equalizer taps to the optimum values at the expense of low rate of convergence. In this case low MSE can be achieved leads to a good overall performance. Low MSE will result in low BER performance.

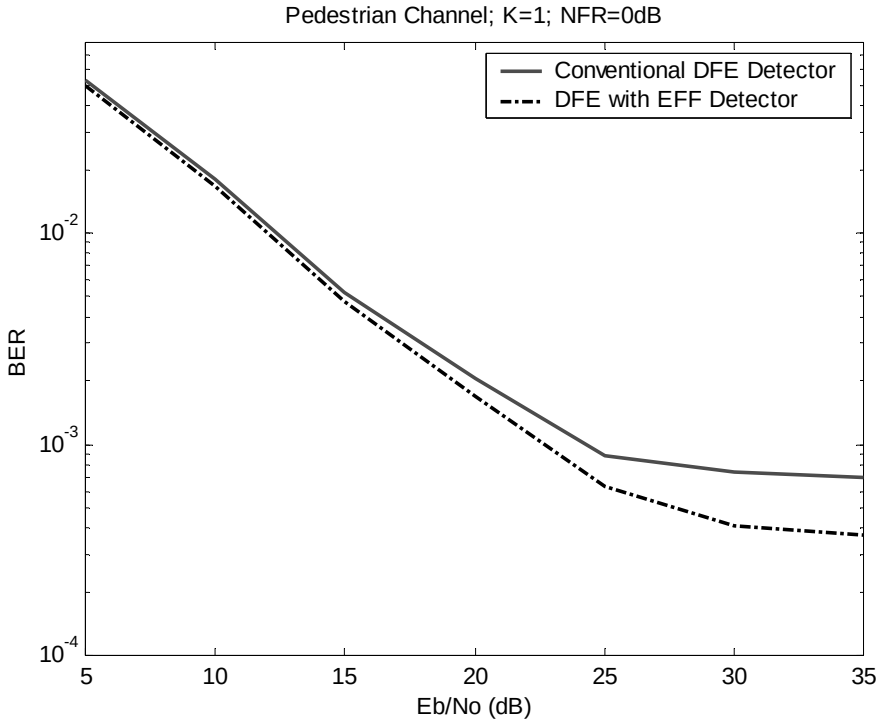

Figure 6.7: Single user bound BER performance of DFE and DFE-EFF detectors under Pedestrian channel (μ=1/aN; a =32; μ_e=0.005).

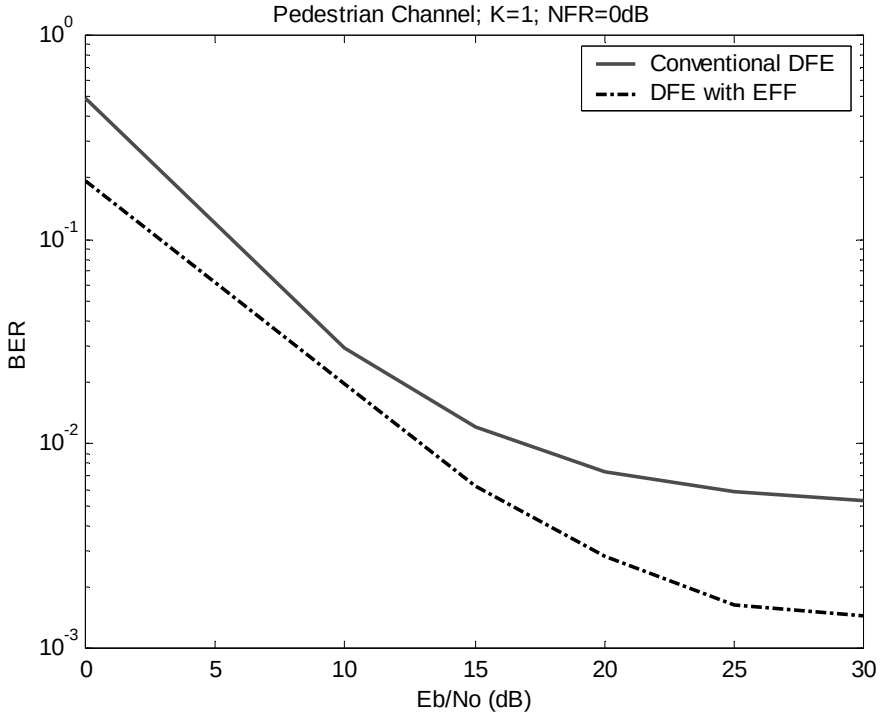

Figure 6.8: Single user bound BER performance of DFE and DFE-EFF detectors under Pedestrian channel (μ=1/aN; a =5; μe=0.008).

The other case is when the step size parameter is large; this will result in high rate of convergence but with high level of miss-adjustment. As consequence of this miss-adjustment high MSE will be observed and hence high BER.

The main disadvantage of small step size parameter is the low rate of convergence of the equalizer taps to the optimum value. Practically, high rate of convergence is needed during the training mode of the equalizer.

Since DFE with EFF can achieve acceptable BER performance with high rate of convergence using a large step size parameter, EFF can be used during the training mode where high rate of convergence is needed. After convergence, i.e. during tracking mode, smaller step size parameter can be used.

Figure 6.9 and Figure 6.10 show the BER performance comparison among different structures under Pedestrian channel. 5 users are in the system. NFR is set to 0dB, i.e. all users are transmitting. The step size parameter used is the case where a=32. Table 6.4 presents Eb/No comparison values among different receiver structures at BER=3.2×10^{-3}.

From the table we can see 2.2dB difference between the DFE-based MUD and DFE-DD. This difference became 0.63dB when EFF is added to the DFE. This is a good result since our aim is to get a performance which is close to the DFE-EFF-DD.

Now the same simulation was repeated but considering the case where a=5 and μ_e=0.008. The result of this case is presented in Figure 6.12. As we can see from the figure, it is difficult to compare among all structures at same BER level. However, comparison is possible among structures at a fixed Eb/No.

Table 6.5 presents BER comparison values among different receiver structures of at Eb/No equal to 25dB.

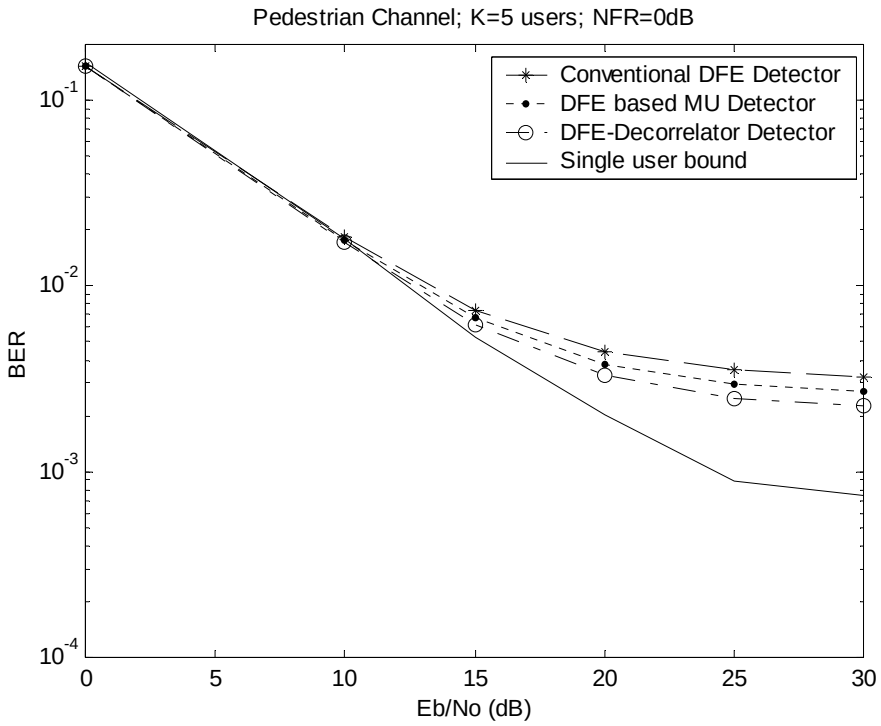

Figure 6.9: BER performance of conventional DFE, DFE-based MUD and DFE-DD under Pedestrian channel (μ=1/aN; a =32; μ_e=0.005).

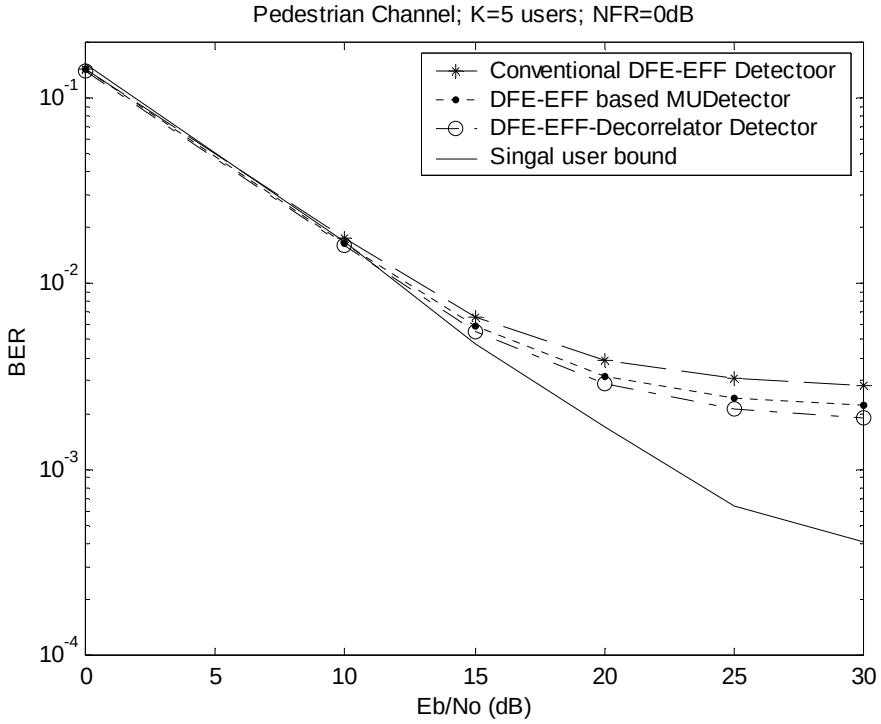

Figure 6.10: BER performance of conventional DFE-EFF, DFE-EFF-based MUD and DFE-EFF-DD under Pedestrian channel (μ=1/aN; a =32; μ_e=0.005).

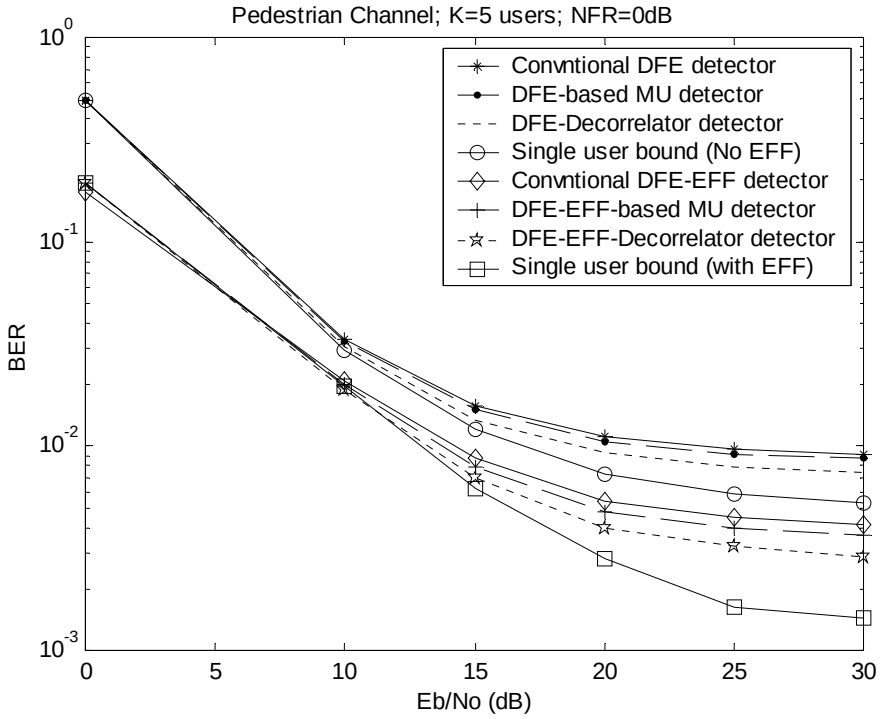

Figure 6.11: BER performance comparison among different receiver structures under Pedestrian channel (μ=1/aN; a =5; μ_e=0.008).

Structure	**Number of users (K)**	**BER**	**Eb/No**
One user DFE-D	1	3.2×10^{-3}	17.5 dB
One user DFE-EFF-D	1	3.2×10^{-3}	16.8 dB
Conventional DFE-D	5	3.2×10^{-3}	29.3 dB
Conventional DFE-EFF-D	5	3.2×10^{-3}	24.1 dB
DFE-based MUD	5	3.2×10^{-3}	22.5 dB
DFE-EFF-based MUD	5	3.2×10^{-3}	19.88 dB
DFE-Decorrelator D	5	3.2×10^{-3}	20.3 dB
DFE-EFF-Decorrelator D	5	3.2×10^{-3}	19.25 dB

Table 6.4: BER comparison among different receiver structures (NFR=0dB, μ=1/aN; a=32; μ_e=0.005)

Structure	Number of users (K)	BER	Eb/No
One user DFE-D	1	1.7×10^{-3}	25
One user DFE-EFF-D	1	5.8×10^{-3}	25
Conventional DFE-D	5	4.3×10^{-3}	25
Conventional DFE-EFF-D	5	9.8×10^{-3}	25
DFE-based MUD	5	3.9×10^{-3}	25
DFE-EFF-based MUD	5	8.9×10^{-3}	25
DFE-Decorrelator D	5	3.2×10^{-3}	25
DFE-EFF-Decorrelator D	5	7.8×10^{-3}	25

Table 6.5: BER comparison among different receiver structures (NFR=0dB, μ=1/aN; a=5; μ_e=0.008)

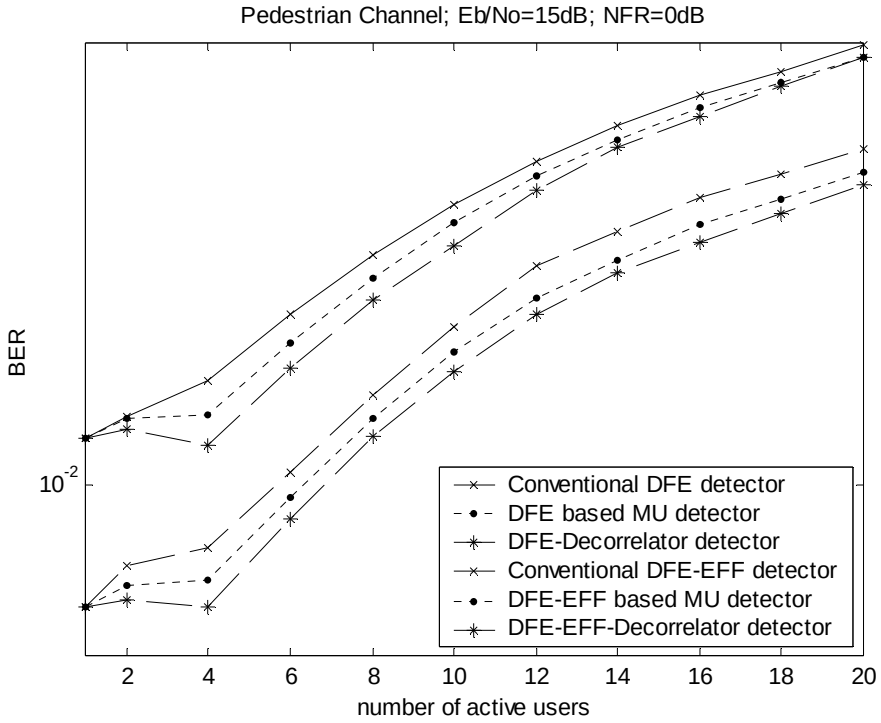

Figure 6.12: System capacity comparison among different receiver structures under Pedestrian channel (μ=1/aN; a =5; μ_e=0.008).

Figure 6.12 shows the system capacity comparison among different receiver structures under Pedestrian channel. Again, we assume all users transmitting at same power level. The step size parameter was chosen such that a =5 and μ_e=0.008. From the figure we can see a big difference between those structures use EFF and those not using EFF. By using EFF, approximately 4 more users can be accommodated at BER=1.3×10^{-2} as shown in Table 6.6. More users can be accommodated at lower BER, around 6 users more at BER=1.3×10^{-2}. Also, we can see there is no much difference between the conventional DFE(EFF) and DFE(EFF)-based MUD. However, it is expected that as the number of users increases and the near-far problem exists, the conventional DFE(EFF) will degrades much more than the DFE(EFF)-based MUD because of the shortage of the conventional DFE(EFF) in canceling MAI.

Structure	**BER**	**System Capacity (K-users)**
Conventional DFE-D	1.3×10^{-2}	2.5
Conventional DFE-EFF-D	1.3×10^{-2}	7.5
DFE-based MUD	1.3×10^{-2}	4.2
DFE-EFF-based MUD	1.3×10^{-2}	8.2
DFE-Decorrelator D	1.3×10^{-2}	5
DFE-EFF-Decorrelator D	1.3×10^{-2}	9

Table 6.6: System capacity comparison among different receiver structures under Pedestrian Channel (Eb/No=15dB and NFR=0dB; μ=1/aN; a =5; μ_e=0.008)

In Figure 6.13, the performance of receiver structures was investigated under near-far effect. 5 users are in the system and one of the users is transmitting at high power. Eb/No was set to 15dB. The step size parameter was chosen such that a =9 and μ_e=0.008. From the figure we can see that both DFE(EFF)-based MUD and DFE(EFF)-DD have better

near-far resistance at high NFR than the conventional DFE(EFF) detector. Table 6.7 gives some comparison values among different structures.

Structure	BER (1)	NFR(1) (dB)	BER (2)	NFR(2) (dB)
Conventional DFE-D	1.1×10^{-2}	0	5×10^{-2}	7.8
Conventional DFE-EFF-D	1.1×10^{-2}	1.3	1.3×10^{-2}	5.8
DFE-based MUD	1.1×10^{-2}	3.3	5×10^{-2}	8.8
DFE-EFF-based MUD	1.1×10^{-2}	5	1.3×10^{-2}	7.6
DFE-Decorrelator D	1.1×10^{-2}	6.3	5×10^{-2}	9
DFE-EFF-Decorrelator D	1.1×10^{-2}	7	1.3×10^{-2}	8.1

Table 6.7: NFR comparison among different receiver structures under Pedestrian channel (Eb/No=15dB)

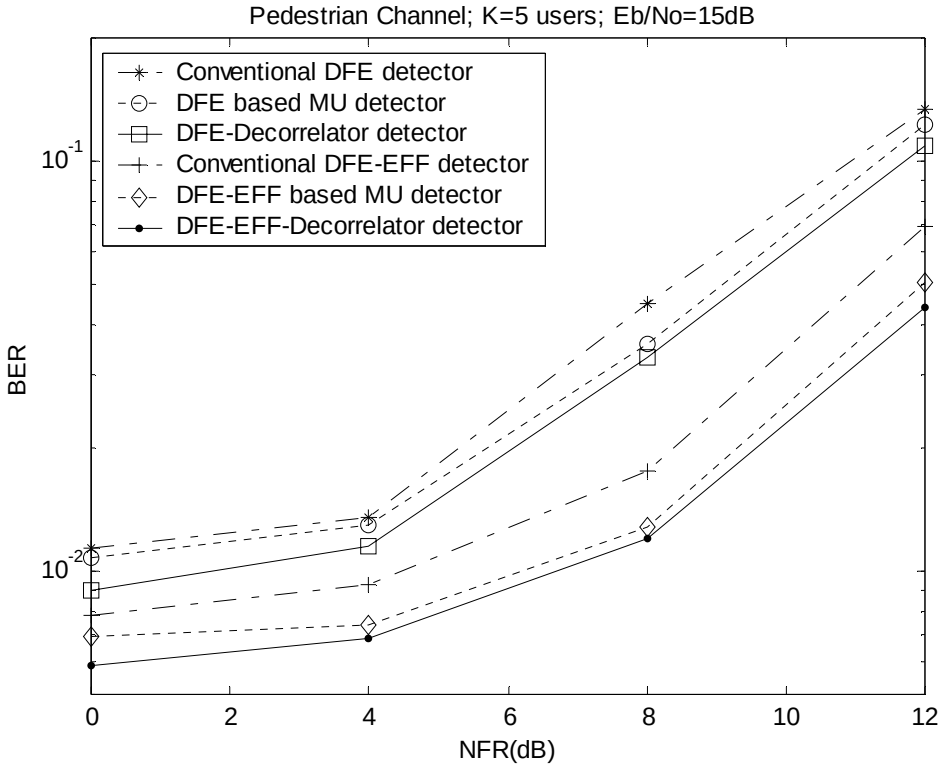

Figure 6.13: NFR comparison of among different receiver structures under Pedestrian channel (μ=1/aN; a =9; μ_e=0.008).

6. 5 Simulation Results under Vehicular Channels

Now we can switch our attention to the situation where the mobile station has a speed grater than the speed considered in the Pedestrian channel, usually known as Vehicular channel. In the Pedestrian channel we considered each path has the same Doppler frequency equal to 10Hz which corresponds to a mobile moving at speed of 5km/h assuming a carrier frequency of 2.2GHz (see Chapter 3, Section 3.6).

In this work, two Vehicular channels were used. For more information about these two channels please refer to Chapter 3, section 3.6.

It is known that when the speed of the mobile station increases, the performance of the receiver will degrades due to the rapid changes in channel characteristics.

Figures 6.14 and 6.15 show single user bound comparison under the different fading channels, namely Pedestrian, Vehicular 1 and Vehicular 2 channels. Figure 6.14 is the case where a =32 and μ_e=0.005 were chosen for the step size parameter and Figure 6.15 is the case where a =5 and μ_e=0.008 were chosen. Tables 6.8 and 6.9 present some comparison values among the different fading channels for the two cases (i.e. a=32 and a=5). It presents the amount of degradation as a result of increasing the mobile speed.

Structure	**Channel**	**BER**	**Eb/No (dB)**
One user DFE-D	Pedestrian	0.9×10^{-3}	25
	Vehicular 1	1.1×10^{-3}	25
	Vehicular 2	1.4×10^{-3}	25
One user DFE-EFF-D	Pedestrian	0.6×10^{-3}	25
	Vehicular 1	0.8×10^{-3}	25
	Vehicular 2	10^{-3}	25

Table 6.8: Single user bound BER comparison among different fading channels (μ=1/aN; a =32; μ_e=0.005)

Structure	Channel	BER	Eb/No (dB)
One user DFE-D	Pedestrian	5.7×10^{-3}	25
	Vehicular 1	6.5×10^{-3}	25
	Vehicular 2	7.3×10^{-3}	25
One user DFE-EFF-D	Pedestrian	1.7×10^{-3}	25
	Vehicular 1	2×10^{-3}	25
	Vehicular 2	2.3×10^{-3}	25

Table 6.9: Single user bound BER comparison among different fading channels (μ=1/aN; a =5; μ_e=0.008)

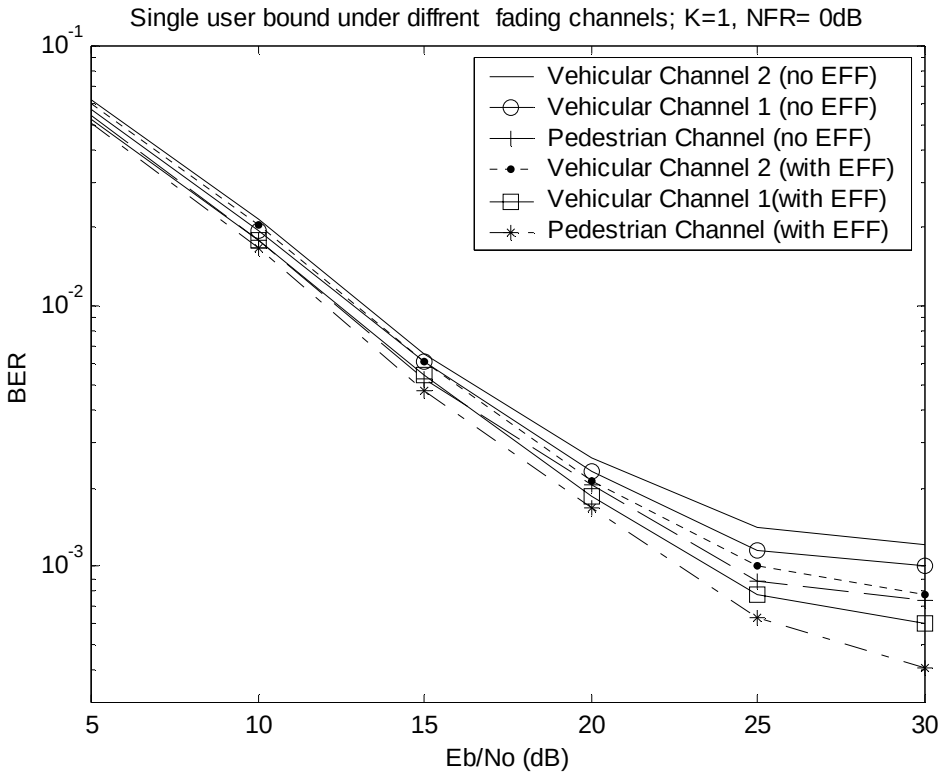

Figure 6.14: Single user bound BER performance of DFE and DFE-EFF detectors under Pedestrian, Vehicular 1 and Vehicular 2 channels (μ=1/aN; a =32; μ_e=0.005).

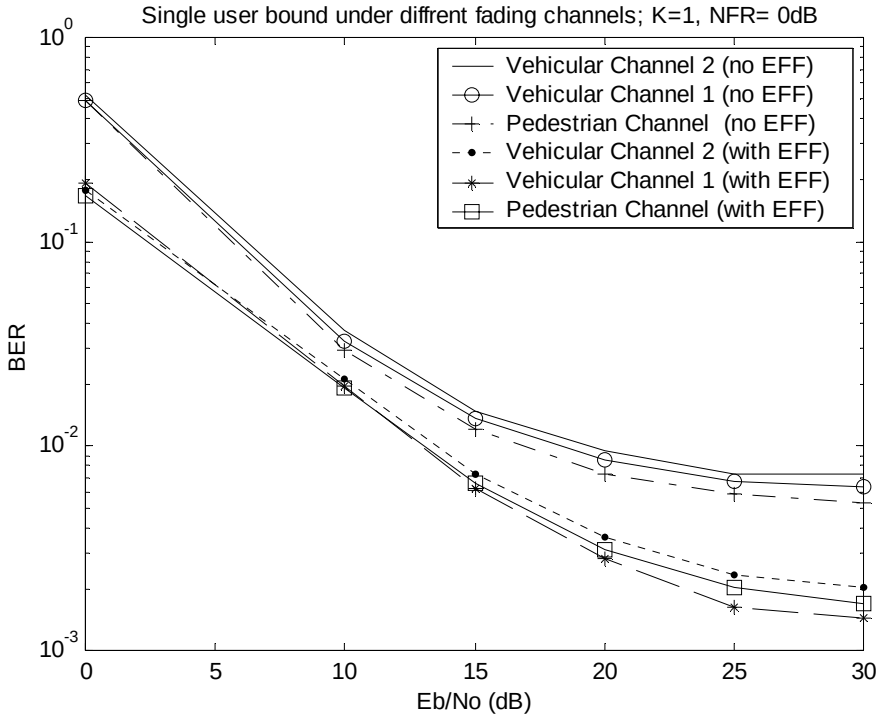

Figure 6.15: Single user bound BER performance of DFE and DFE-EFF detectors under Pedestrian, Vehicular 1 and Vehicular 2 channels (μ=1/aN; a =5; μ_e=0.008).

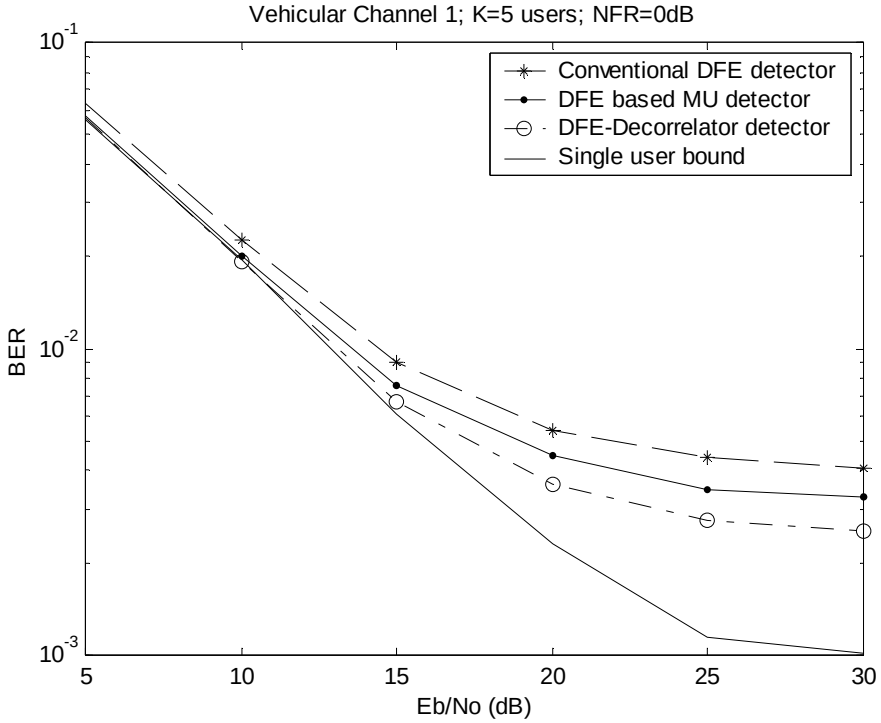

Figure 6.16: BER performance of conventional DFE, DFE-based MUD and DFE-DD under Vehicular channel 1 (μ=1/aN; a =32; μ_e=0.005).

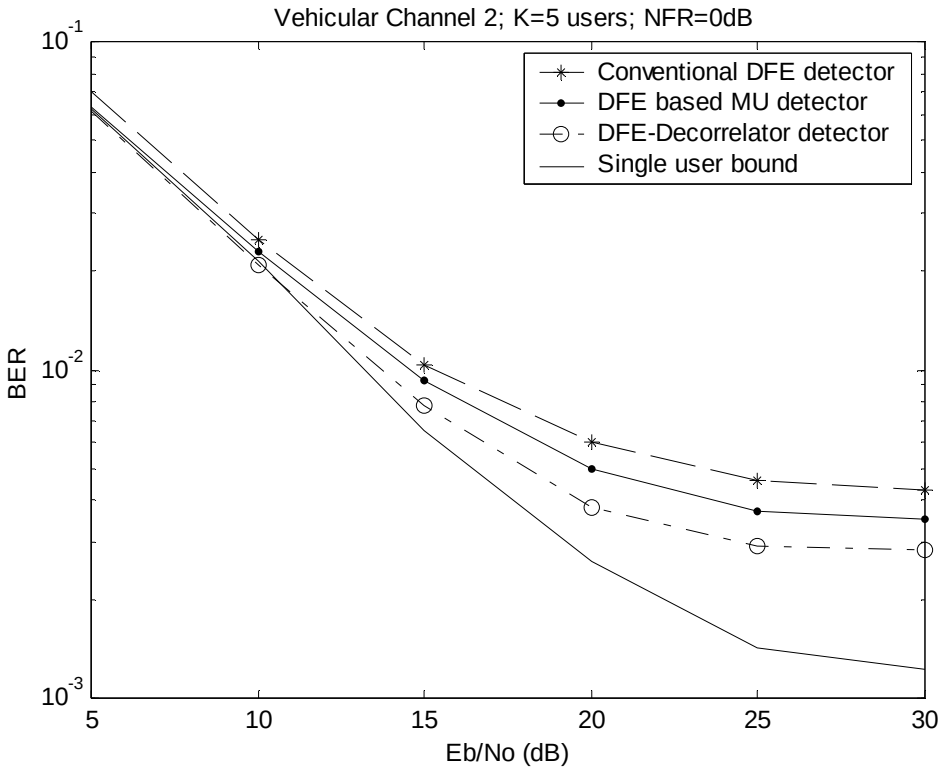

Figure 6.17: BER performance of conventional DFE, DFE-based MUD and DFE-DD under Vehicular channel 2 (μ=1/aN; a =32; μ_e=0.005).

Structure	**Channel**	**BER**	**Eb/No (dB)**
One user bound	Vehicular 1	6×10^{-3}	15.1
	Vehicular 2	6×10^{-3}	15.5
Conventional DFE	Vehicular 1	6×10^{-3}	19
	Vehicular 2	6×10^{-3}	20
DFE-based MUD	Vehicular 1	6×10^{-3}	17.3
	Vehicular 2	6×10^{-3}	18.3
DFE-DD	Vehicular 1	6×10^{-3}	15.9
	Vehicular 2	6×10^{-3}	16.7

Table 6.10: BER comparison among different receiver structures (NFR=0dB, μ=1/aN; a=32; μ_e=0.005)

Figures 6.16 and 6.17 show the BER performance comparison of the conventional DFE, DFE-based MUD and DFE-DD for Vehicular channel 1 and 2, respectively. In the simulation of these figures, 5 users are considered active and all have the same power level. The step size parameter used is the first case where a =32 and μ_e=0.005. It is obvious that the performance of the receivers in case of Vehicular channel 1 is better than of those in the case of Vehicular channel 2. For a better insight, Table 6.10 presents some Eb/No comparison for these receivers under the two channels at a given BER. As we can see from Table 6.10, around 1dB degradation is noted at BER=6×10^{-3} in the case of conventional DFE and DFE-based MUD as a result of increasing the Doppler frequency from 100Hz to 135Hz. In the case of DFE-DD around 0.8dB difference is noted. In the simulation of Figures 6.16 and 6.17, no EFF is used. Figures 6.18 and 6.19 present the case where EFF is used. Again, for a good comparison among the different receiver structures under Vehicular channel 1 and 2, Table 6.11 presents some comparison values. In the case of conventional DFE-EFF detector, 1.5dB difference was noted between Vehicular channel 1 and 2 at BER=6×10^{-3}. For DFE-EFF-based MUD, 0.7dB difference was noted which mean that this structure is less sensitive to the increase in Doppler frequency than the conventional DFE-EFF detector. For the third structure which is the DFE-EFF-DD, 0.6dB difference was noted which is close to the DFE-EFF-based MUD.

Now for the case where the step size parameter is large (i.e. a=5 and μ_e=0.008), Figures 6.20 and 6.21 show the BER performance comparison of all receiver structures under Vehicular channel 1 and 2.

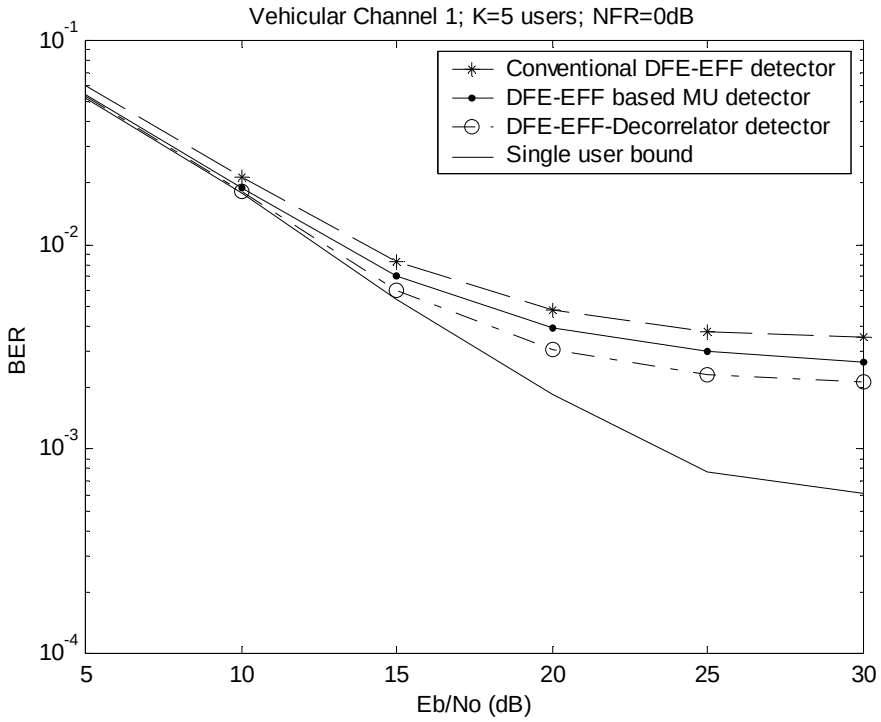

Figure 6.18: BER performance of conventional DFE-EFF, DFE-EFF-based MUD and DFE-EFF-DD under Vehicular channel 1 (μ=1/aN; a =32; μ_e=0.005).

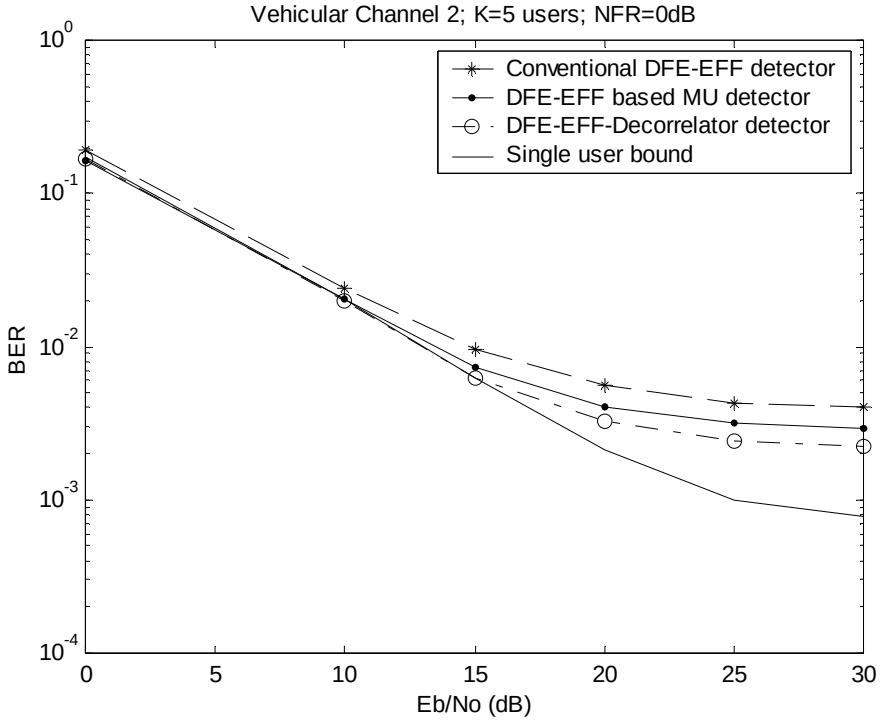

Figure 6.19: BER performance of conventional DFE-EFF, DFE-EFF-based MUD and DFE-EFF-DD under Vehicular channel 2 (μ=1/aN; a =32; μ_e=0.005).

Structure	Channel	BER	Eb/No (dB)
One user bound	Vehicular 1	6×10^{-3}	14.6
	Vehicular 2	6×10^{-3}	15
Conventional DFE-EFF	Vehicular 1	6×10^{-3}	17.9
	Vehicular 2	6×10^{-3}	19.4
DFE-EFF-based MUD	Vehicular 1	6×10^{-3}	16.2
	Vehicular 2	6×10^{-3}	16.9
DFE-EFF-DD	Vehicular 1	6×10^{-3}	15.2
	Vehicular 2	6×10^{-3}	15.8

Table 6.11: BER comparison among different receiver structures (NFR=0dB, μ=1/aN; a=32; μ_e=0.005)

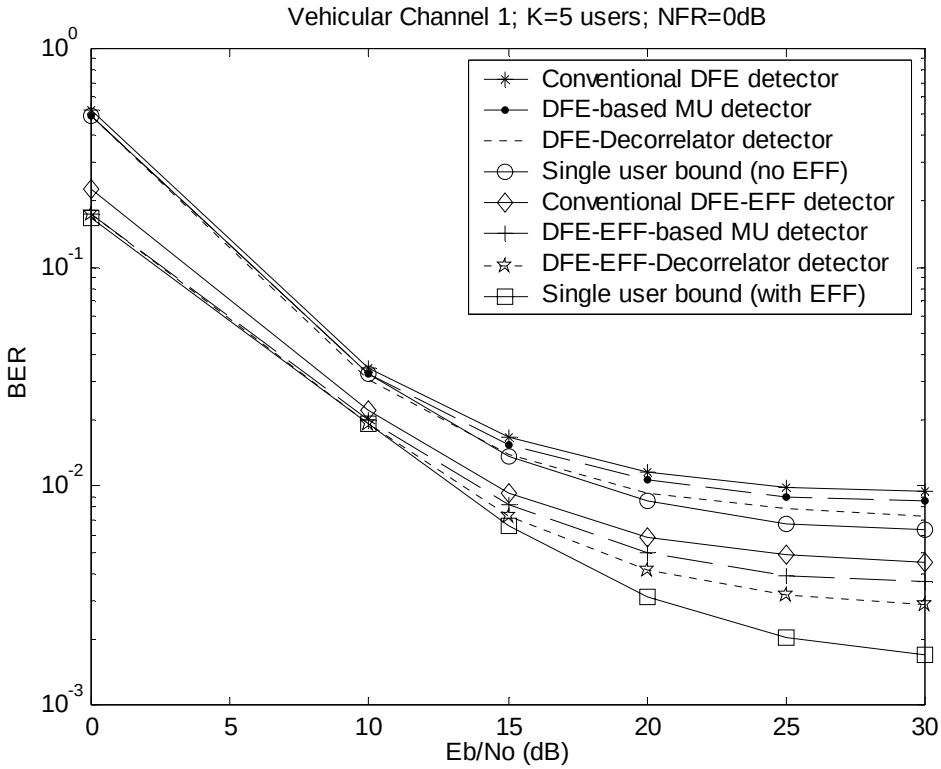

Figure 6.20: BER performance comparison among different receiver structures under Vehicular channel 1 (μ=1/aN; a =5; μ_e=0.008).

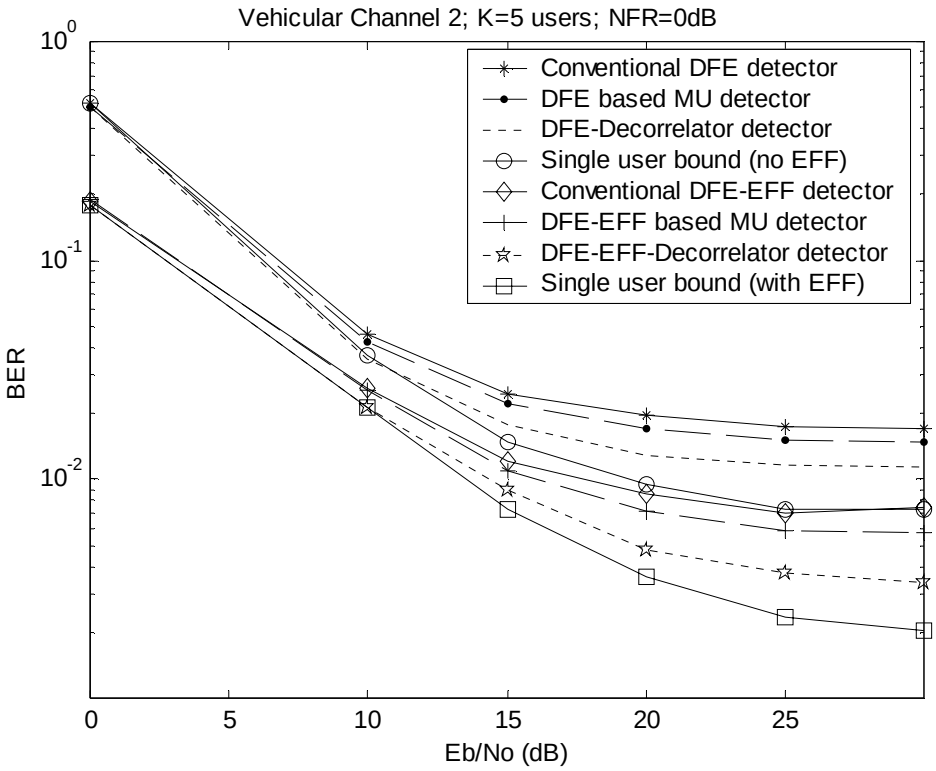

Figure 6.21: BER performance comparison among different receiver structures under Vehicular channel 2 (μ=1/aN; a =5; μ_e=0.008).

Structure	**Channel**	**BER**	**Eb/No (dB)**
One user bound	Vehicular 1	1.6×10^{-2}	14.13
	Vehicular 2	1.6×10^{-2}	14.71
Conventional DFE	Vehicular 1	1.6×10^{-2}	15.7
	Vehicular 2	1.6×10^{-2}	30
DFE-based MUD	Vehicular 1	1.6×10^{-2}	14.8
	Vehicular 2	1.6×10^{-2}	22.5
DFE-DD	Vehicular 1	1.6×10^{-2}	14.23
	Vehicular 2	1.6×10^{-2}	16.6

Table 6.12: BER comparison among different receiver structures (NFR=0dB, μ=1/aN; a=5; μ_e=0.008)

Table 6.12 presents some Eb/No comparison values between Vehicular channel 1 and 2 at a given BER for structures that have no EFF, while Table 6.13 presents the same thing but with structures that have EFF. As we can see from Table 6.12, the difference between Vehicular channel 1 and Vehicular channel 2 in case of Conventional DFE is around 15dB at BER=1.6×10^{-2}. A difference of 7.7dB was noted in the case of DFE-based MUD while a difference of 2.4dB was noted in the case of DFE-DD.

In the case of using EFF, Table 6.13 shows a difference of 8dB at BER=0.7×10^{-2} in the case of conventional DFE-EFF. It was difficult to compare at BER=1.6×10^{-2} as in the previous case due to the big gap between the performance of structures with EFF and without EFF as it can be seen from Figures 6.20 and 6.21. Now in the case of DFE-EFF-based MUD a difference of 3.3dB was noted while a difference of 1.5dB was noted in the case of DFE-EFF-DD.

Structure	**Channel**	**BER**	**Eb/No (dB)**
One user bound	Vehicular 1	0.7×10^{-2}	14.66
	Vehicular 2	0.7×10^{-2}	15.34
Conventional DFE-EFF	Vehicular 1	0.7×10^{-2}	18.2
	Vehicular 2	0.7×10^{-2}	26.2
DFE-EFF-based MUD	Vehicular 1	0.7×10^{-2}	16.6
	Vehicular 2	0.7×10^{-2}	19.93
DFE-EFF-DD	Vehicular 1	0.7×10^{-2}	15.44
	Vehicular 2	0.7×10^{-2}	16.94

Table 6.13: BER comparison among different receiver structures (NFR=0dB, $\mu=1/aN$; $a=5$; $\mu_e=0.008$)

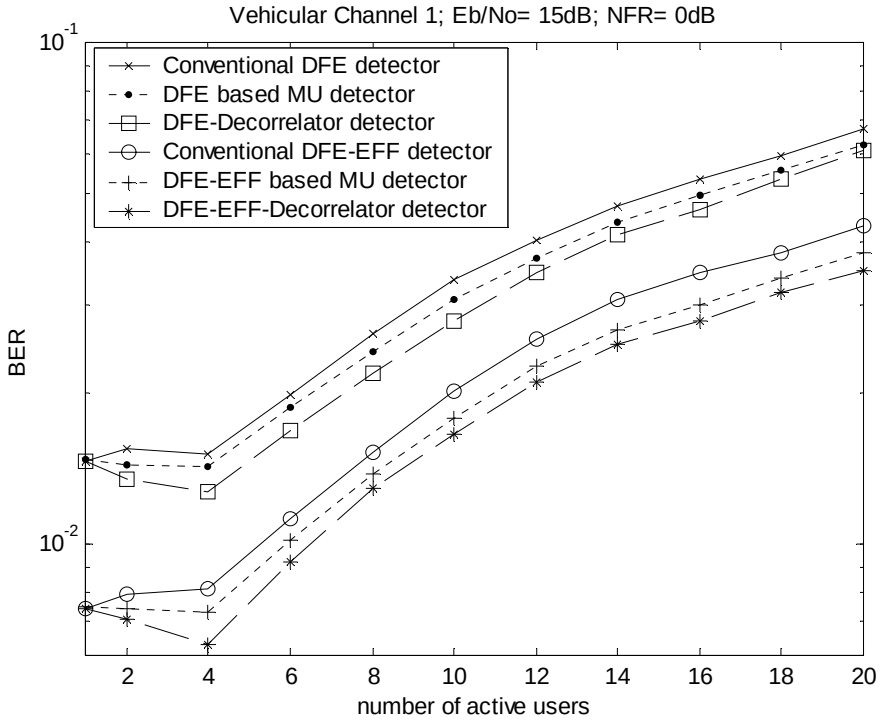

Figure 6.22: System capacity comparison among different receiver structures under Vehicular channel 1 (μ=1/aN; a =5; μ_e=0.008).

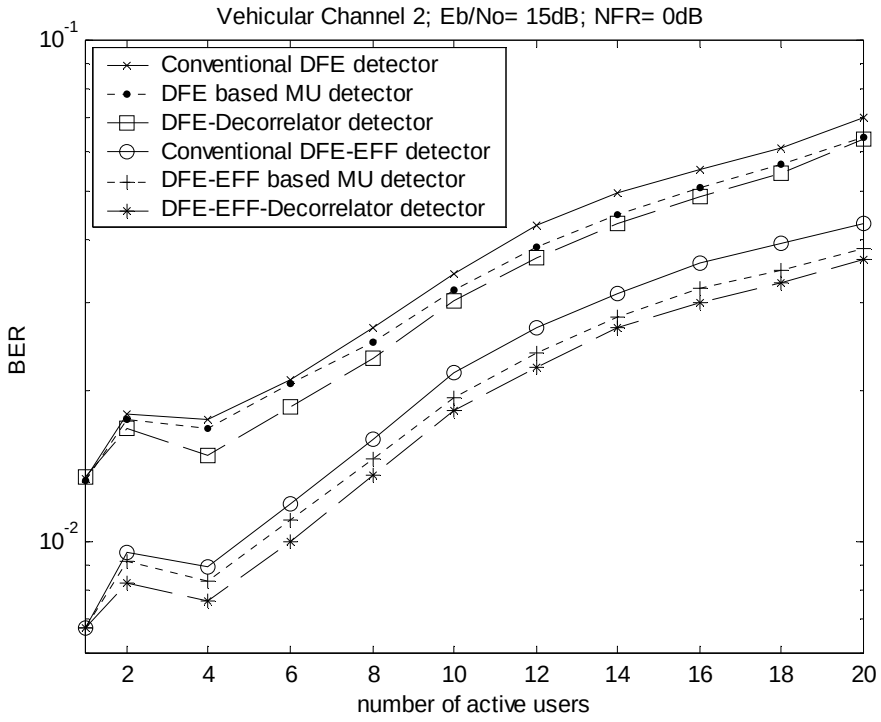

Figure 6.23: System capacity comparison among different receiver structures under Vehicular channel 2 (μ=1/aN; a =5; μ_e=0.008).

Figures 6.22 and 6.23 show the system capacity comparison among different receiver structures under Vehicular channel 1 and Vehicular channel 2, respectively. We assume all users transmitting at same power level. The step size parameter was chosen such that a=5 and μ_e=0.008. From the figures we can see a big difference between those structures use EFF and those not using EFF. By using EFF, an average of 5 more users can be accommodated at BER=1.5×10^{-2} as shown in Table 6.14 when the channel is the Vehicular channel 1. In the case of Vehicular channel 2, By using EFF, an average of 6 more users can be accommodated at BER=1.8×10^{-2} as shown in Table 6.15.

As in the case of Pedestrian channel, we can see there is no much difference between the conventional DFE(EFF) and DFE(EFF)-based MUD either in the case where Vehicular channel 1 used or Vehicular channel 2. However, it is expected that as the number of users increases and the near-far problem exists, the conventional DFE(EFF) will degrades much more than the DFE(EFF)-based MUD because of the shortage of the conventional DFE(EFF) in canceling MAI.

Structure	BER	System Capacity (K-users)
Conventional DFE-D	1.5×10^{-2}	1.5
Conventional DFE-EFF-D	1.5×10^{-2}	8
DFE-based MUD	1.5×10^{-2}	4.4
DFE-EFF-based MUD	1.5×10^{-2}	9
DFE-Decorrelator D	1.5×10^{-2}	5.4
DFE-EFF-Decorrelator D	1.5×10^{-2}	9.4

Table 6.14: System capacity comparison among different receiver structures under Vehicular Channel 1 (Eb/No=15dB and NFR=0dB; μ=1/aN; a =5; μ_e=0.008)

Structure	BER	System Capacity (K-users)
Conventional DFE-D	1.8×10^{-2}	2
Conventional DFE-EFF-D	1.8×10^{-2}	8.8
DFE-based MUD	1.8×10^{-2}	4.7
DFE-EFF-based MUD	1.8×10^{-2}	9.6
DFE-Decorrelator D	1.8×10^{-2}	5.7
DFE-EFF-Decorrelator D	1.8×10^{-2}	10

Table 6.15: System capacity comparison among different receiver structures under Vehicular Channel 2 (Eb/No=15dB and NFR=0dB; $\mu=1/aN$; a =5; μ_e=0.008)

Structure	BER (1)	NFR(1) (dB)	BER (2)	NFR(2) (dB)
Conventional DFE-D	1.1×10^{-2}	0.3	5.2×10^{-2}	8
Conventional DFE-EFF-D	1.1×10^{-2}	5.13	1.4×10^{-2}	6.14
DFE-based MUD	1.1×10^{-2}	1.14	5.2×10^{-2}	9
DFE-EFF-based MUD	1.1×10^{-2}	6.6	1.4×10^{-2}	8
DFE-Decorrelator D	1.1×10^{-2}	3.33	5.2×10^{-2}	9.25
DFE-EFF-Decorrelator D	1.1×10^{-2}	7.3	1.4×10^{-2}	8.3

Table 6.16: NFR comparison among different receiver structures under Vehicular channel 1(Eb/No=15dB)

In Figures 6.24 and 6.25, the performance of receiver structures was investigated under near-far effect for both Vehicular channel 1 and Vehicular channel 2, respectively. 5 users are in the system and one of the users is transmitting at high power. Eb/No was set to 15dB. The step size parameter is the same as in Pedestrian channel i.e. a =9 and μ_e=0.008. From the figures we can see that both DFE(EFF)-based MUD and DFE(EFF)-DD have better near-far resistance at high NFR than the conventional DFE(EFF) detector. Tables 6.16 and 6.17 give some comparison values among different structures.

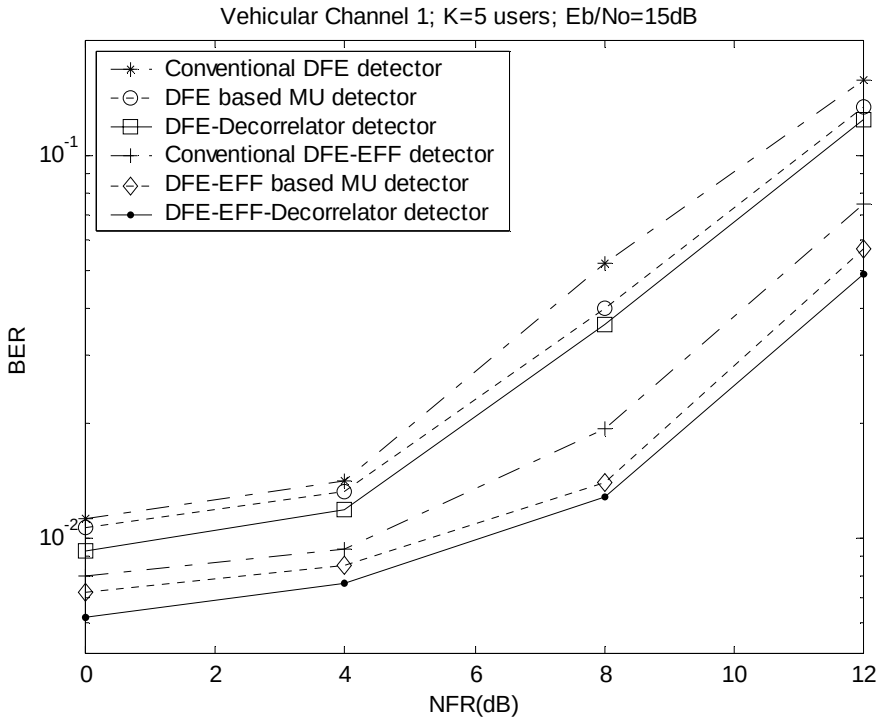

Figure 6.24: NFR comparison of among different receiver structures under Vehicular channel 1 (μ=1/aN; a =9; μ_e=0.008).

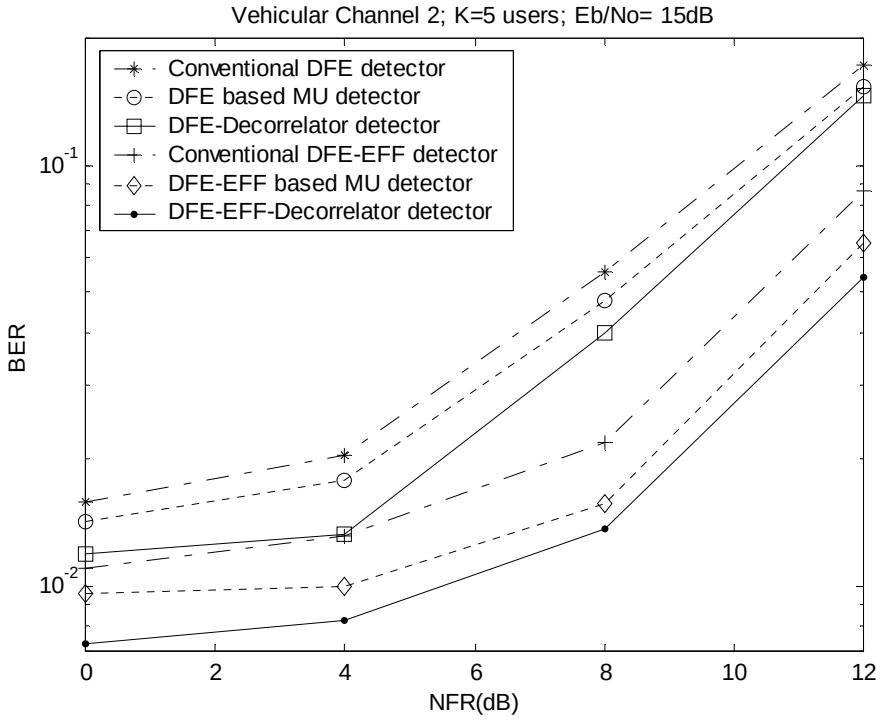

Figure 6.25: NFR comparison of among different receiver structures under Vehicular channel 2 (μ=1/aN; a =9; μ_e=0.008).

Structure	BER (1)	NFR(1) (dB)	BER (2)	NFR(2) (dB)
Conventional DFE-D	1.7×10^{-2}	1.1	10^{-1}	10
Conventional DFE-EFF-D	1.7×10^{-2}	6	2×10^{-2}	7.3
DFE-based MUD	1.7×10^{-2}	3.23	10^{-1}	10.6
DFE-EFF-based MUD	1.7×10^{-2}	8.2	2×10^{-2}	8.7
DFE-Decorrelator D	1.7×10^{-2}	4.9	10^{-1}	10.8
DFE-EFF-Decorrelator D	1.7×10^{-2}	8.6	2×10^{-2}	9.1

Table 6.17: NFR comparison among different receiver structures under Vehicular channel 2 (Eb/No=15dB)

Now, to see the effect of Doppler frequency on the receiver structures under near-far problem, a comparison among the 3 different fading channels had been made. Figures 6.26, 6.27 and 6.28 presents a comparison among Pedestrian, Vehicular 1 and Vehicular 2 channels for the conventional DFE(EFF) detector, DFE(EFF)-based MUD and DFE(EFF)-DD, respectively.

By looking to Figure 6.26, the conventional DFE detector under Pedestrian and Vehicular channel 1 almost have the same near far resistance when NFR varies from 0 to 7dB. This is also true when EFF is used. However, after 8dB the performance under Vehicular channel 1 start to degrade such that the performance reaches the Vehicular channel 2. When the channel is Vehicular channel 2, around 5.5dB difference is noted between this channel and the other two channels at BER=1.6×10^{-2} in case EFF is not used and the same difference is noted at BER=1.1×10^{-2} in case EFF is used.

Now the second case is when DFE(EFF)-base MUD is used. By looking to Figure 6.27, the DFE-based MUD under Pedestrian and Vehicular channel 1 almost have the same near far resistance when NFR varies from 0 to 7dB. However, this is not the case when EFF is used. Comparing among the different three channels, there is a difference of 4.5dB between the Vehicular channel 2 and the other two channels at BER=1.4×10^{-2} in

case EFF is not used. In the case where EFF is used, a difference of 5.1dB is noted between the Vehicular channel 1 and 2 at BER=9.5×10^{-3} and a difference of 0.8dB between the Vehicular channel 1 and the Pedestrian channel at the same BER level.

Finally, Figure 6.28, presents the case where DFE(EFF)-DD is used. It can be noted that the DFE-DD approximately has the same near-far resistance performance up to 8dB when the channels are Vehicular 1 and Pedestrian. This not the case when EFF is used. A difference of 1dB between the Pedestrian and Vehicular channel 1 is noted at BER=7.3×10^{-3} and a difference of 3.4dB at the same BER is noted between the Vehicular channels 1 and 2.

One thing to be noted is that, in all different structures under the different channels used in this work, a good power control is needed for NFR grater than 6dB.

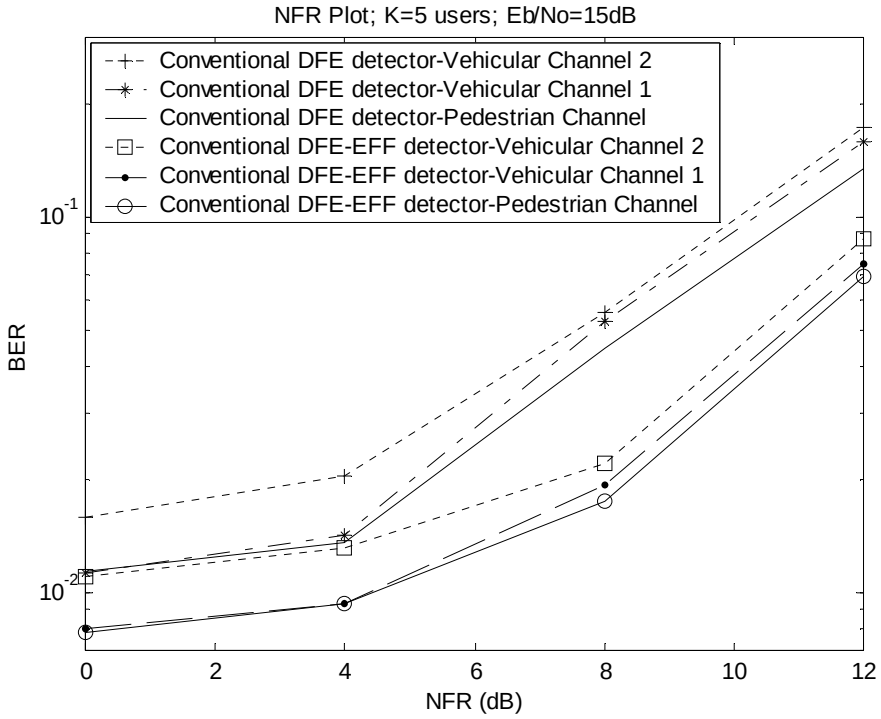

Figure 6.26: NFR comparison of among different fading channel for both Conventional DFE and DFE-EFF detector (μ=1/aN; a =9; μ_e=0.008).

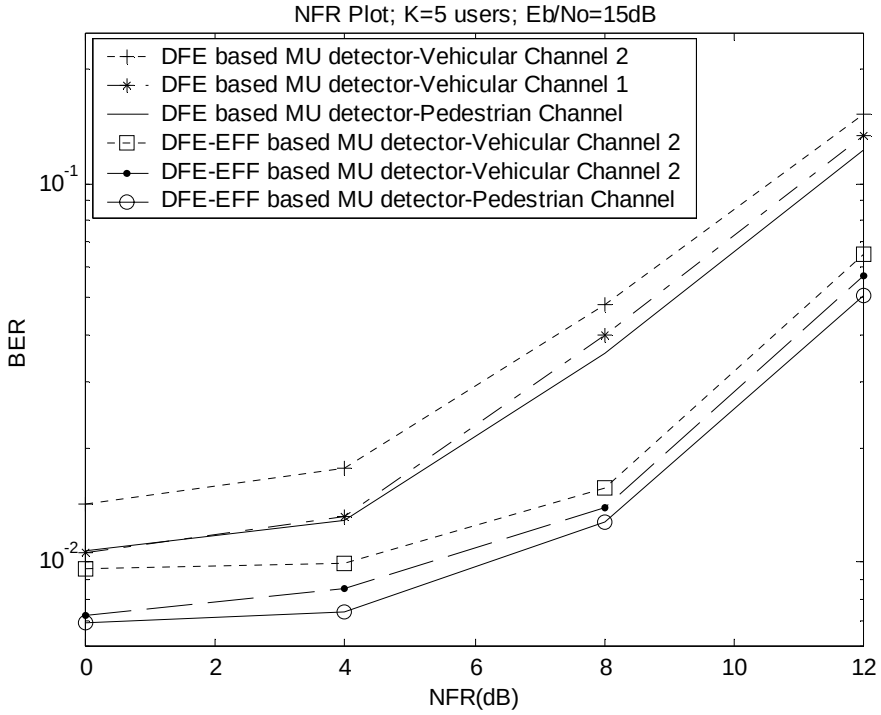

Figure 6.27: NFR comparison of among different fading channel for both DFE and DFE-EFF-based MUDs (μ=1/aN; a =9; μ_e=0.008).

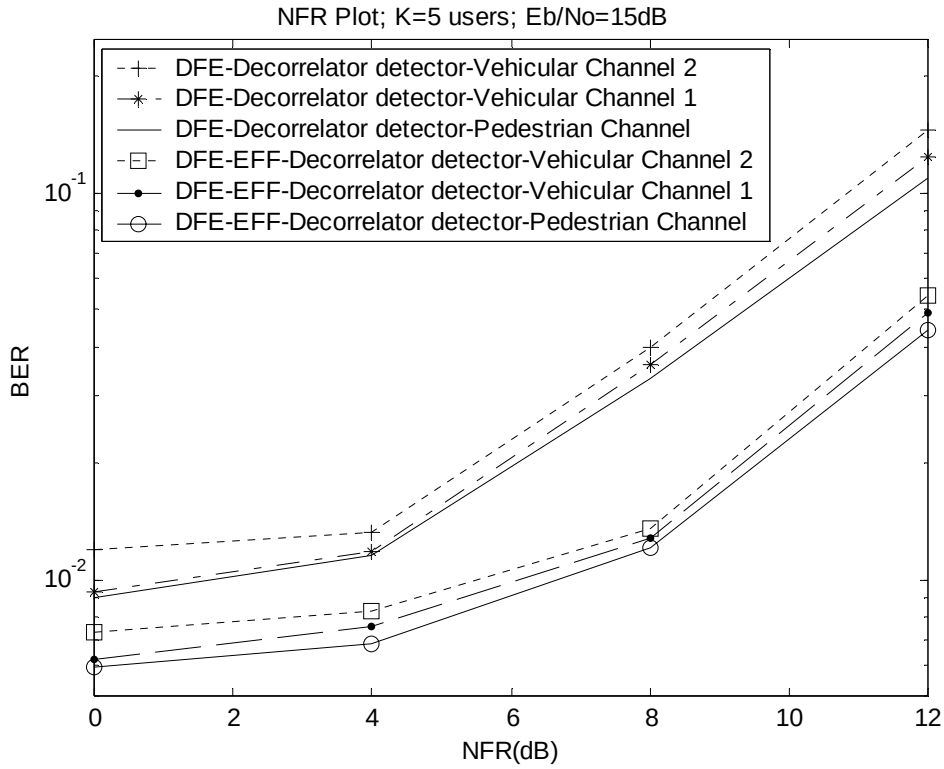

Figure 6.28: NFR comparison of among different fading channel for both DFE-DD and DFE-EFF-DD (μ=1/aN; a =9; μ_e=0.008).

Chapter 7

Conclusions and Future Work

This chapter concludes the thesis by summarizing the important observations, contributions, results and advantages and disadvantages of the receiver structures. It also highlights some research work that can be done in future.

7.1 Conclusions

In this work, a new MUD detector was proposed. In this new structure the DFE was used as a MUD detector in which MAI is cancelled from all users after equalizing and detecting a bit. This structure has been modified by adding and error feedback filter to enhance the performance of the DFE-based MUD. It has been shown that this structure gives better performance than the conventional DFE detector and acceptable performance compared to the Decorrelator detector.

In the simulation results it has been observed that under static channels, adding EFF to the DFE will enhance the overall performance by around 1 dB at BER=10^{-3}. Also, the performance of DFE-EFF-based MUD approaches the performance of the DFE-EFF-DD at high Eb/No under the assumption of perfect power control which means the same performance but with low complexity. Moreover, the performance of the conventional

DFE(EFF) detector under near-far problem degrades while both DFE(EFF) based MUD and DFE(EFF)-DD give a reasonable performance. The reason for bad performance of the conventional DFE(EFF) is that this detector has no way of canceling MAI as a result of increasing the number of active users.

Another thing that has been observed is that the DFE with EFF performs well in a noisy environment. This is obvious, since a noisy environment will lead to high probability of error, which means more errors, and hence more contribution from the EFF.

Moreover, a strong relationship among the MSE, BER and the step size parameter of the LMS algorithm has been observed. There are two cases; one is when the step size parameter is small and the other is when this parameter is large. The first case is when we have a small step size parameter. This case will result in low level of miss-adjustment of the equalizer taps to the optimum values with the expense of low rate of convergence. As a result, low MSE can be achieved, which leads to a good overall performance. Note that, low MSE will result in low BER performance.

The other case is when the step size parameter is large. In this case high rate of convergence will be observed but with high level of miss-adjustment. As consequence of this miss-adjustment high MSE will be observed and hence high BER.

The main disadvantage of small step size parameter is the low rate of convergence of the equalizer taps to the optimum value. Practically, high rate of convergence is needed during the training mode of the equalizer.

Since DFE with EFF can achieve acceptable BER performance with high rate of convergence using large step size parameter, EFF can be used during the training mode

where high rate of convergence is needed. After convergence, i.e. during tracking mode, a smaller step size parameter can be used.

Another thing that should be noted is that a large step size parameter for the EFF should be avoided because it might lead to stability problems. Instead of compensating for the errors, more errors might be added.

Under fading channels, the DFE(EFF) based MUD gives an overall acceptable performance in the sense of BER, system capacity and near far resistance. However, it has been observed that the overall performance of all receiver structures degrades as a result of an increase in the Doppler frequency.

The advantages and disadvantages of the conventional DFE(EFF), the DFE(EFF)-based MUD and the DFE(EFF)-Decorrelator detector were discussed.

The main advantage of the conventional DFE(EFF) detector is its simplicity. This detector follows single user detection process. It doesn't require the pervious knowledge of all users PN codes, only the intended user code. The complexity of this detector is the lowest among the other detectors as we saw.

However, the main disadvantage of this detector is its poor performance as a result of an increase in the number of active users. This detector has no way to cancel MAI. Also, this detector has less near-far resistance capability.

The second detector, which is the DFE(EFF)-Decorrelator detector, has the best performance among the others. However, it is the most complex detector due to the need of matrix inversion. The decorrelator alone has a complexity of order $O(K^3)$ where K is the number of users. Another disadvantage of this detector is the need for the knowledge of PN codes of all active users.

The third detector is the DFE(EFF)-based MUD, which is the proposed one. This detector has better performance than the conventional DFE(EFF) detector and acceptable performance compared to the DFE(EFF) decorrelator detector. It has a reasonable complexity. However, this detector has a disadvantage. When a wrong bit is detected, degradation in performance will result because instead of canceling MAI from other users, error will be added. However, the effect of this problem can be solved or reduced by partial cancellation, i.e. instead of canceling a complete bit, a partial of a bit is used to cancel MAI. This can be done by adding a tap that can be updated with an adaptive algorithm.

7.2 Future Work

The following things can be considered in future work:

- Comparison between the performance of the DFE(EFF)-Decorrelator detector and the Decorrelator-DFE(EFF) detector. In other word, instead of applying the Decorrelator after equalization, it can be done before equalization.
- Investigation of the performance of DFE(EFF)-based MUD when partial MAI cancellation is considered.
- Trying to improve the performance of the DFE and find a proper solution to the error propagation problem.

Bibliography

[1] S. Verdu, Multiuser Detection, Cambridge University Press. 1998.

[2] A.J. Viterbi, CDMA Principles of Spread-Spectrum Communications, Reading. Mass.: Addison-Wesley Publishing Company, 1995.

[3] H. Liu. Signal Processing Applications in CDMA Communications, Artech House, Inc. 2000.

[4] J. B. Groe and L. E. Larson, CDMA Mobile Radio Design, Artech House, Inc. 2000.

[5] S. Moshavi, “Multiuser Detection for DS-CDMA Communications," IEEE Communications magazine, pp. 124-136, Oct. 1996.

[6] S. Qureshi, “Adaptive Equalization” Proc. IEEE, vol. 73, pp. 1349-1387, September 1985.

[7] J. Proakis, Digital Communications, 3rd edition, McGraw-Hall, 1995.

[8] A. Klein, G. K. Kaleh and P. W. Baier. “Equalizers for multi-user detection in code division multiple access mobile radio systems,” IEEE. 1994.

[9] K. Schneider, “Optimum Detection of Code Division Multiplexed Signals,” IEEE Trans. Aerospace Elect. Sys. Vol. AES-15, Jun. 1979, pp. 181-185.

[10] R. Kohno, M. Hatori, and H. Imai, “Cancellation Techniques of Co-Channel Interference in Asynchronous Spread Spectrum Multiple Access Systems,” Elect. And Commun. in Japan, vol. 66-A, no.5 1983, pp. 20-29.

[11] R. Lupas and S. Verdu, “Near-Far Resistance of Multi-User Detectors in Asynchronous Channels,” IEEE Trans. Commun. vol. 38, no. 4, Apr. 1990, pp. 496-508.

[12] R. Lupas and S. Verdu, “Linear Multiuser Detectors for Synchronous Code Division Multiple-Access Channels,” IEEE Trans. Info. Theory, vol. 35, no. 1, Jan. 19989, pp. 123-136.

[13] G. Xue, J. Weng, T. Le-Ngoc and S. Tahar, “Multiuser Detection Techniques: An Overview.” Department of Electrical and Computer Engineering, Concordia University, October 1998.

[14] P. Patel and J. Holtzman, “Analysis of a simple successive interference cancellation scheme in DS/CDMA system,” IEEE J. Select. Areas Communication, vol. 12, pp. 509-519, June 1994.

[15] M. K. Varanasi and B. Aazhang, “Near-optimum detection in synchronous code-division multiple-access communications,” IEEE Trans. Communication., vol. 39, pp.725-736, May 1991.

[16] N. Buehrer and B. Woerner, “A comparison of multiuser reciver for cellular CDMA,” in Proc. IEEE Globecom’96, pp. 1571-1577, Nov.1996.

[17] M. Juntti, M. Latva-aho and M. Heikkila, “Performance comparison of PIC and decorating multiuser receiver in fading channels,” in Proc. IEEE Globecom’97, pp. 609-613, 1997.

[18] D.W. Kim, S.H. Han, M.S. Eun, J.S. Choi and Y.S.Cho, “ An Adaptive Decision Feedback Equalizer using Error Feedback,” IEEE Trans. on Consumer Electronics, Vol.42, no. 3, August 1996.

[19] T. S. Rappaport, B D Woerner, and J H Reed, Wireless Personal Communications, Kluwer Academic Publishers, 1996.

[20] R. L. Pickholtz, , D. L. Schilling and L. B. Milstein,“Theory of Spread-Spectrum Communications—A Tutorial” IEEE Trans. Commun., vol. 30, no. 5, pp 855-884, May 1982.

[21] An overview of the application of code division multiple access (cdma) to digital cellular systems and personal cellular networks. Qualcomm Inc., 1992.

[22] Robert A. Scholtz, “The Origins of Spread-Spectrum Communications”, IEEE Transactions on Communications, Vol.Com.-30, No. 5, May 1982.

[23] Robert C. Dixon, Spread Spectrum Systems with Commercial Applications, 3rd edition, 1994, John Wiley & Sons.

[24] J. D. Gipson, The Communications Handbook, CRC Press, IEEE Press 1997.

[25] T. Ojanperä, P. Ranta, S. Hämäläinen, A. Lappeteläinen, Analysis of CDMA and TDMA for 3rd Generation Mobile Radio Systems, VTC’97.

[26] Nathan Yee, Jean-Paul M.G. Linnartz, and Gerhard. Fettweis. Multi-carrier-cdma in indoor wireless network. *IEICE Transaction on Communications, Japan*, E77 B(7):900-904, July 1994.

[27] R. L. Peterson, R. E. Ziemer, D. E. Borth, Introduction to Spread Spectrum Communications, Prentice-Hall, 1995.

[28] D. L. Nicholson, Spread Spectrum Signal Design, Computer Science Press, Maryland, 1988.

[29] D. V. Sarwate and M. B. Pursley, “Cross-correlation Properties of Pesudo-random and Related Sequences,” Pro. IEEE, Vol. 68, pp. 593-619, May 1980.

[30] Stefan Parkvall, “Variability of User Performance in Cellular DS-CDMA–Long versus Short Spreading Sequences”, IEEE Transactions on Communications, Vol. 48, No. 7, July 2000

[31] S. Ulukus and R. D. Yates, “Stochastic Power Control for cellular Radio Systems” IEEE Trans. On Communications, Vol. 46, No. 6, June 1998.

[32] A. Duel-Hallen, J. Holtzman, and Z. Zvonar, “Multiuser Detection for CDMA Sysems” IEEE Personal Communications. April 1995

[33] S. Verdu,“Minmum Probability of Error for Asynchronous Multiuser Channels” IEEE Trans. Info. Theory, vol 32, no.1, pp.85-96. Jan. 1986.

[34] Bernard Sklar. “Rayleigh Fading Channels in Mobile Digital communication Systems; Part I: Characterization.” IEEE communications Magazine, July 1997.

[35] Michel C. Jeruchim, Philip Balaban, K. Sam Shanmugan, Simulation Of Communication Systems. Publisher: Plenum, 1992.

[36] Akbar M. Sayeed and Behnaam Aazhang. “Communcation over Multipath Fading Cahnnels: A Time-Frequencey Perspective.” PIMRC’97, Helsinki, Finland, September 1997.

[37] P. A. Bello, “Characterization of randomly time-varying linaer channels”, IEEE Trans. on Commun. Syst., vol. 11, pp. 360-393, December 1963.

[38] W. C. Jakes, Microwave Mobile Communication. Newyork, Willey, 1974.

[39] R. H. Clarke, “A statistical theory of mobile-radio reception”, Bell System Technical Journal, vol. 47, pp. 957-1000, July-August 1968.

[40] M. F. Pop and N. Beaulieu, “Statistical investigation of sum-of-sinusoids fading channel simulators,” in Global Telecommunications Conference (GLOBECOM '99), vol. 1a, pp. 419-426, 2000.

[41] M. Patzold, U. Killat, F. Laue, and Y. Li, “On the statistical properties of deterministic simulation models for mobile fading channels”, itvt, vol. 47, Feb.1998.

[42] P. Dent, G. Bottomley, and T. Croft, “Jakes fading model revisited”, Electronics Letters, vol. 29, pp. 1162-1163, 24 June 1993.

[43] ETSI Tech. Rep. 101 112 V3.2.0, “UMTS; Selection procedures for the choice of RTT of the UMTS," April 1998.

[44] S. Haykin, Adaptive Filter Theory. Upper Saddle River, NJ, Prentice Hall, 1996.

[45] B. Widrow, J.R. Glover, Jr., J.M. McCool, J. Kaunitz, C.S. Williams, J.R. Zeidler, E. Dong, Jr., and R.C. Goodlin, “Adaptive noise cancelling: Principles and applications,” IEEE Proceedings, vol. 63, no. 12, pp. 1692-1716, 1975.

[46] L. Makhoul, “Linear predition a tutorail review,” IEEE Proceedings, vol. 63, no. 4, pp. 561-580, 1975.

[47] C. Cowan and P. Grant, Adaptive Filters. Englewood Clifs, NJ: Prentice Hall, 1985.

[48] Iliev, G. and Kasabov, N. “ Channel Equalization Using Adaptive Filtering With Averaging’. http//:divcom.otago.ac.nz/infosxi/KEL/CBIIS.html.

[49] Haykin, S. Communication Systems, John Wiley & Sons, Inc, 3rd edition. 1994, pp.424-465.

[50] Odile Macchi, Adaptive Processing The Least Mean Squares Approach With Application In Transmission, John Wiley & Sons, 1996.

[51] B. Widrow, J.M. McCool, M.G. Larimore, and C.R. Johnson, “Stationary and Nonstationary Learning Characteristics of the LMS Adaptive Filter”, IEEE Proceedings, vol. 64, no. 8, pp. 1151-1162, 1976.

[52] L. Ljung, M. Morf and D. Falconer, “Fast calculation of gain matrices for recursive estimation schemes,” Int. J. Contr, vol. 27, pp. 1-19, 1978.

[53] S. Vaseghi, Advance Signal Processing and Digital Noise Reduction, John Wiley & Sons, Inc. 1996, pp.164-183.

[54] R. H. Kwong and E. W. Johnston, “A Variable Stepsize LMS algorithm”, IEEE transactions on signal procssing, vol. 40, pp. 1633-1642, 1992.

[55] T. J. Shan and T. Kailath, “Adaptive algorithms with an automatic gain control feature”, IEEE transactions on Acoustic, Speech and Signal Processing, vol. 35, pp. 122-127, 1988.

[56] J.I., Nagumo and A. Noda, “A learning method for system identifcation”, IEEE Transactions, Automatic control, vol. AC-12, pp. 282-287, 1967.

[57] N.J. Bershad, “Analysis of the normalized LMS algorithm with Gaussian inputs” IEEE transactions on Acoustic, Speech and Signal Processing, vol. ASSP-34, pp. 793-806, 1986.

[58] TIA/EIA/IS-95 Interim Standard, Mobile Station-Base Station Compatibility Standard for Dual-mode Wideband Spread Spectrum Cellular System. TIA, July 1993.

[59] M. Honig and M. K. Tsatsanis, “Adaptive Techniques for Multiuser CDMA Receivers” IEEE Signal Processing Magazine, May 2000.

[60] M. Abdulrahman, D. Falconer and A. Sheikh, “Equalization for Iinterference Cancellation in Spread Spectrum multiple access systems” IEEE 42nd Vehic. Technol.Conf., pp.71-74. 1992.

[61] M. Abdulrahman, A. Sheikh and D. Falconer,“Decision Feedback Equalization for CDMA in Indoor Wireless Communications” IEEE Journal on Selected Areas in Comm., Vol. 12, No. 4. May 1994.

[62] M. Raju, and A. Chockalingam, “Decision Feedback Equalizer Based Multiuser Detection in DS-CDMA Systems”

[63] J. Palicot, “A Weighted Decision Feedback Equalizer with Limited Error Propagation”, ICC 2000, New Orleans, June 2000.

[64] Gordon L. Stuber, Principles of mobile communication, 2 nd edition, 2001, Kluwer Academic Publishers.

Vita

- Waleed A. Saif.
- Born in Taiz, Yemen on July 27, 1977.
- Received Bachelor of Sciences (B.S.) degree in Electrical Engineering from King Fahd University of Petroleum and Minerals, Dhahran, Saudi Arabia in 2000.
- Joined King Fahd University of Petroleum and Minerals in January 2000 for Master studies in the field of Telecommunication Engineering.
- Email: waleedsaif@yahoo.com